A Simultaneous Physically and Chemically Gelling Polymer System for Endovascular Embolization of Cerebral Aneurysms

by

Hanin H. Bearat

A Dissertation Presented in Partial Fulfillment
of the Requirements for the Degree
Doctor of Philosophy

Approved April 2012 by the
Graduate Supervisory Committee:

Brent Vernon, Chair
David Frakes
Francisco Solis
Mark Preul
Christine Pauken
Stephen Massia

ARIZONA STATE UNIVERSITY

May 2012

ABSTRACT

Current treatment methods for cerebral aneurysms are providing life-saving measures for patients suffering from these blood vessel wall protrusions; however, the drawbacks present unfortunate circumstances in the invasive procedure or with efficient occlusion of the aneurysms. With the advancement of medical devices, liquid-to-solid gelling materials that could be delivered endovascularly have gained interest. The development of these systems stems from the need to circumvent surgical methods and the requirement for improved occlusion of aneurysms to prevent recanalization and potential complications.

The work presented herein reports on a liquid-to-solid gelling material, which undergoes gelation via dual mechanisms. Using a temperature-responsive polymer, poly(N-isopropylacrylamide) (poly(NIPAAm), the gelling system can transition from a solution at low temperatures to a gel at body temperature (physical gelation). Additionally, by conjugating reactive functional groups onto the polymers, covalent cross-links can be formed via chemical reaction between the two moieties (chemical gelation). The advantage of this gelling system comprises of its water-based properties as well as the ability of the physical and chemical gelation to occur within physiological conditions. By developing the polymer gelling system in a ground-up approach via synthesis, its added benefit is the capability of modifying the properties of the system as needed for particular applications, in this case for embolization of cerebral aneurysms.

The studies provided in this doctoral work highlight the synthesis, characterization and testing of these polymer gelling systems for occlusion of

aneurysms. Conducted experiments include thermal, mechanical, structural and chemical characterization, as well as analysis of swelling, degradation, kinetics, cytotoxicity, *in vitro* glass models and *in vivo* swine study. Data on thermoresponsive poly(NIPAAm) indicated that the phase transition it undertakes comes as a result of the polymer chains associating as temperature is increased. Poly(NIPAAm) was functionalized with thiols and vinyls to provide for added chemical cross-linking. By combining both modes of gelation, physical and chemical, a gel with reduced creep flow and increased strength was developed. Being waterborne, the gels demonstrated excellent biocompatibility and were easily delivered via catheters and injected within aneurysms, without undergoing degradation. The dual gelling polymer systems demonstrated potential in use as embolic agents for cerebral aneurysm embolization.

To my parents, my eternal flames, Hamdallah and Nadia Bearat

To my sisters, my shining stars, Hayat and Lina Bearat

To my best friend, Chetan Patel

To my beautiful homeland, Palestine

ACKNOWLEDGMENTS

Many individuals have in some way or another been instrumental in the compilation of this doctoral work, to whom special thanks is presented. First and foremost, I am thankful to my advisor Dr. Brent Vernon for providing me the opportunity to pursue my doctoral studies under his supervision, after having had my first taste of research as an undergraduate in his lab. With his exceptional guidance, support and intellectual contributions, I have grown into a better person. Gratitude goes to Dr. Francisco Solis for his vision and passion in my work. I would also like to acknowledge my committee members for providing me with their expertise in particular fields of my research: Dr. David Frakes for assistance with aneurysm glass models, Dr. Stephen Massia for the opportunity and training in teaching Biomaterials, Dr. Christine Pauken for her experience and knowledge with cell studies and Dr. Mark Preul for his support and mentorship with the *in vitro* glass models and *in vivo* swine studies. I would like to particularly thank Dr. Bae Hoon Lee for his excellent scientific training, guidance and insightful discussions. I am also thankful for the professional feedback and fun times spent with my lab colleagues.

I am also indebted to the incredible surgical skills of Dr. Bill Bichard and to the Barrow Neurological Institute staff in their help in conducting the *in vitro* glass models and the *in vivo* swine studies. Additionally, I am grateful for Dr. Soenke Seifert for his superior experience and resourcefulness in conducting the SAXS studies and to the Advanced Photon Source at Argonne National Laboratories for the opportunity to fulfill my passion for the SAXS experiments.

Research could not be carried out without the presence of substantial funding resources. Recognition is presented to the Science Foundation Arizona for their doctoral fellowship and the Arizona Biomedical Research Commission for their research support. I thank the National Science Foundation for their research funding and for their GK12 program doctoral fellowship. I also acknowledge the Bioengineering department and the Graduate and Professional Student Association for their financial aid in travel to conferences as well as the allocation of a Graduate Research Support Program grant.

Lastly, certain individuals have made a tremendous impact on my life, at all levels. I am so touched by the incredible friendships of my peers, Veronica Clavijo Jordan and Liliana Rincon, who have made this doctoral experience unforgettable. No words can possibly explain the appreciation I feel towards my best friend Chetan Patel. It is with unparalleled support, advice, cherishing, intelligence and eloquence that he has accompanied me throughout this journey, and I only hope I can nearly reciprocate it. Finally, it is beyond expression the impact my family has imprinted on me. I owe utmost respect and eternal gratitude to my parents, Hamdallah and Nadia Bearat, and to my sisters, Hayat and Lina Bearat, for their constant surrounding of love, encouragement and belief in me with which they have helped me take each step, not only within this doctoral experience, but throughout my lifetime. Je vous aime.

TABLE OF CONTENTS

Page

CHAPTER Page

CHAPTER Page

CHAPTER Page

CHAPTER Page

LIST OF TABLES

Table Page

LIST OF FIGURES

Figure Page

Figure Page

CHAPTER 1

AN INTRODUCTION TO THERMORESPONSIVE POLYMERS

1.1 Introduction

Smart materials have been under immense investigation in all fields of science and in all corners of the world, over the past decades. Smart materials consist of materials which respond to changes in their environment, thus rendering them stimuli-responsive. This work focuses on use of environmentally-responsive hydrogels, essentially polymer networks which are capable of retaining large amounts of water without altering their structure. Many hydrogels possess the ability to undergo reversible changes in phase transition, from a solution-to-gel or gel-to-solution, depending on their chemical properties as well as the type of stimulus they are subjected to. The array of stimuli observed to trigger such changes includes temperature, electric field, pH, light, pressure, magnetic field, and ionic strength. Additionally, other hydrogels have shown to be responsive to biomolecules including antigens, glucose, enzymes and thrombin.

There is demand for more effective, localized, and need-based systems, which can be used in a plethora of biomedical applications, such as cancer targeting, controlled drug delivery, tissue engineering or biosensors. By developing injectable hydrogels which can respond to variations in their environment and which can achieve the desired outcome (releasing a drug or biological molecule, targeting cancerous cells, or cell differentiation in scaffolds), better medical techniques can be attained.

1.2 Temperature-responsive polymers

1.2.1 Properties

Thermoresponsive materials have received much attention in recent years due to their unique characteristics when exposed to various temperatures, particularly at physiological conditions. Since temperature acts as the stimulus, these materials undergo gelation upon increase or decrease in temperature, such as a change from room to body temperature. The event of a transformation from solution to gel in an aqueous environment is known as a sol-gel transition (Klouda & Mikos, 2008). This transition is marked by a critical temperature which can either be a lower critical solution temperature (LCST) or an upper critical solution temperature (UCST) (Moelbert & De Los Rios, 2003; Ougizawa, Inoue, & Kammer, 1985). Below the LCST, the polymer is hydrophilic and soluble, and can thus be found in a solution state. However, as temperature is increased to above the LCST, the polymer becomes more hydrophobic and insoluble, thus causing a collapse into a gel form (Henderson et al., 2008; Klouda & Mikos, 2008; H. Liu & Zhu, 1999). In the case of a UCST, a phase separation occurs at a low temperatures and the polymer solution converts into a gel as cooling occurs (Moelbert & De Los Rios, 2003; Ougizawa et al., 1985). The phase transition temperature can be altered by varying the composition of comonomers in the polymer structure. With addition of hydrophobic comonomers, the LCST can be decreased while incorporation of hydrophilic comonomers results in an increase in LCST (Cui, Lee, & Vernon, 2007). It has been demonstrated that the addition

of acrylic acid to poly(N-isopropylacrylamide) leads to an increase in its LCST (B. H. Lee & Vernon, 2005; Vernon, Kim, & Bae, 2000), while incorporation of hydroxyethyl methacrylate-acrylate lowers its LCST (B. H. Lee, West, McLemore, Pauken, & Vernon, 2006). It has also been shown that increasing the molecular weight of a polymer may increase its UCST and decrease its LCST (Y. C. Bae, Lambert, Soane, & Prausnitz, 1991).

Although complete understanding of the phase transition of such systems has not yet been attained, various hypotheses are present. One proposition is that a LCST exists due to a local structural transition, which involves the presence of water molecules around specific portions of the polymer in solution (Solis, Weiss-Malik, & Vernon, 2005). At low temperatures, the water molecules tend to be frozen in place, forming a clathrate structure around segments of the polymer. When at lower temperatures, the water molecules do not possess sufficient energy to alter the bonding pattern and thus maintain their location within the lattice structure (Plummer & Chen, 1983). This structure causes the polymer to remain water soluble and in solution form. With an increase in temperature, the water molecules gain energy, resulting in an increase of librational motion of the bonds which in turn causes hydrogen bonding disruption (Plummer & Chen, 1983). The disruption of hydrogen bonds of the water molecules within the clathrate structure allows for associations to be formed between newly exposed monomers. Exposure of monomers leads to more chances of entanglement, and thus, formation of a gel.

The behavior of polymers in solution and their phase transition at different temperatures can also be described thermodynamically. Three types of interactions can occur once a polymer is dissolved in water: water-polymer, water-water, and polymer-polymer (Klouda & Mikos, 2008; Solis et al., 2005), and they can be analyzed using the free Gibbs energy equation given below:

$$\Delta G = \Delta H - T\Delta S \qquad \textit{Eqn. 1}$$

where ΔG is the change in free energy of the system, ΔH is the change in the enthalpy of the system, T is the absolute temperature and ΔS is the change in entropy of the system. As can be seen from the equation, as temperature is increased, the entropy term ($T\,\Delta S$) becomes more negative compared to the enthalpy term (ΔH), leading to a negative free energy term (ΔG). What this translates to for polymers with an LCST is that as temperature is increased, a decrease in the free energy of the system occurs, which results in unfavorable conditions for polymer-water interaction and more favorable conditions for water-water and polymer-polymer interactions (Klouda & Mikos, 2008). Frank and Evans in 1945 studied this phenomenon and noted that when a non-polar molecule dissolves in water at room temperature, the water molecules tend to orient themselves in a manner to produce greatest "crystallinity" (Frank & Evans, 1945). What they describe as the "freezing" of the water molecules, as in a clathrate-like structure, was coined as the "iceberg" theory. In this manner, the water molecules would rather form hydrogen bonds with other adjacent water molecules to construct a cage around the non-polar molecule. The greater the non-polar molecule, the greater the iceberg or cage formed. From a thermodynamic

point, at low temperatures, processes tend to lower their enthalpies whereas at high temperatures, these processes reach higher entropy (Southall, Dill, & Haymet, 2002). Thus, as temperature is increased, the water molecules in this cage will gain entropy by rearranging themselves to widen their distribution; however, as they do so, the bonds between the water molecules will break, resulting in an increase in enthalpy (Southall et al., 2002). Different polymers behave differently at their phase transition temperature. The following sections discuss various thermoresponsive polymers as well as their respective properties and applications.

1.2.2 N-isopropylacrylamide

Temperature-responsive polymers are most likely the most investigated environmental stimuli responsive materials (Qiu & Park, 2001b), especially for biomedical purposes. One of the well-known thermoresponsive polymers is poly(N-isopropylacrylamide), abbreviated as poly(NIPAAm), with its chemical structure shown in Figure 1.1.

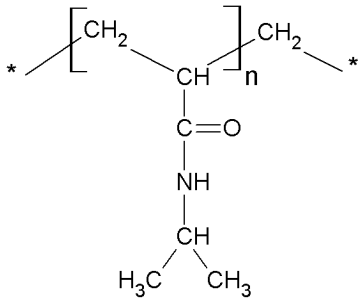

Figure 1.1 Chemical structure of thermoresponsive polymer poly(N-isopropylacrylamide), known as NIPAAm.

This particular polymer has an LCST around 32°C. Below its LCST, NIPAAm is hydrophilic and soluble in aqueous solutions. As temperature is increased above 32°C, the polymer becomes hydrophobic and insoluble, resulting in its collapse into a gel. The behavior of NIPAAm around its phase transition temperature has not been fully uncovered. A possibility is, as explained earlier, that as the temperature is increased, the water molecules which formed a clathrate structure around the hydrophobic methyl groups, will unfreeze. This in turn allows the polymer chains to entangle, cross-link, and form a gel, as seen in Figure 1.2.

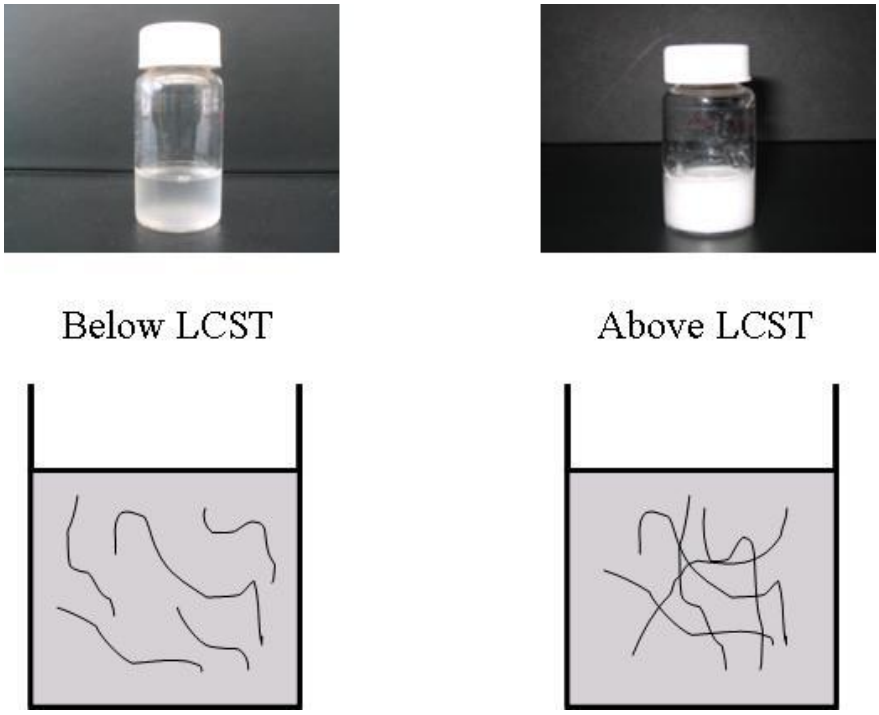

Figure 1.2 Demonstration of a thermoresponsive polymer below and above its LCST. Below LCST, the polymer is hydrophilic and remains in solution form. As temperature is increased to above its LCST, the polymer becomes insoluble and collapses to form a gel.

NIPAAm possesses great potential for medical use due to an LCST close to body temperature. It is also important to note that the LCST of NIPAAm can be altered by copolymerization of other monomers to the poly(NIPAAm) backbone. The addition of a hydrophobic monomer leads to a decrease in the LCST, whereas the addition of a hydrophilic monomer results in an increase in LCST. An example of copolymerization of a hydrophobic monomer to poly(NIPAAm) has been done by (B. H. Lee et al., 2006). Through free radical polymerization, the

group has added hydroxyethylmethacrylate-acrylate (HEMA-acrylate) to the backbone, resulting in poly(NIPAAm-co-HEMA-acrylate) seen in Figure 1.3.

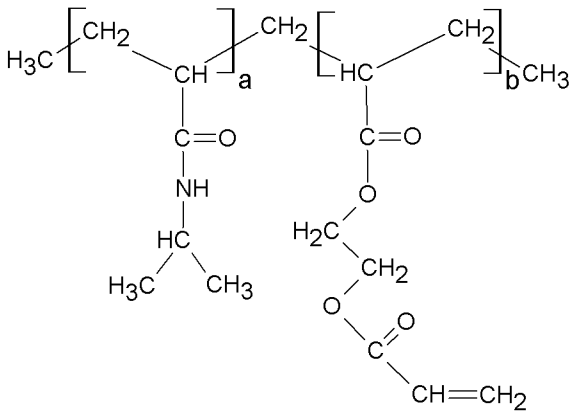

Figure 1.3 Chemical structure of thermoresponsive polymer poly(N-isopropylacrylamide-co-hydroxyethyl methacrylate acrylate), or poly(NIPAAm-co-HEMA-acrylate). By the copolymerization of HEMA-acrylate, a hydrophobic monomer, the LCST of the polymer decreases.

The hydrophobicity of the HEMA-acrylate monomer caused the LCST of the copolymer to decrease to 23°C (B. H. Lee et al., 2006). Contrarily, by the copolymerization of acrylic acid to poly(NIPAAm), structure shown in Figure 1.4, (Vernon & Martinez, 2005) witnessed that as the content of acrylic acid (AAc) in the polymer is increased, an increase in LCST is simultaneously observed. They recorded that at 0 mol% AAc in THF, the LCST was 32.87°C, with 1.33 mol% AAc the LCST increased to 38.17°C, whereas with 1.99 mol% AAc, the LCST reached 39.1°C (Vernon & Martinez, 2005).

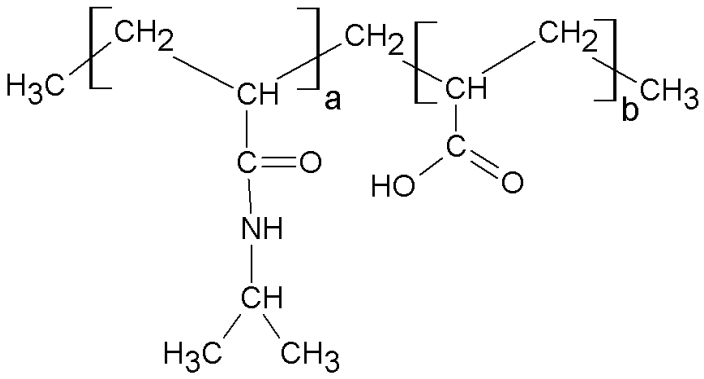

Figure 1.4 Chemical structure of thermoresponsive polymer poly(N-isopropylacrylamide-co-acrylic acid), or poly(NIPAAm-co-AAc). Since acrylic acid is a hydrophilic moiety, its conjugation increases the original LCST.

(Feil, Bae, Feijen, & Kim, 1993b)) have also investigated the addition of different comonomers to poly(NIPAAm-co-butyl methacrylate-X) where X is a hydrophobic, hydrophilic, cationic, or anionic comonomer. Their study showed that the addition of hydrophilic or charged comonomers had no direct effect on the water structure around the hydrophobic groups of the polymer, but rather caused an increase in the LCST due to the influence on the overall hydrophilicity of the polymer (Feil, Bae, Feijen, & Kim, 1993b).

Poly(NIPAAm) being one of the most studied thermoresponsive polymers has thus found itself used in various biomedical applications. (B. H. Lee et al., 2006; Robb, Lee, McLemore, & Vernon, 2007a) have taken advantage of the thermal characteristics of poly(NIPAAm) and combined it with the Michael-type addition reaction which occurs between thiols on one NIPAAm copolymer with the olefins on the second NIPAAm copolymer to form an *in situ* gel used for

potential endovascular embolization of aneurysms and arteriovenous malformations (B. H. Lee et al., 2006; Robb, Lee, McLemore, & Vernon, 2007a). Cui et al. (2007) synthesized poly(NIPAAm) with dimethyl-γ-butyrolactone acrylate to form a hydrolysis-dependent thermoresponsive gelling system, rendering the copolymer biodegradable, for injectable drug delivery (Cui et al., 2007). By conjugating poly(NIPAAm) with acrylic acid (AAc) and HEMA-poly(trimethylene carbonate), a biodegradable and thermoresponsive copolymer was achieved for injection into the ventricular wall to prevent progressive remodeling of the left ventricle after myocardial infarction (Fujimoto et al., 2009). NIPAAm and AAc combination was also used as a carrier of chondrocytes and transforming growth factor ß3 to cartilage tissue (Yun & Moon, 2008). After 8 weeks of implantation in cartilage of mice, Yun and Moon (2008) observed normal histological and biochemical characteristics, and concluded this hydrogel can be used for neocartilage formation. Grafting of NIPAAm on collagen/chitosan-immobilized polypropylene nonwoven fabric has shown improved healing as well as better remodeling of the veins, epidermis and dermis of the skin injury, when compared to the non-NIPAAm grafted fabric (C. C. Wang, Su, & Chen, 2008). Kim and Lee (2009) obtained a thermoresponsive gel with an LCST around 34.5°C by preparing NIPAAm with vinyl phosphonic acid. The hydrogel was then biomineralized with urea-mediation and was loaded with bovine serum albumin for a drug release model. They determined that drug release was affected by drug loading, water content and biomineralization. Through protein delivery and biomineralization, this hydrogel has potential for

bone regeneration (Kim & Lee, 2009). By forming branched copolymers of NIPAAm and poly(ethylene glycol) (PEG), a highly elastic and stiff material was achieved to be used for replacement of the nucleus pulposus of the intervertebral discs (Vernengo, Fussell, Smith, & Lowman, 2008).

1.2.3 Natural thermoresponsive polymers

Natural polymers have also been used as thermoresponsive hydrogels, either on their own or in combination with other synthetic polymers. Popular natural polymers include chitosan, cellulose derivatives, dextran, xyloglucan and gelatin (Klouda & Mikos, 2008). Chitosan is a polysaccharide derived from the shells of crustaceans and is produced by deacetylation of chitin, basically through the removal of the acetyl group using a concentrated NaOH solution.

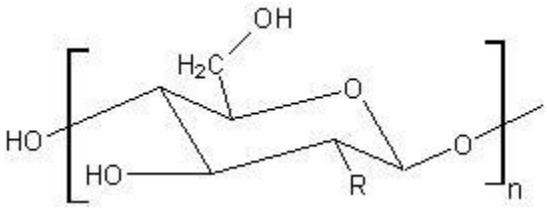

Figure 1.5 Chemical structure of chitosan, a natural thermoresponsive polymer.

The main advantage of chitosan, chemical structure shown in Figure 1.5, for medical and pharmaceutical applications is its biocompatibility and inertness when in contact with human cells (Kumar, Muzzarelli, Muzzarelli, Sashiwa, & Domb, 2004). It is also quite unique in that it can be degraded in the human body by enzymatic action, but can also be recognized by tumor cells and thus be used

for drug delivery applications. An extensive review is written on the chemistry and applications of chitosan, highly recommended for further reading (Kumar et al., 2004). The Leroux group has also elaborately investigated use of chitosan in drug delivery applications. Chitosan is soluble up to a slightly acidic pH of 6.2 at 85% degree of deacetylation. Once the pH is brought above this value, a gel is formed. They have determined that by using a polyol counterionic monohead salt to neutralize the pH, the chitosan solution was found to remain in liquid form for an extended period of time at or below room temperature. This discovery is important in that it allows chitosan solutions to possess pH values closer to the physiological pH of 7.4 and also results in dependence on temperature to determine the liquid or gel phase, with gel formation occurring at higher temperatures (Chenite et al., 2000). Chenite et al. (2000) used the chitosan/polyol salt solution for delivery of biologically active growth factors *in vivo* and also utilized it for tissue engineering techniques as an encapsulating matrix for living chondrocytes. The same group looked into using chitosan with glycerophosphate (GP). They found that gelation rate depended on temperature and degree of deacetylation of chitosan (Ruel-Gariepy, Chenite, Chaput, Guirguis, & Leroux, 2000). When tested *in vitro*, the release profile of the chitosan/GP solution with different modeled compounds was related to GP present in the solution, molecular weight and lysozyme presence in the release media. Studies have been done which use chitosan for delivery of bovine serum albumin and anti-tumor necrosis factor agents (Shamji et al., 2008), for local sustained release of paclitaxel against tumor growth (Ruel-Gariépy et al., 2004), for nasal drug delivery by combination

with poly(ethylene glycol) (Wu, Wei, Wang, Su, & Ma, 2007) or thiolated chitosan microparticles for nasal peptide delivery (Krauland, Guggi, & Bernkop-Schnürch, 2006), ocular delivery of liposome-chitosan nanoparticles (Diebold et al., 2007) and fluorescently-labeled chitosan nanoparticles (de Salamanca et al., 2006), as well as microspheres for a sustained and controlled drug carrier to the systemic circulation (Denkbas & Ottenbrite, 2006).

Cellulose is a polysaccharide commonly found in nature which is insoluble in water. Its insolubility can be altered by substituting the hydroxyl groups on its chiral structure to hydrophobic groups, such as methyl or hydroxypropyl groups (Klouda & Mikos, 2008). Methylcellulose and hydroxypropyl methylcellulose undergo similar gel formation as poly(NIPAAm), in that at low temperature (and low concentrations of 1-10wt%), they can be found in liquid form. The chemical structure of methylcellulose can be seen in Figure 1.6.

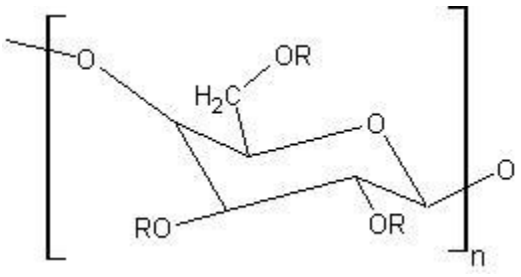

Figure 1.6 Chemical structure of methylcellulose, a derivative of the naturally-occurring temperature-responsive cellulose.

Once exposed to higher temperatures, the methylcellulose and hydroxypropyl methylcellulose solutions form gels, between 40 to 50°C and 75 to 90°C, respectively (Ruel-Gariépy & Leroux, 2004). Studies done by Sarkar (1979) demonstrated that the temperature at which the phase transition of either solution occurs decreases at first with increasing concentration, up to a critical concentration; above this value, temperature is faintly influenced by changes in concentration (Sarkar, 1979). It was also shown that strength of the resulting gels is time-dependent, that it increases with an increase in molecular weight and decreases with greater hydroxypropyl substitution (Sarkar, 1979). A hydrophobically-modified methyl cellulose (HMMC) with NaCl solution provided much faster gelation (S. C. Lee, Cho, & Park, 2005). Also by adjusting the concentration of HMMC and NaCl, S. C. Lee, Cho, and Park (2005) were able to obtain a sol-gel transition at body temperature and a gel-sol transition at room temperature. Siepmann and Peppas (2001) have modeled different drug delivery systems consisting of hydroxypropyl methylcellulose (Siepmann & Peppas, 2001). Cellulose derivatives have been used in various applications, which include substitutes for bone repair when mixed with biphasic calcium phosphate (Fellah et al., 2006) or as an injectable bone substitute for dental sockets (Weiss et al., 2007). Methylcellulose can also be combined with gelatin type A and chondroitin 6-sulfate to serve as a combination gel for protein drug delivery (Jin & Kim, 2008). Although this section was mainly focused on chitosan and cellulose derivatives, there are quite a few other naturally-occuring polymers used for medical applications. Xyloglucan, a polysaccharide which originates from

tamarind seeds, shows thermally reversible gelation as its galactose side chains are partially degraded (Ruel-Gariépy & Leroux, 2004). It has a broad gelation range, from 5 to 50°C, and a morphology dependent on the hydrogel concentration (Nisbet et al., 2006). Xyloglucan has been used to coat layered double hydroxides for drug delivery (Ribeiro, Arizaga, Wypych, & Sierakowski, 2009) as well as to obtain nanocomposites with hydrophobic matrices (Zhou, Rutland, Teeri, & Brumer, 2007). Gelatin is also used as a thermoresponsive polymer as it is found in gel form below 25°C and returns to its liquid form above 30°C (Klouda & Mikos, 2008). It is a collagen-derived protein; however, since it is found in liquid state at body temperature, studies have been performed to chemically cross-link gelatin to improve its gelation properties, such as cross-linking it with hyaluronan for extracellular matrix (Weng, Pan, & Chen, 2008). Gelatin has also been used to serve as a scaffold for chondrogenic differentiation of adult stem cells (Awad, Quinn Wickham, Leddy, Gimble, & Guilak, 2004).

1.2.4 Pluronics

Pluronics, also known as poloxamers, are a class of synthetic block copolymers which consist of hydrophilic poly(ethylene oxide) (PEO) and hydrophobic poly(propylene oxide) (PPO), arranged in an A-B-A triblock structure, thus giving PEO-PPO-PEO structure, as shown in Figure 1.7 (Batrakova & Kabanov, 2008).

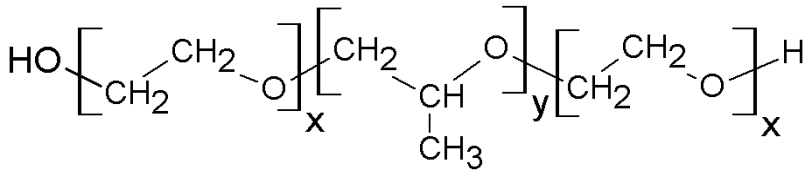

Figure 1.7 Poloxamer, poly(ethylene oxide)-poly(propylene oxide)-poly(ethylene oxide) (PEO-PPO-PEO).

They can be found either as liquids, pastes or solids (Ruel-Gariépy & Leroux, 2004). Due to their amphiphilic characteristics (presence of hydrophobic and hydrophilic components), pluronics possess surfactant properties which allow them to interact with hydrophobic surfaces and biological membranes (Batrakova & Kabanov, 2008). Being amphiphilic also results in the ability of the individual block copolymers, known as unimers, to combine and form micelles in aqueous solutions. When the concentration of the block copolymers is below that of the critical micelle concentration (CMC), the unimers remain as molecular solutions in water. However, as the block copolymer concentration is increased above the CMC, the unimers will self-assemble and form micelles, which can take on spherical, rod-shaped or lamellar geometries. Their shapes depend on the length and concentration of the block copolymers (i.e. EO and PO), and the temperature (Kabanov, Batrakova, & Alakhov, 2002). Micelles usually have a hydrophobic core, in this case the PO chains, and a hydrophilic shell, the EO chains.

The formation of micelles in Pluronics has lead to a plethora of studies in the field of drug delivery. Micelles have a feasible structure for drug loading, since drugs can be incorporated into the core of the micelle at high loads. A

characteristic of micelle use is that the distribution of the drug from the drug-loaded micelles is not so much dependent on the drug itself, but rather on the size and surface properties of the micelles, which can be tailored with chemical techniques (Kataoka, Harada, & Nagasaki, 2001). By doing so, the solubility, metabolic activity and circulation time of the drug can be increased (Kabanov et al., 2002). Poloxamer 407 in conjuction with HPMC has been used for rectal delivery of quinine in children (Koffi et al., 2008). Use of poloxamer 188 as a membrane sealant on *in vitro* studies of cardiac myocytes showed signs of possible prevention of cardiomyopathy and heart failure in muscular dystrophy (Yasuda et al., 2005). A combination of poloxamer 407, poloxamer 188 and carbopol was utilized as an ophthalmic delivery system for puerarin, thus providing an alternative for longer-lasting drug availability to the precorneal area (Qi et al., 2007). Poloxamer 407 has also shown prolonged duration of the painkiller, lidocaine, at the injection site as well as sustained drug release and increased therapeutic efficacy (Ricci, Lunardi, Nanclares, & Marchetti, 2005). Batrakova et al. (2006) investigated the use of Pluronic P85 with the antineoplastic drug, doxorubicin, and determined that presence of pluronic resulted in the inability of human breast cancer cells to grow (Batrakova et al., 2006). Other studies of pluronics involve use of Pluronic F127 for delivery of human growth hormone (Chung, Lee, & Park, 2008), combination of Pluronic F127 with chitosan as an injectable cell delivery carrier for cartilage regeneration (Park et al., 2009), and for enhanced transcription of reporter genes (Sriadibhatla, Yang, Gebhart, Alakhov, & Kabanov, 2006).

1.2.5 PEG-PLGA-PEG

Poly(ethylene glycol) (PEG) is quite a popular polymer in biomedical applications due to its hydrophilicity and biocompatibility. When PEG is copolymerized with poly(D,L-lactic acid co-glycolic acid) (PLGA) as a triblock copolymer, the polymer has shown to possess biocompatibility, biodegradability and a sol-gel phase transition (Jeong & Gutowska, 2002b). The triblock chemical structure of PEG-PLGA-PEG can be seen in Figure 1.8, depicting the various copolymers in the structure.

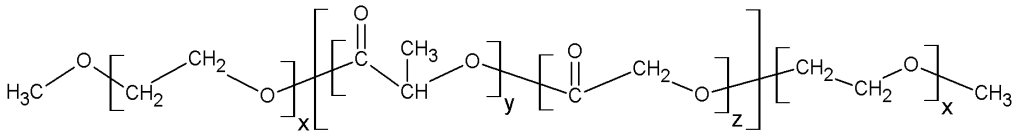

Figure 1.8 Thermoresponsive copolymer PEG-PLGA-PEG, which consists of poly(ethylene glycol) (PEG) and poly(D,L-lactic acid co-glycolic acid) (PLGA).

At higher temperatures (around 45°C), the polymer can be found as a solution and therefore allows for loading of bioactive molecules. Once the polymer is injected at body temperature, the decrease in temperature permits the hydrogel to form a gel. The creation of a gel consisting of loaded bioactive molecules renders the system appropriate for sustained release of drugs from the matrix (Jeong & Gutowska, 2002b). Further work has demonstrated that alteration to the gelation temperature can be achieved by increasing the concentration of PEG in the copolymer (Tarasevich, Gutowska, Li, & Jeong, 2009). The study also concluded

that the gelation temperature was also dependent on molecular weight of the polymer as well as concentration. The PEG-PLGA-PEG copolymer was also used for delivery of plasmid DNA in rat models and it was determined that the copolymer has the potential to improve gene delivery efficiency (Chang et al., 2007). P. Y. Lee, Cobain, Huard, and Huang (2007) investigated the properties of the copolymer for wound dressing and scaffold of diabetic skin wounds (P. Y. Lee, Cobain, Huard, & Huang, 2007). They witnessed an increase in engraftment of muscle-derived stem cells, which in turn allowed for better wound healing and collagen deposition. Poly(D,L-lactide-co-glycolide) (PLGA) microspheres dispersed within a PEG-PLGA-PEG gel were used for the sustained release of ganciclovir, an antiviral drug (Duvvuri, Janoria, & Mitra, 2005). The group witnessed a decrease in the drug release rate from the microspheres within the gel, compared to the microspheres alone. They also developed a set of equations to describe the various phases of drug release from the microspheres, these stages being initial diffusion, matrix hydration and degradation (Duvvuri et al., 2005). By coating a PEGylated monoclonal antibody, which has high affinity for an antigen on prostate cancer cells, with PLGA-PEG-PLGA, an enhanced transfection efficiency and uptake of the plasmid was seen due to copolymer coating (Moffatt & Cristiano, 2006).

1.3 Conclusions

As seen in this work, hydrogels can be made to respond to various environmental stimuli. Temperature and pH are stimuli present in the body which can be employed to trigger changes in a hydrogel form. Due to their amphiphilic nature, thermoresponsive hydrogels undergo a sol-gel phase transition upon reaching a particular temperature (LCST/UCST). This characteristic allows them to be used for controlled drug delivery purposes, as this transition is reversible. Having polyelectrolyte properties, pH, ionic strength, light and electro-sensitive hydrogels experience swelling and shrinking behaviors upon stimulation. By controlling glucose concentration or magnetic field application, a modulated response can be obtained to achieve pulsatile release. With the diverse stimuli available for managing hydrogel characteristics, a plethora of biomedical applications can take advantage of these mechanisms. These include controlled drug delivery, bone regeneration, scaffolds for cell differentiation, enhanced gene transcription and therapy, muscle actuators, and lubricants for joint diseases, to name a few. These environmentally-responsive hydrogels are advantageous in that they provide for easier drug administration, they do not use organic solvents, they enhance localization and specificity, as well as allow for a sustained drug release.

Although tremendous work has been accomplished in the field of stimuli-responsive materials, there is room for improvement in providing more suitable systems. Hydrogels need to possess faster gelation time and appropriate temperature and pH values to maintain homeostasis. Due to their high water

content, the mechanical strength of hydrogels can sometimes fall short of the required mechanical strength needed for physiological applications. Additionally, biocompatibility and biodegradability, when necessary, are essential components for success of a hydrogel. With degradable compounds, proper elimination from the body must be ascertained. Most of the complications with hydrogels listed above can be ameliorated via manipulation of copolymerization. By utilizing diverse copolymers, the hydrophobic-hydrophilic interactions can be altered, resulting in different mechanical strength, swelling behavior, and gelation temperature. The molecular weight of the copolymers can also be adjusted for better clearance from the body and the biocompatibility can also be amended for more feasible physiological applications.

CHAPTER 2

SYNTHESIS, CHARACTERIZATION AND PROPERTIES OF POLY(NIPAAM-CO-CYSTEAMINE) AND POLY(NIPAAM-CO-HEMA-ACRYLATE) GELLING SYSTEM

2.1 Introduction

In the last decades, there has been a growing demand for materials which can gel *in situ* and which can be manipulated to accommodate for various applications in the medicinal sciences. As such, recent research has found diverse uses of *in situ* gelling biomaterials, including cancer targeting (Cui et al., 2007), controlled drug delivery (Ruel-Gariépy & Leroux, 2004; Ruel-Gariépy et al., 2004; Shamji et al., 2008), tissue engineering (Awad et al., 2004; Vernon et al., 2000) and biosensors (Li & Luo, 2009). These materials are ideal in that they take the shape of their local environment and this gelation can be triggered by different environmental stimuli.

Thermoresponsive materials are one of the most investigated environmentally-responsive materials due to their unique characteristics when exposed to various temperatures, particularly at physiological conditions. Temperature being their stimulus, these materials form gels upon an increase or decrease in temperature, such as an increase from room to body temperature. The particular temperature at which the sol-gel transition occurs in an aqueous environment is referred to as the lower critical solution temperature (LCST) (Klouda & Mikos, 2008). Below the LCST, the material is found to be in solution

state due to its hydrophilicity and solubility; however, as temperature is increased above its LCST, the material becomes hydrophobic and insoluble, experiencing a collapse into gel form (Henderson et al., 2008; H. Y. Liu & Zhu, 1999). One particularly interesting polymeric material which has such thermoresponsive properties is poly(N-isopropylacrylamide), abbreviated as poly(NIPAAm). It has an LCST around 32°C; thus below this temperature, the polymer is hydrophilic and soluble in the aqueous environment due to the hydrogen bonds formed between the water molecules and the hydrophilic amide group on poly(NIPAAm). As temperature is increased above 32°C, the polymer undergoes phase transition, becoming hydrophobic and insoluble (Qiu & Park, 2001b). This results from the breaking of hydrogen bonds and dispersion of the water molecules, as more energy is added to the system (Jeong & Gutowska, 2002b). The hydrophobic methyl groups on poly(NIPAAm) then collapse (Jeong, Kim, & Bae, 2002)(Jeong & Gutowska, 2002b) and allow for entanglements of the polymer chains, resulting in a gel.

Many *in situ* gelling polymeric systems require use of organic solvents to dissolve hydrophobic and water-insoluble polymers. However, these organic solvents can cause toxicity when injected intra-arterially. The commonly used organic solvent, dimethyl sulfoxide (DMSO), shows signs of a local dose-related toxic effect on vessel and brain tissue when injected intravascularly in pigs (Mottu, Gailloud, Massuelle, Rüfenacht, & Doelker, 2000), while ethanol, at high concentrations, can cause severe local histopathological changes (Sampei et al., 1996). Similarly, acetone and *N*-methyl-2-pyrrolidone (NMP) have demonstrated

systemic, mutagenic, teratogenic and local toxic effects (Mottu, Laurent, Rüfenacht, & Doelker, 2000). Thus, a water-based gelling polymer system is needed to minimize toxic effects. Poly(NIPAAm) is ideal in that it is soluble in aqueous solutions and would thus circumvent use of organic solvents for preparation of gels.

The work herein investigated a waterborne *in situ* gelling polymer system for endovascular embolization techniques, consisting of copolymers of NIPAAm that undergo simultaneous physical and chemical gelation. By mixing poly(NIPAAm-*co*-HEMA-acrylate) with poly(NIPAAm-*co*-cysteamine), chemical gelation occurs through a Michael-type addition reaction between the thiol group on the cysteamine and the vinyl group on the acrylate, resulting in a cross-link. The advantage with the Michael-type addition reaction is that the initiation step, which involves the deprotonation of the thiol, can be done at the physiological pH of 7.4 (Lutolf & Hubbell, 2003b). Additionally, this reaction is highly selective, allowing thiols to react with acrylates at orders of magnitude faster than acrylates would react with amines or nucleophilic molecules in the body (Vernon, Tirelli, Bächi, Haldimann, & Hubbell, 2003). Aside for the cross-links formed through the chemical reaction, further cross-linking in the polymer system occurs due to the thermoresponsive properties of poly(NIPAAm). As the gel is exposed to body temperature (temperature higher than the LCST of the copolymers), NIPAAm chains on the copolymers will collapse and form cross-links. The benefits of the proposed system are that by simultaneous chemical and physical gelation, improved mechanical properties can be developed for the *in situ*

gel. Whereas solely chemical gels experience a large extent of swelling in aqueous solutions, unless they are highly cross-linked (Metters & Hubbell, 2005), and solely physical gels show signs of creep at low frequencies due to their viscoelastic properties (F. Tanaka & Edwards, 1992c), a chemical-physical gel will attain a more creep-resistant system when exposed to constant stress and provide better mechanical properties for the gel to be used endovascularly for embolization. Hubbell's group have developed a combined thermal gelling and chemical cross-linking system through a similar mechanism of Michael-type addition reaction (Cellesi, Tirelli, & Hubbell, 2004). The gels demonstrate potential for low cytotoxicity and improved biocompatibility. Hennink's group have explored core-cross-linked, thermally gelling micelles which maintained their physical stability and biodegradability (Rijcken, Snel, Schiffelers, Van Nostrum, & Hennink, 2007). Our group has also investigated physical-chemical gels, however, employing poly(NIPAAm). Vernon's group used poly(NIPAAm-*co*-HEMA-acrylate) mixed with pentaerythritol tetrakis 3-mercaptopropionate (QT) to form a physical-chemical gel (B. H. Lee et al., 2006) as wells as combining poly(NIPAAm-*co*-cysteamine) with poly(ethylene glycol) diacrylate (PEGDA) to obtain another simultaneously gelling system (Robb, Lee, McLemore, & Vernon, 2007b). Some difficulties observed with the former system is the high pH required for QT solubility as well as the challenging control of its kinetics (McLemore, Lee, & Vernon, 2009). In the latter system, PEGDA is highly hydrophilic and causes the gel to swell. A system whose properties can be changed as required and whose characteristics are ideal for use in biological and

physiological contexts is highly needed. In the proposed work, the properties of both components of the gelling system can be altered as needed by conjugating different monomers to poly(NIPAAm) at various ratios through free radical polymerization. This allows for more flexibility in the obtained gel properties, as an array of copolymers can be developed, stemming from poly(NIPAAm). An important aspect of this *in situ* gelling system is that it can be performed at physiological conditions, mainly at a pH of 7.4 and body temperature of 37°C, with the simultaneous use of a Michael-type addition reaction and the thermoresponsive properties of poly(NIPAAm). The mixed copolymers, once exposed to body temperature, can undergo physical gelation instantly, while further curing can occur through the chemical reaction between the thiol and acrylate functional groups on each copolymer.

2.2 Materials and Methods

2.2.1 Materials

N-isopropylacrylamide (NIPAAm; Aldrich 97%) was purified by recrystallization in hexanes and dried under vacuum for 4 days. 2,2'-Azobisisobutyronitrile (AIBN; Sigma-Aldrich 98%) was purified by recrystallization in methanol. Hydroxyethyl methacrylate (HEMA; Aldrich 98%), acryloyl chloride (Aldrich 97%), cysteamine hydrochloride (Fluka 98%), *N*-acryloxysuccinimide (NASI; Acros 99%) and 5,5'-dithiobis-(2-nitrobenzoic acid) (DTNB; Sigma) were used as received. Tetrahydrofuran (THF; Sigma-Aldrich,

HPLC grade 99.9%) was dried using sodium and triethylamine (TEA; Sigma-Aldrich 99.5%) was dried with barium oxide. Diethyl ether (Spectrum, anhydrous), hydrochloric acid (HCl; Mallinckrodt 37%), and anhydrous dichloromethane (MC; Sigma-Aldrich 99.8%) were used as received.

2.2.2 Synthesis of Poly(NIPAAm-*co*-HEMA-acrylate) and Poly(NIPAAm-*co*-cysteamine)

Poly(NIPAAm-*co*-HEMA) was synthesized by radical polymerization in THF at a NIPAAm:HEMA feed ratio of 95:5, as in the literature (B. H. Lee & Vernon, 2005; B. H. Lee et al., 2006). Briefly, NIPAAm and HEMA were dissolved in THF at 0.1g/mL (10w/v). AIBN was used as the initiator. At temperatures above 50°C, AIBN degrades to form a stable nitrogen molecule as well as two free-radical containing molecules, which initiate the polymerization reaction (Peppas, Keys, Torres-Lugo, & Lowman, 1999). Batches of approximately 20g were prepared. Prior to addition of the initiator, the solution was nitrogen bubbled at room temperature for 15 min to minimize oxygen content in the polymerization reaction. The copolymerization reaction was performed at 65°C for 20h under a nitrogen atmosphere. The copolymer was then precipitated in excess diethyl ether, filtered and vacuum dried. The copolymer was dissolved in water, dialyzed for 3 days in 3,500 MWCO dialysis membranes, frozen at -80°C and lyophilized. About 20g of poly(NIPAAm-*co*-HEMA) was then dried under vacuum at room temperature for 24h and dissolved in approximately 200mL of THF and 2.2mL of TEA (4 equiv per OH group). A volume of roughly

1mL acryloyl chloride (2 equiv per OH group) was added to the solution. The flask containing the mixture was covered with Al foil and left to react for 16h, while on ice for 2h and at room temperature for the remaining hours. Filtration was used to remove the triethylammonium chloride salt and the remainder of the solution was precipitated in 9-fold excess diethyl ether, filtered and vacuum dried for 24h. The copolymer was then dissolved in water, dialyzed for 3 days against 3,500 MWCO at 4°C, and lyophilized to obtain the final product. The copolymerization reaction can be seen in Figure 2.1A.

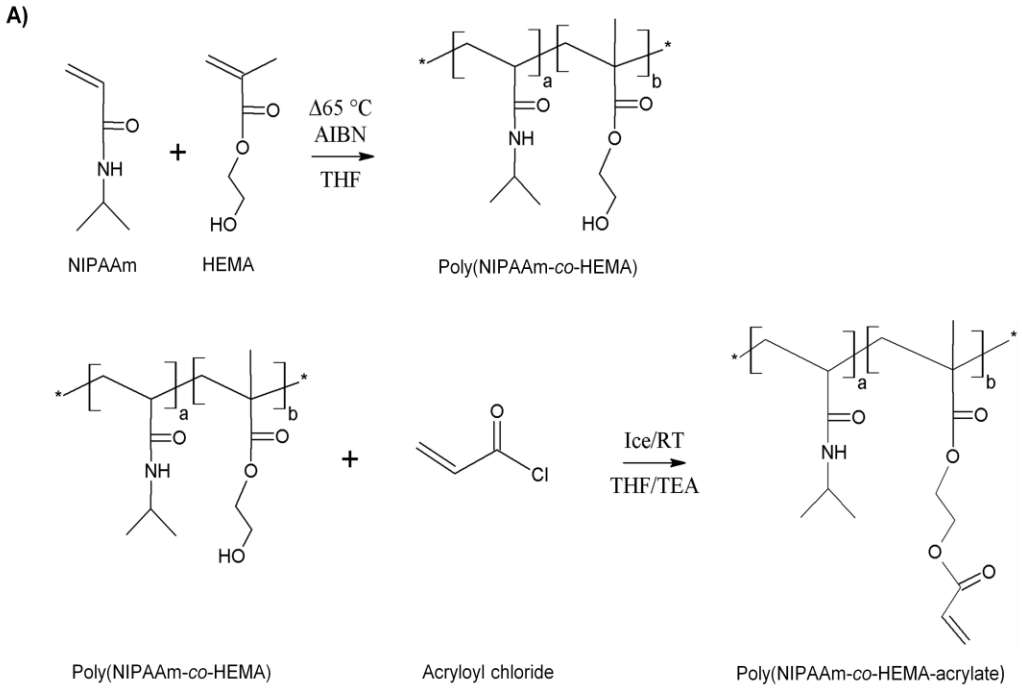

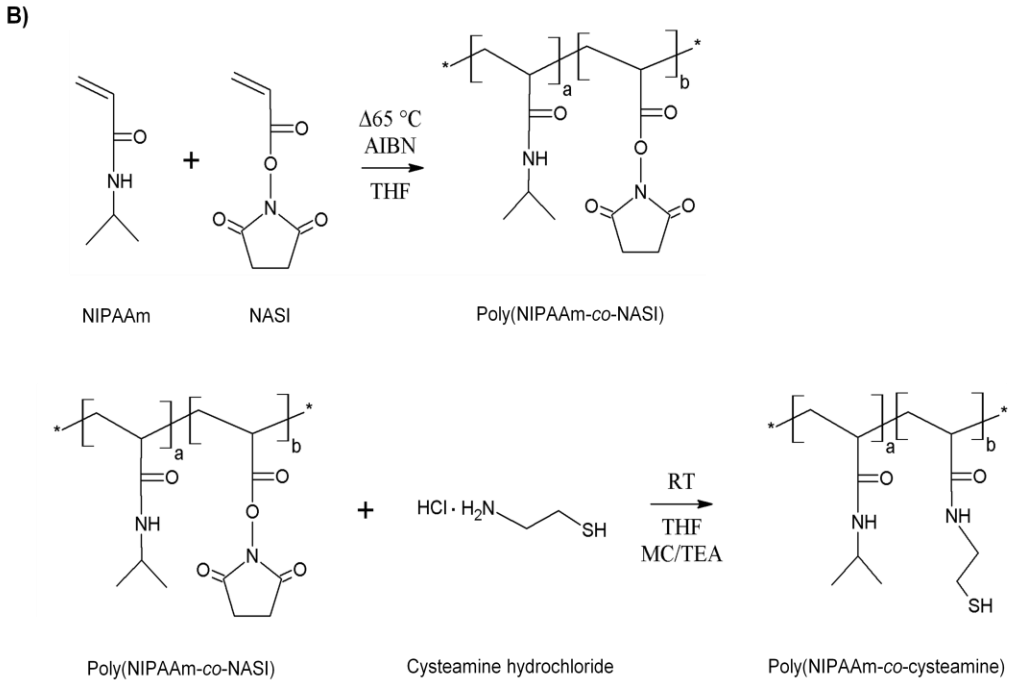

Figure 2.1 Free radical polymerization synthesis schemes of A) poly(NIPAAm-*co*-HEMA-acrylate) and B) poly(NIPAAm-*co*-cysteamine).

Synthesis of poly(NIPAAm-*co*-cysteamine) follows similar steps as that of poly(NIPAAm-*co*-HEMA-acrylate) and as reported in the literature (Robb, Lee, McLemore, & Vernon, 2007b). Briefly, NIPAAm and NASI were first dried at under vacuum for 24h and then dissolved in THF at a feed ratio of 98:2. The solution was nitrogen bubbled for 15 min and AIBN was added. The reaction was left for 16h at 65°C, under nitrogen. Poly(NIPAAm-*co*-NASI) was obtained after precipitation in excess diethyl ether, filtration and drying. For replacement and conjugation of cysteamine, 18g of poly(NIPAAm-*co*-NASI) and 0.524g of cysteamine hydrochloride (2 equiv per NASI group) were dried separately under vacuum at room temperature for 24h to minimize water presence. Poly(NIPAAm-

co-NASI) was then dissolved in THF while cysteamine chloride was dissolved in anhydrous MC. Two milliliters of TEA was added to the cysteamine chloride flask to assist in deprotecting hydrochloride. Once dissolved, the solutions of both flasks were combined using a double-tip needle under nitrogen and allowed to stir for 24h. The polymer solution was then precipitated in excess diethyl ether, filtered, and dried. The polymer was dialyzed for 5 days (at 4°C against 3,500 MWCO) in distilled water containing a solution of 5mM HCl (0.33mL HCl for 4L of water) to prevent disulfide bonding and 1 day in distilled water alone. After undergoing dialysis, the polymer solution was frozen and lyophilized. The copolymerization scheme for the synthesis of poly(NIPAAm-*co*-cysteamine) can be seen in Figure 2.1B. To form the gel, the synthesized copolymers were mixed stoichiometrically, with physical and chemical gelation occurring as indicated in Figure 2.2.

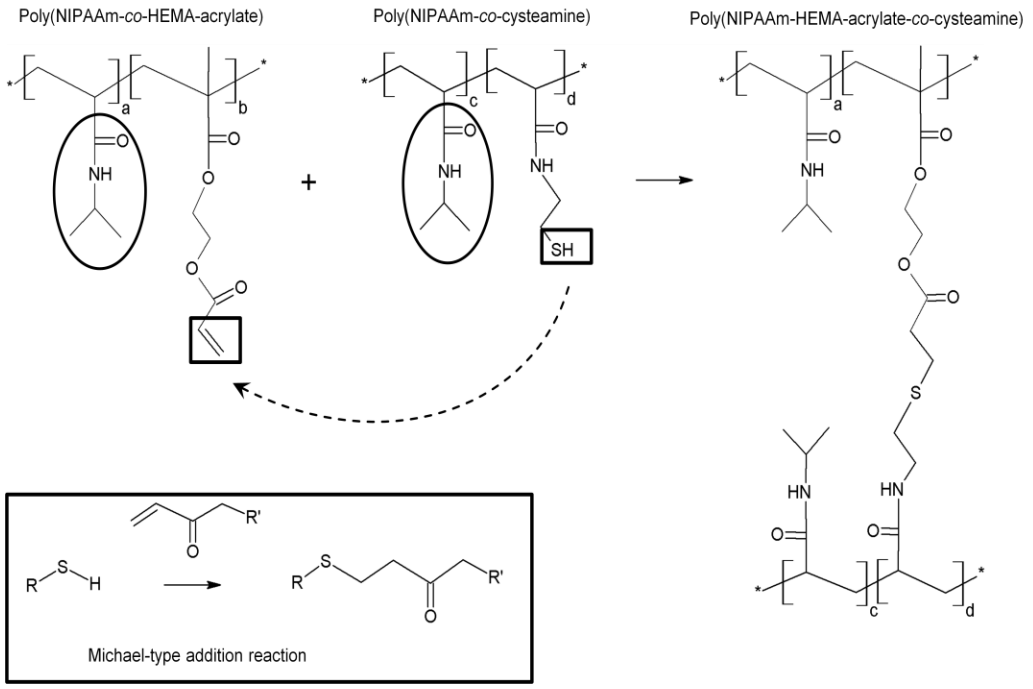

Figure 2.2 Demonstration of the two forms of gelation present upon mixing of poly(NIPAAm-*co*-HEMA-acrylate) and poly(NIPAAm-*co*-cysteamine); with chemical gelation taking place through a Michael-type addition reaction and physical gelation occurring at temperatures above the LCST.

2.2.3 ^{1}H Nuclear Magnetic Resonance Spectroscopy (^{1}H NMR)

^{1}H NMR measurements were made using a Varian Gemini-400 spectrometer operating at 400 MHz in Fourier-transform mode. Samples were dissolved in D_2O and TMS was used as the standard.

2.2.4 Fourier Transform Infrared Spectroscopy (FTIR)

The chemical composition of the synthesized copolymers was determined using FTIR (Thermoelectron Nexus 470). ATR-FTIR was conducted on small

pieces of the synthesized copolymers, enough to cover the diamond ATR crystal. Number of scans was set at 60.

2.2.5 Differential Scanning Calorimetry (DSC)

The thermal properties of the polymers were determined by measuring their lower critical solution temperature (LCST) using a CSC 4100 multicell differential scanning calorimeter. Samples were prepared with 5 wt% polymer solutions dissolved in 0.1M PBS at pH 7.4. Scans were run from 0 to 80°C at a scan rate of 1°C/min and in triplicates.

2.2.6 Cloud Point

For further investigation of the thermal properties and the LCST values of the copolymers, cloud point was conducted by dissolving each copolymer at 1 wt% in 0.1M PBS, pH 7.4 (n = 3). The samples were placed in a water bath which gradually increased the water temperature from 0 to 31°C and measurements were taken at 1°C intervals. However, only values from 8 to 22°C were recorded for poly(NIPAAm-*co*-HEMA-acrylate) and 20 to 31°C for poly(NIPAAm-*co*-cysteamine) since the excluded data remained constant. At each specific degree, 1mL of each copolymer sample was placed in a cuvette and its % transmission was measured using a UV spectrophotometer at 500nm (Ultrospec 3000, Pharmacia Biotech). Measurements were repeated 3 times for each copolymer at each degree. The reference point was set for each copolymer by using clear solutions of each.

2.2.7 Free Thiol Determination

To determine the content of free thiols present in the poly(NIPAAm-*co*-cysteamine) copolymer, Ellman's method was conducted (Ellman, 1958). To do so, polymer samples were dissolved at 1mg/mL in 0.1M PBS, pH 7.4 and 10mM DTNB [5,5'-dithiobis-(2-nitrobenzoic acid)] solution was added. For each 0.5mL of the copolymer solution, 0.1mL of DTNB was added. Absorbance was measured at 415nm using a FLUOstar Omega microplate reader (BMG Labtech), with n = 4. A cysteine calibration curve of thiol content vs absorbance was used to evaluate thiol content.

2.2.8 Molecular Weight and Polydispersity

The molecular weight and polydispersity index of the synthesized copolymers were determined using gel permeation chromatography (GPC) in conjunction with static light scattering (Wyatt Minidawn, Santa Barbara CA). GPC (Shimadzu, micro-styragel HR-4 and 6 columns) was performed on the copolymers using THF as the mobile phase and a flow rate of 0.8mL/min. The copolymer samples were prepared in THF at a concentration of 5mg/mL.

2.2.9 Gelation Properties

For analysis of the mechanical properties of the hydrogels, rheological studies were performed using a Physica MCR 101, Anton Paar rheometer, with a sandblasted measuring plate of a 25mm diameter and a gap of 0.5 mm. Measurements of the elastic (or storage) modulus (G') and the viscous (or loss)

modulus (G'') were conducted and gelation point was identified as the crosspoint of G' and G''. Samples were prepared for each copolymer by dissolving in 0.1M PBS, pH 7.4 at 30 wt%. The physical, chemical and physical-chemical gelation properties of the copolymers were analyzed, as well as the gel point. Time sweeps (4500 sec) of the copolymers mixed at 2, 3, and 4 minutes were performed at 37°C with a frequency of 1Hz, a normal force control of 1N and a controlled stress of 10Pa. The copolymers were mixed stoichiometrically at a ratio of 0.48: 1 (poly(NIPAAm-*co*-HEMA-acrylate): poly(NIPAAm-*co*-cysteamine)) in 3cc syringes via syringe couplers, at 2 strokes per minute, and 0.6mL of the solution was injected upon the rheometer plate. The copolymers were mixed at room temperature. The mixing of the components results in the chemical reaction between the acrylates of the poly(NIPAAm-*co*-HEMA-acrylate) and the thiols of poly(NIPAAm-*co*-cysteamine), and thus, cross-linking of the polymer network. Following gelation, frequency sweeps were conducted with a logarithmic ramp ranging from 0.01 to 100Hz at 20°C (for chemical gels) and 37°C (for physical gels), under similar conditions. For physical-chemical gelation, the copolymers were mixed as described above, loaded onto the rheometer plate (0.6mL) at 37°C, followed by measurements performed with time and frequency sweeps as described above.

2.2.10 Swelling Test

Each copolymer was dissolved at 15 wt% in 0.1M PBS, pH 7.4, mixed stoichiometrically at a ratio of 0.48: 1 (poly(NIPAAm-*co*-HEMA-acrylate):

poly(NIPAAm-*co*-cysteamine)) for 1 min at room temperature using 3cc syringes and a syringe coupler. The copolymer system was placed in a hot room at 37°C for 24h to allow for further curing. The cylinder-shaped gel was then removed from the syringe, cut into 1cm long pieces (total of 9 pieces) and lyophilized. Following lyophilization, the dried samples were weighed and then incubated in PBS, pH 7.4 vials at 4, 20 and 37°C. Samples (n = 3 for each copolymer) were weighed (after dabbing with wet towel) at time intervals of 30min, 1, 2, 4, 6, 12h, 1, 2, 3, 4, 6, 8, and 10 days. The degree of swelling was defined as $[100(W - W_0)/W_0]$, where W is the weight of the swollen gel and W_0 is the weight of the dried polymer.

2.2.11 Statistical Analysis

The means and standard deviations of the swelling data were analyzed using a two-sided *t*-test, with a level of significance set at $p < 0.05$.

2.3 Results and Discussion

2.3.1 Structural and Chemical Verification

The copolymers were synthesized through free radical polymerization. The advantage of synthesizing both components of the gelling system is that the properties of either copolymer can be modified to better suit the application needed. This is done by conjugating various comonomers to poly(NIPAAm). Poly(NIPAAm-*co*-HEMA) was first prepared through free radical polymerization,

and acryloyl chloride was then added and allowed to react with the terminal OH groups of the HEMA to result in poly(NIPAAm-*co*-HEMA-acrylate) (Figure 2.1A). The composition of the copolymer was determined from the ^{1}H NMR spectra. The mole ratio was calculated using the methyl protons (6H) ((C*H*$_3$)$_2$CHNHCO-) of NIPAAm and the methylene protons of the HEMA-acrylate (2H) (CH_2═CH-COOCH_2C*H*$_2$OCO), appearing at 1.1 and 4.1ppm, respectively, as demonstrated in Figure 2.3 (B. H. Lee et al., 2006).

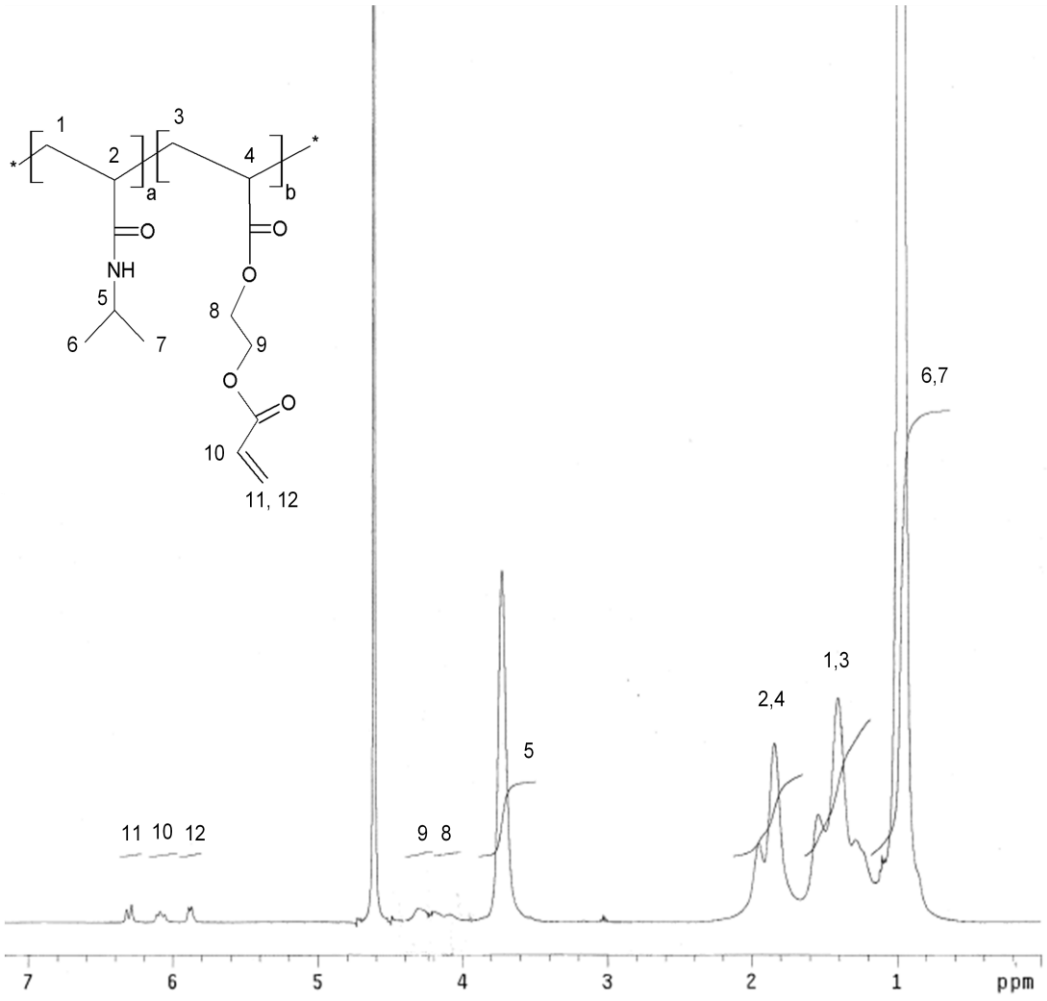

Figure 2.3 ^{1}H NMR spectrum of poly(NIPAAm-*co*-HEMA-acrylate), identifying the corresponding peaks of its structure.

The poly(NIPAAm-*co*-HEMA-acrylate) ratio was measured to be approximately 97:3 (NIPAAm:HEMA-acrylate). The decrease in the actual molar ratio compared to the feed molar ratio can be due to the variability in the copolymer composition combinations which can be obtained through free radical polymerization. Poly(NIPAAm-*co*-cysteamine) was prepared by free radical polymerization as well, with a poly(NIPAAm-*co*-NASI) intermediate. Cysteamine hydrochloride was dissolved in methylene chloride and triethylamine was added to deprotect hydrochloride and allow the reaction to proceed. The cysteamine then performed a nucleophilic substitution on the carbonyl group of the NASI, allowing the replacement of the NASI, a good leaving group, with cysteamine, to result in the final product poly(NIPAAm-*co*-cysteamine) (Figure 2.1B). The composition of this copolymer was similarly analyzed using ^{1}H NMR. The mole ratio was calculated using the methyl groups (6H) ((CH_3)$_2$CHNHCO-) of NIPAAm and the methylene protons (4H) (NHCH_2CH_2SH) of cysteamine, appearing at 1.1, 3.25, and 2.55ppm, respectively, as shown in Figure 2.4. The mole ratio was determined to be about 99:1 (NIPAAm:cysteamine). The mole ratio was also evaluated through Ellman's method.

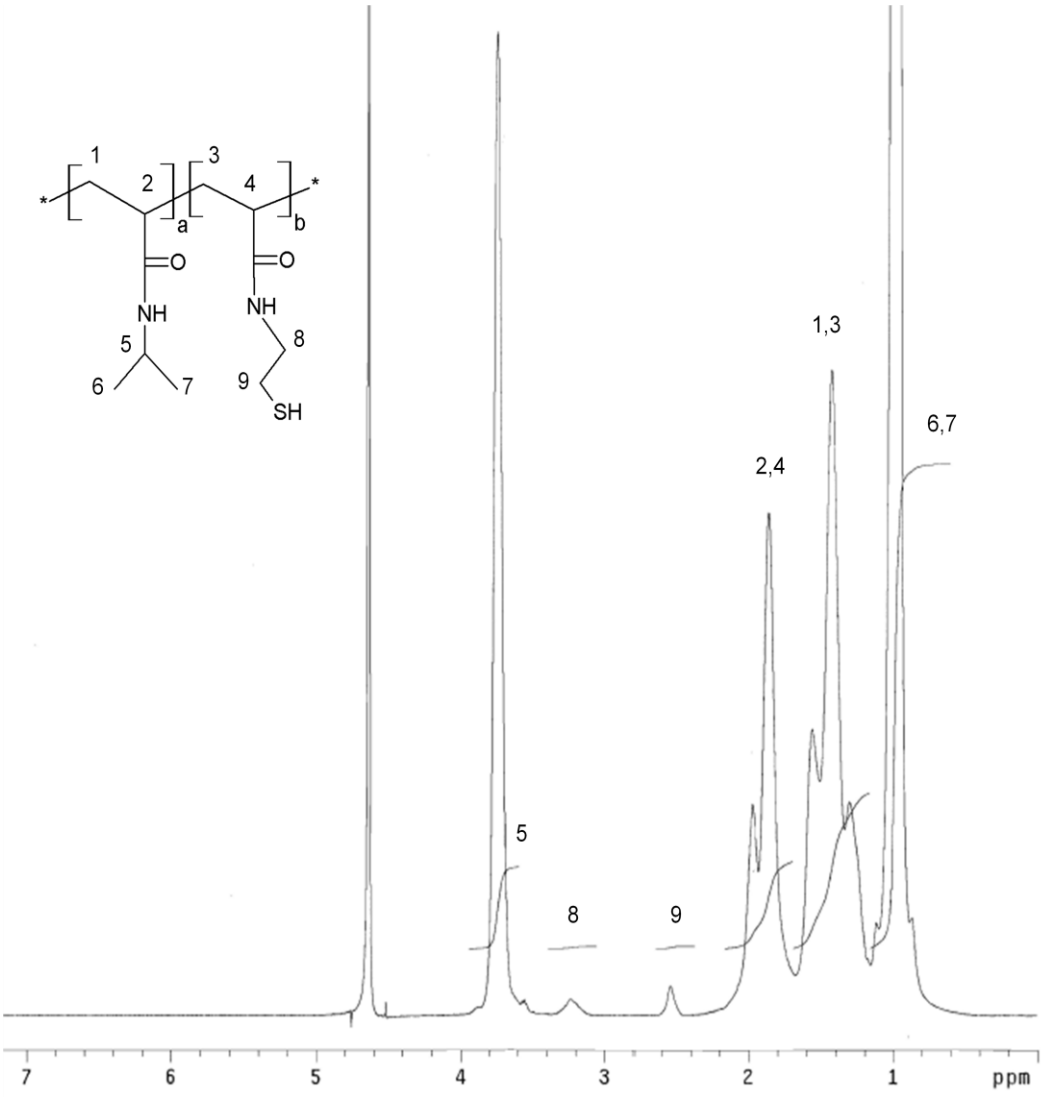

Figure 2.4 ^{1}H NMR spectrum of poly(NIPAAm-*co*-cysteamine), with labels of the respective H atoms.

The chemical composition of each copolymer was verified through ^{1}H NMR and FTIR. As seen in Figure 2.3, the ^{1}H NMR results of poly(NIPAAm-*co*-HEMA-acrylate) show distinctive peaks at positions 4.1 and 4.3ppm, indicative of the methylene protons between the ester groups. The peak present at 5.9, 6.1 and 6.3ppm represent the protons on the terminal vinyl. The solvent peak for D_2O is

observed at 4.79ppm. The remaining peaks on the spectra show the protons representative of the poly(NIPAAm) structure. As can be noticed, the peak of the HEMA-acrylate protons have much smaller amplitudes than the protons of poly(NIPAAm) due to the larger amount of NIPAAm in the copolymer compared to HEMA-acrylate. The poly(NIPAAm-*co*-HEMA-acrylate) structure was also verified through FTIR, as seen in Figure 2.5.

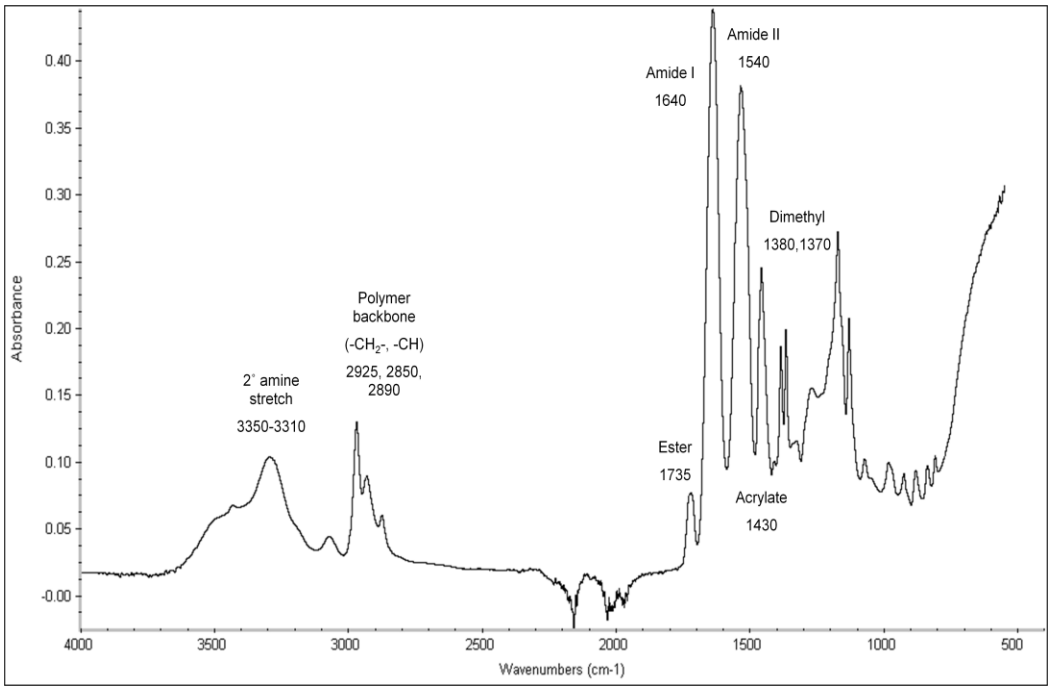

Figure 2.5 FTIR spectrum of poly(NIPAAm-*co*-HEMA-acrylate), verifying the structural composition of the copolymer.

The main observations are the ester peak at 1735 cm^{-1} and the acrylate peak at 1430 cm^{-1} (Silverstein & Webster, 2006). The pair of peaks at 1640 and 1540 cm^{-1}

is characteristic of amide stretching (Amide I) and bending (Amide II) bands; the former representing the C═O stretch of the amide and the latter demonstrating N–H bending and C–N stretching of the amide (Silverstein & Webster, 2006). The doublet seen at 1370 and 1380 cm^{-1} denotes the geminal dimethyl group of the NIPAAm structure. The peaks generated between 2850 and 3000 cm^{-1} symbolize the –CH– and $–CH_2–$ stretching of the polymer backbone, and at 1470 cm^{-1} the $–CH_2–$ bending. The ^1H NMR spectra of poly(NIPAAm-*co*-cysteamine), shown in Figure 2.4, has distinguishing peaks for the methylene protons of the cysteamine at 2.5 and 3.2ppm. The D_2O solvent peak is also seen at 4.79ppm. Thiols have high variability in the S–H absorbance in ^1H NMR due to the proton exchange which occurs and causes the proton to go through various environments during the exchange, thus resulting in absorption at a wide range of frequencies and field strengths. It is therefore difficult to observe a thiol peak in this ^1H NMR spectra.

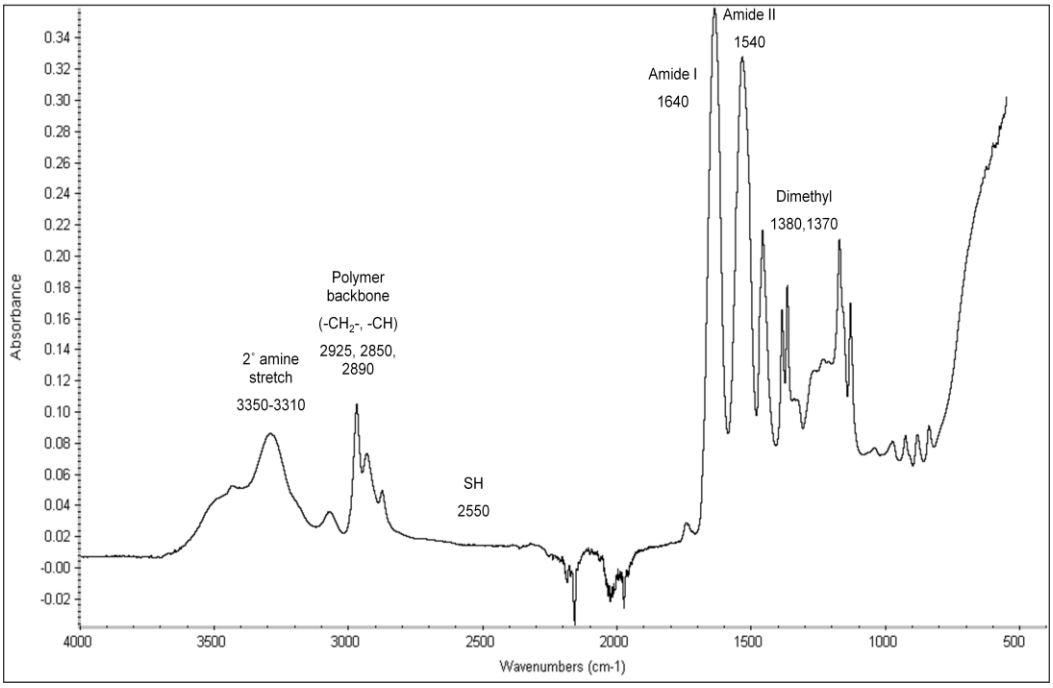

Figure 2.6 FTIR spectrum of poly(NIPAAm-*co*-cysteamine), demonstrating its chemical structure.

Similarly, the thiol peak in the FTIR spectra (Figure 2.6) of poly(NIPAAm-*co*-cysteamine) should emerge at 2550 cm^{-1} (Silverstein & Webster, 2006), however, no detection is seen at that location, not only because the S–H bond is weak, but also due to the lower molar ratio of cysteamine to NIPAAm in the copolymer. The remaining peaks in the FTIR spectra are identical to those seen in the spectra of poly(NIPAAm-*co*-HEMA-acrylate) since they correspond to the NIPAAm structure. The negative peaks found between 1900 and 2300 cm^{-1} in both spectra result from the background effect.

2.3.2 Thermal Analysis

Analysis of the thermal properties of the synthesized copolymers is important to understanding their phase transition behaviors as well as determining at what temperature this phase transition occurs and if it is feasible to their potential applications. The LCST of poly(NIPAAm-*co*-HEMA-acrylate) was determined through DSC and cloud point (50% transmission). Using DSC, the copolymer LCST was found to be 29.1°C. This indicates a lower LCST value due to the hydrophobic nature of the acrylate group. However, the LCST value obtained from cloud point was around 15°C, as shown in Figure 2.7.

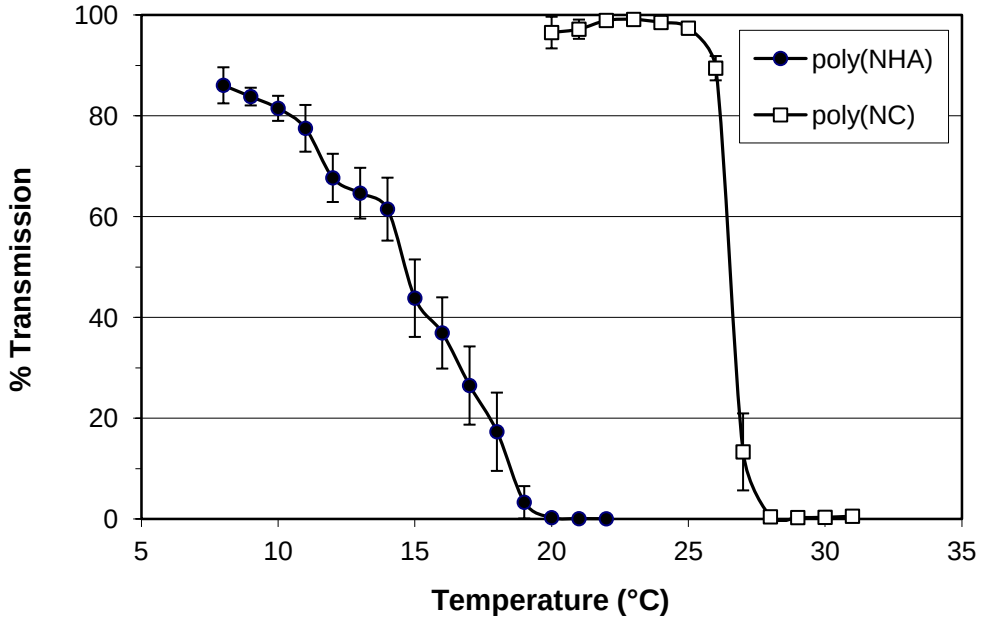

Figure 2.7 Cloud point data of both copolymers, illustrating a gradual change in the phase transition temperature of poly(NIPAAm-*co*-HEMA-acrylate), abbreviated as poly(NHA), whereas poly(NIPAAm-*co*-cysteamine), or poly(NC), has a sharp drop indicating its transition (n = 3); cloud point was defined at 50% transmission.

Although it is different from the value acquired by DSC, it is mainly because this copolymer forms an opaque solution at low temperatures. When measuring light transmission with the UV spectrophotometer, the opacity of the copolymer solution leads to a gradual but early drop in % transmission. There is also some variability between each 1°C interval and between each replica due to its unstable opacity throughout the run of the experiment. Looking at the shape of the DSC curve for this copolymer in Figure 2.8, it is important to note the broader peak, with an increasing slope starting around 10°C, which corresponds with the gradual decrease in % transmission in cloud point. The early onset of its phase transition and opacity suggests that poly(NIPAAm-*co*-HEMA-acrylate)'s hydrophobicity leads to some chains collapsing earlier than others, even at temperatures below the gelation temperature (B. H. Lee & Vernon, 2005). It can also be noted that the area near the sharp peak is indicative of the phase separation of the high molecular weight chains of the copolymer, whereas the broader areas leading away from the peak can be associated with the shorter chains of the copolymer (Schild & Tirrell, 1990b). The LCST of poly(NIPAAm-*co*-cysteamine) was determined to be 30.4°C with DSC. Through cloud point, the observed LCST for this copolymer was around 27°C. Similarly, the cloud point LCST value is slightly different than those obtained through DSC, but the difference here is much smaller than that with the poly(NIPAAm-*co*-HEMA-acrylate) copolymer. As can be seen in the cloud point curve of poly(NIPAAm-*co*-cysteamine) (Figure 2.7), there is a sudden and more pronounced drop in % transmission at a particular temperature, which here is 27°C. This observation

displays an abrupt change in the opacity of the copolymer solution, indicating an immediate phase transition from a clear solution at lower temperatures, into an opaque and more viscous compound at temperatures beyond 27°C. This drastic change corresponds with the DSC endotherm acquired for this copolymer, seen in Figure 2.8.

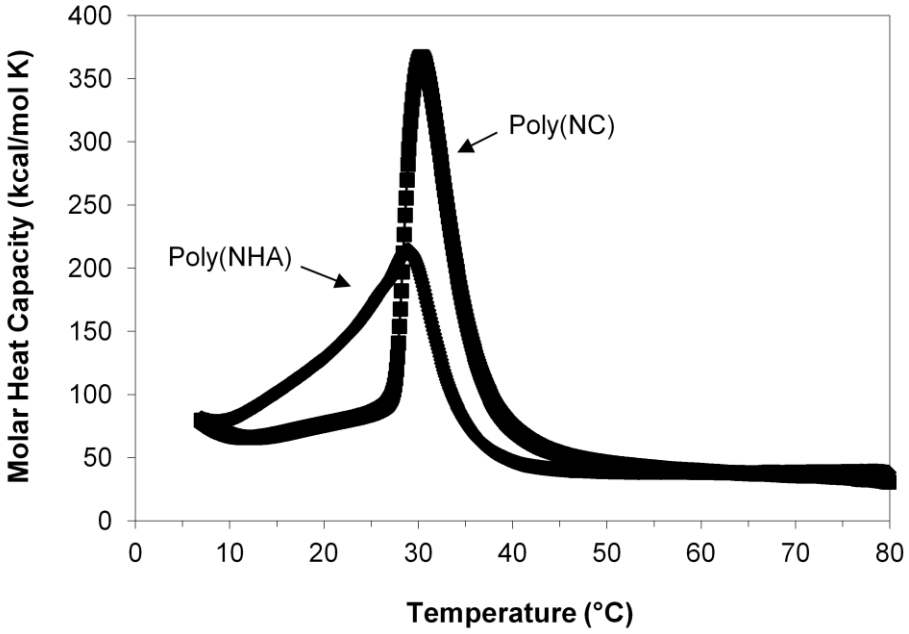

Figure 2.8 DSC curves of the copolymers, with the peaks indicating their LCST point.

The endotherm peak for poly(NIPAAm-*co*-cysteamine) is sharper and narrower in shape than that displayed by poly(NIPAAm-*co*-HEMA-acrylate). The different character of the poly(NIPAAm-*co*-cysteamine) DSC peak indicates the more homogeneous composition of this copolymer, suggesting more of a simultaneous collapse of the polymer chains within a narrower range of temperatures. It has

been noted that the NIPAAm homopolymer has a sharp and narrow DSC peak; however, copolymers show a broader peak. Additionally, an increase in the comonomer content also results in a broader peak (Y. H. Bae, Okano, & Kim, 1991). Thus, the observed broader peak of poly(NIPAAm-*co*-HEMA-acrylate) is justified by the larger content of the (HEMA-acrylate) comonomer to NIPAAm, compared to the lesser content of cysteamine comonomer to NIPAAm. It is also important to note that poly(NIPAAm-*co*-HEMA-acrylate) has a lower molar heat capacity than poly(NIPAAm-*co*-cysteamine), averaging 1900 ±194 kcal/molK and 2470 ± 57 kcal/molK, respectively. With the former copolymer having a smaller molar ratio of NIPAAm than the latter, it therefore requires less energy to break the hydrogen bonds formed between the water molecules and NIPAAm (Robb, Lee, McLemore, & Vernon, 2007a).

2.3.3 Mechanical and Gelation Properties

The mechanical properties of a hydrogel are highly important for the potential application it is designed for. Physical gels are characterized by chains which physically cross-link or entangle, resulting in a network. How these non-covalent cross-links form is not fully understood due to the various interactions which may cause the chains to collapse. These forces include, but are not limited to, dipole-dipole, van der Waals, hydrophobic and hydrogen bonding (Kavanagh & Ross-Murphy, 1998). Since these chains can diffuse through the network, even though they are partially connected to the greater network structure, an internal fluidity is present in the system. Due to these characteristics, physical gels tend to

experience creep flow when exposed to external forces for a long period of time (F. Tanaka & Edwards, 1992a). This may in turn render the gel too weak and result in the undesirable leaking of the gel *in vivo* (Ramakrishna, Mayer, Wintermantel, & Leong, 2001). A chemical gel differs from a physical gel due to the covalent cross-links formed within the gel structure, which are dependent on the reactivity ratios of the monomers and cross-linkers present (Norisuye et al., 2002). Due to the inhomogeneous cross-linking network formed, chemical gels reach an equilibrium swelling when in aqueous solutions. The degree of swelling is dependent on the cross-link density of the hydrogel network, as well as the concentration, molecular weight and degree of substitution (Hiemstra, van der Aa, Zhong, Dijkstra, & Feijen, 2007; Hoffman, 2002). High swelling can be particularly difficult to manage *in vivo* and thus would need to be controlled accordingly. An ideal hydrogel would consist of a combination of a physical gel and a chemical gel. By merging the two kinds of gels, one would anticipate a reduction in the viscoelastic flow seen with physical gels under constant stress and a decrease in the swelling experienced by chemical gels. A physical-chemical gel would overall improve the mechanical properties of the resultant hydrogel.

To investigate the mechanical properties of the hydrogels and develop a comparison of the physical, chemical, and physical-chemical gels, rheology was utilized, as demonstrated in Figure 2.9. Poly(NIPAAm-*co*-cysteamine) and poly(NIPAAm-*co*-HEMA-acrylate) each are physical gels and can undergo transition from a solution to a gel at their respective LCSTs. Thus, each copolymer was placed on the rheometer plate and allowed to gel at 37°C, prior to

the frequency sweep. As can be noted, poly(NIPAAm-*co*-cysteamine) shows signs of viscoelastic flow as well as a weak gel under constant, low frequency stress. Similarly, poly(NIPAAm-*co*-HEMA-acrylate) illustrates a loss in strength, which is witnessed by purely physical gels at low frequencies. There appears to be some disturbance in the points measured at frequencies above 1Hz. This may be due to the slight shrinking which this copolymer experiences and thus results in expulsion of some water, allowing the rheometer to record the behavior of the water layer, sporadically. Poly(NIPAAm-*co*-HEMA-acrylate) also attains higher values of *G'* than poly(NIPAAm-*co*-cysteamine). This behavior can be attributed to the more hydrophobic nature of this copolymer, due to the presence of acrylates. Hydrophobic components have been used to increase the mechanical stability of gels (Feil, Bae, Feijen, & Kim, 1992). To observe the chemical gel, the copolymers were mixed at room temperature, allowing the chemical reaction to occur and form cross-links, and the gel was deposited on the rheometer plate at 20°C. The data obtained for the chemical gel demonstrates less viscoelastic flow at low frequencies. Nonetheless, the solely chemical gel portrays characteristics of a weak hydrogel, since it never surpasses *G'* values higher than 1000 Pa. To observe the mechanical properties of the physical-chemical gel, the copolymers were first mixed at room temperature and then injected onto the rheometer plate at 37°C. In contrast to the purely physical and purely chemical gels, the physical-chemical gel reveals less viscoelastic flow under constant, low frequency stress and higher *G'* values, ranging from 10,000 to 100,000 Pa. Although a slight degree of water expulsion is noticed for the mixed system, water does not seem to

perturb the rheological measurements, as in the case of poly(NIPAAm-*co*-HEMA-acrylate), again demonstrating greater stability than seen with each copolymer independently. Thus, a stronger and more stable gel is formed due to the combined gelation mechanisms: a physical gel at higher temperatures and a chemical gel through the Michael-type addition reaction as the copolymers are mixed.

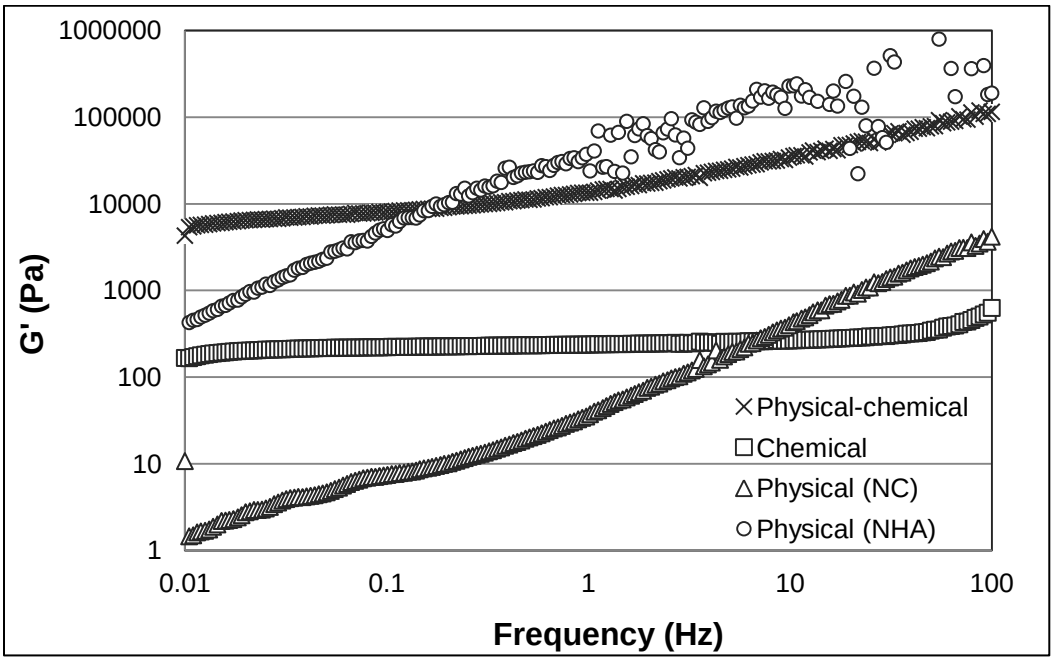

Figure 2.9 Frequency sweeps performed on a rheometer for the purely physical gels, poly(NIPAAm-*co*-HEMA-acrylate) at 37°C (○) and poly(NIPAAm-*co*-cysteamine) at 37°C (Δ); the chemical gel, the mixed copolymers at 20°C (□), as well as the physical-chemical gel, the mixed copolymers at 37°C (×).

The time needed for the copolymers to undergo transition from solution to gel is important, especially when injected *in vivo.* Various factors can have an

effect on the gel point, including concentration, mixing time, pH, etc. Gel point is defined as the crosspoint of *G'* and *G''*. As the material becomes a gel, behaving as an elastic solid, the elastic modulus (*G'*) becomes more dominant while the viscous modulus (*G''*), which represents the viscous component of the hydrogel, is dominant in the liquid phase. Here, rheology was also utilized to investigate the time to gel point when the copolymers are combined at different mixing times. This was accomplished by mixing the two copolymers at mixing times of 2, 3 and 4 minutes, followed by deposition and exposure of the solution to a constant oscillatory stress and frequency on the rheometer plate. As can be seen in Figure 2.8, when the copolymers were mixed for 4 minutes, gel point was reached after 1500 seconds, or 25 minutes. However, as the mixing time was decreased to 3 and 2 minutes, time to gel point increased to 2010 and 2310 seconds, respectively. The trend of a decrease time to gel point with an increase in mixing time has been observed in past studies (B. H. Lee et al., 2006). It is obvious that as the copolymers are mixed for a longer period of time, the mixture of the two copolymers becomes more homogeneous and the reaction takes place for a longer period of time before being placed on the rheometer plate, which in turn provides more opportunities for chemical cross-links to form. Thus, less time is needed to attain gel point since the mixture has undergone chemical gelation to a larger extent than when mixed for a lesser amount of time. It can also be noted that with longer mixing, higher *G'* values are reached. This behavior can also be attributed to the more homogeneous solution and the greater extent of chemical cross-linking taking place.

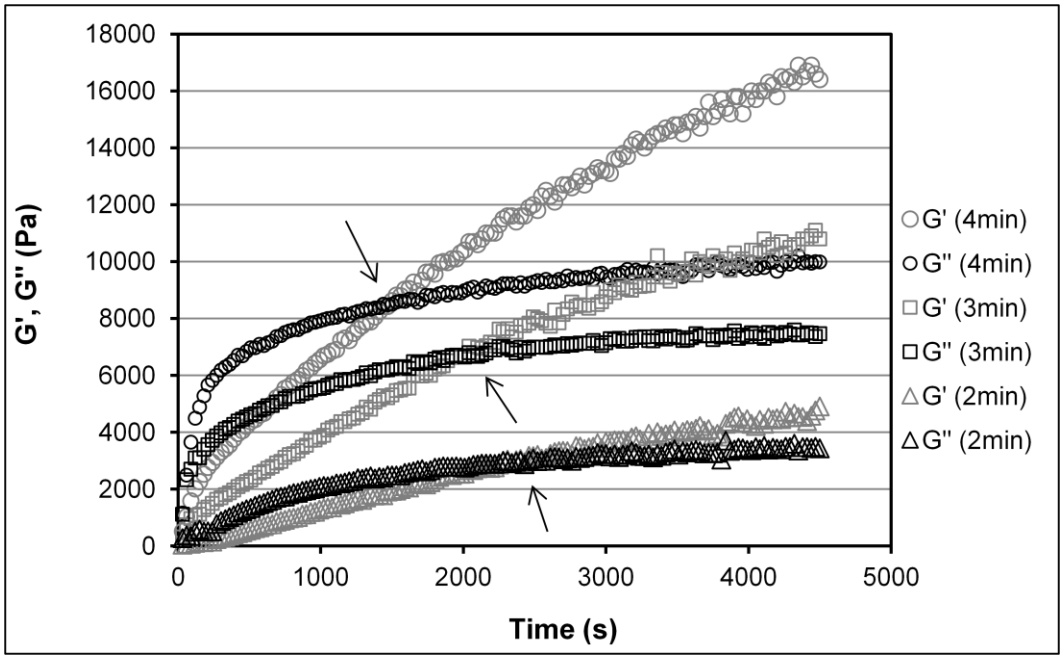

Figure 2.10 Time sweep done on physical-chemical gels with different mixing times (2, 3, and 4 minutes). Gel points of the various gels (defined as the crossover of *G'* and *G''*) are indicated by arrows, demonstrating a faster achievement of gel point with a longer period of mixing.

2.3.4 Swelling Properties

As previously mentioned, controlling the swelling behavior of the hydrogel is important, especially for biomedical applications. Previous studies on the swelling properties of copolymers of poly(NIPAAm) have reported a decrease in the swelling ratio with an increase in temperature (Feil et al., 1992; Matsuo & Tanaka, 1988; T. Tanaka, Sato, Hirokawa, Hirotsu, & Peetermans, 1985). A similar trend is observed here with the swelling study of the physical-chemical gel (poly(NIPAAm-HEMA-acrylate-*co*-cysteamine)). When the gel pieces were

placed at 4°C, the largest degree of swelling was experienced, reaching a swelling ratio of about 800% after 48 hours, as seen in Figure 2.11.

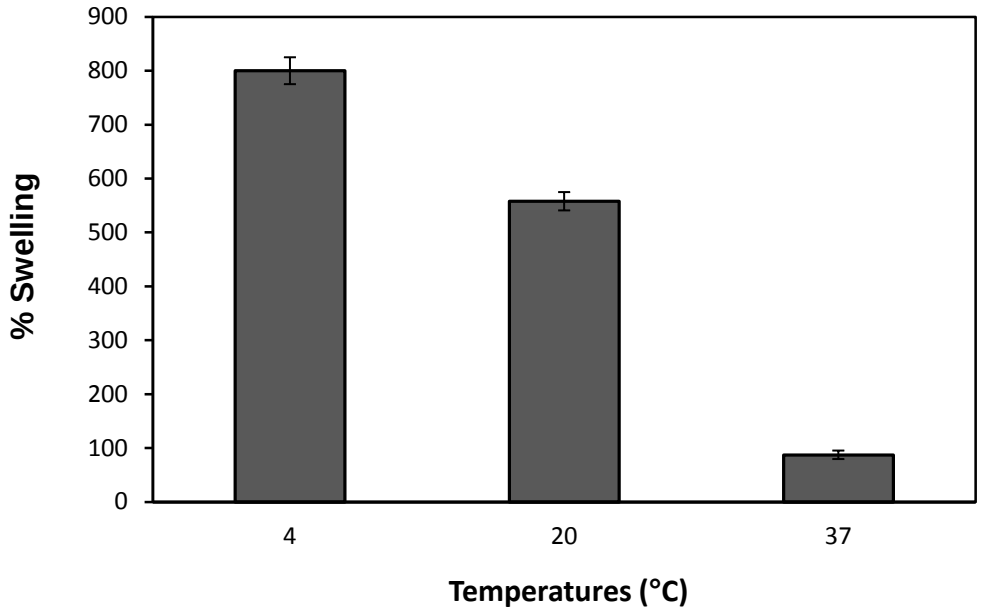

Figure 2.11 Swelling of the physically and chemically gelled system at 4°C, 20°C and 37°C, after 48 hours. The observed trend shows a decrease in the percent swelling with an increase in temperature, (n = 3 for all).

At 20°C, the swelling ratio at 48 hours decreased to about 558%, whereas the least amount of swelling was witnessed at 37°C, with a swelling ratio of 87%. The decrease in swelling with an increase in temperature, particularly above the LCST, can be explained by the physical association of NIPAAm chains at higher temperature. At 4°C and 20°C, the gel samples are mainly chemically cross-linked, since the temperature is below the LCST, allowing for larger degrees of

swelling. At 37°C, physical gelation occurs in addition to chemical gelation, resulting in more cross-links in the polymer network and thus, less swelling. The swelling study was conducted for 10 days, with the 2, 6 and 10 day intervals shown in Figure 2.12. It was determined that there is no significant difference between the 2, 6 and 10-day data points at each temperature ($p > 0.05$). Thus, no significant increase or decrease in the swelling ratio was recorded, over the 10-day duration, suggesting that the samples had already reached equilibrium swelling after 2 days.

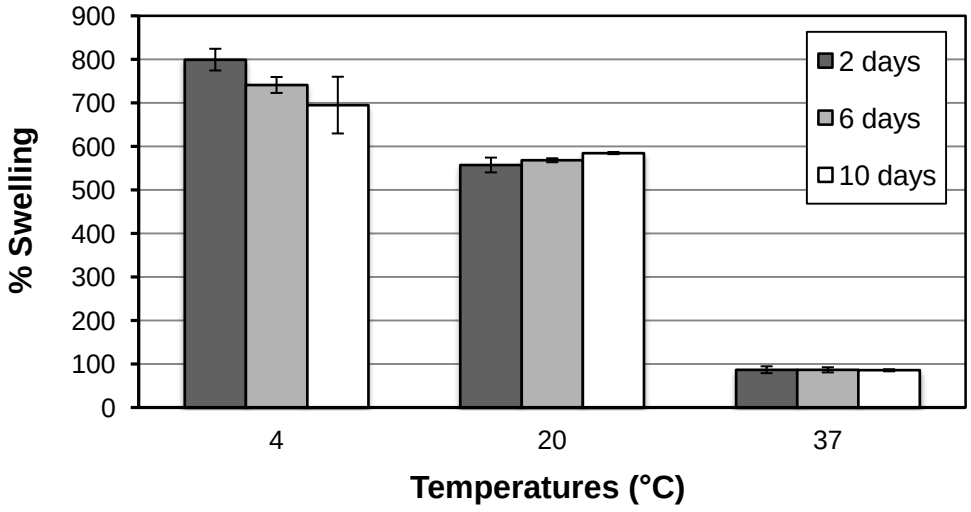

Figure 2.12 Swelling of the physical-chemical gel after 2, 6 and 10 day-intervals, at different temperatures (4°C, 20°C and 37°C), (n = 3 for all).

Although this particular NIPAAm-based physical-chemical gel, employing poly(NIPAAm-*co*-HEMA-acrylate) with poly(NIPAAm-*co*-cysteamine), has demonstrated feasible properties, when compared to the use of

poly(NIPAAm-*co*-HEMA-acrylate) with QT by Lee et al. or poly(NIPAAm-*co*-cysteamine) with PEGDA by Robb et al., some strengths and weaknesses are uncovered. Whereas *G'* values on the order of millions of Pa were achieved with Robb's material, the highest *G'* values reached here are in the hundreds of thousands of Pa, indicating a slightly weaker gel. Likewise, although creep was reduced in this system through the use of the simultaneous physical and chemical cross-linking, Robb and Lee showed greater reduction in creep at low frequencies. Difference in mechanical strength and creep resistance between the previous studies and the work here can be due to the different molecular weights of the copolymers used in the gelling system. Nonetheless, this polymer gelling system has shown compatible thermal properties, as well as plausible mechanical and swelling characteristics. The advantage with this system is the ability to alter its properties through synthesis adjustments, whether manipulating solvents, comonomers or molar feed ratios.

2.4 Conclusions

A simultaneous physical and chemical gelling polymer system was developed by synthesizing thiol-functionalized poly(NIPAAm-*co*-cysteamine) and vinyl-terminated poly(NIPAAm-*co*-HEMA-acrylate). The copolymers underwent a phase transition at their respective LCSTs, with a difference in LCST presented by the hydrophobic/hydrophilic elements of each copolymer as well as the molar feed ratios at which each copolymer was synthesized. Physical gelation occurred through the temperature sensitivity of poly(NIPAAm), whose chains

collapse and entangle at the LCST, while chemical gelation took place through a Michael-type addition reaction between the thiols and the vinyls, forming a covalent cross-link. The combination of both gelation systems allowed for a reduction in the frequency response experienced at constant, low frequency stress, as well as an increase in strength, when compared to solely physical and solely chemical gels. Rheological time measurements also illustrated that gel point is dependent on mixing time. As the copolymers were mixed longer, more chemical cross-links could be formed, resulting in a shorter time to gelation. The swelling behavior of the physical-chemical gel was shown to be dependent on temperature; showing a decrease in the percent swelling with an increase in temperature, mainly due to the association of the NIPAAm chains. As the swelling of the gel samples was monitored for a longer duration than 48 hours, no significant difference was observed in the swelling behavior with respect to time. With improved features, this physical-chemical gel could potentially be used *in vivo* for various biomedical applications, specifically for endovascular embolization of aneurysms or arteriovenous malformations.

CHAPTER 3

ON THE PHASE TRANSITION OF POLY(N-ISOPROPYLACRYLAMIDE) AND COPOLYMERS: THERMAL AND X-RAY SCATTERING ANALYSIS

3.1 Introduction

Temperature-responsive materials have been widely used over the last decades in all ranges of science and engineering. Because of their response to temperature as a form of stimuli, a change in the properties of these materials can easily be triggered by increasing or decreasing the temperature of the environment. One particularly popular thermoresponsive material is poly(N-isopropylacrylamide), abbreviated as poly(NIPAAm). What has long been known about poly(NIPAAm) is that in an aqueous environment and in appropriate concentrations, it undergoes a phase transition from a solution to a gel as temperature is increased above a specific threshold. This phase transition threshold is termed the lower critical solution temperature (LCST) and occurs around 31°C (Heskins & Guillet, 1968). Common knowledge of the phase transition behavior entails that at temperatures below its LCST, poly(NIPAAm) is hydrophilic and soluble in the aqueous environment, remaining in solution state. As the temperature is increased above its LCST, poly(NIPAAm) becomes hydrophobic, expelling water molecules which facilitates the transition to a gel. Not only is this sol-gel phase transition unique, but it also can be manipulated. The LCST of poly(NIPAAm) can be altered with the conjugation of comonomers.

With the addition of hydrophilic monomers, the LCST can be increased. Feil et al. noted that an increase in LCST occurred with the conjugation of acrylic acid, (diethylamino)-ethyl methacrylate and acrylamide and that the LCST was also increased with increasing comonomers content (Feil, Bae, Feijen, & Kim, 1993a). Similarly, Vernon et al.(2000) noticed that the higher the content of acrylic acid that was conjugated to poly(NIPAAm), the higher the LCST was raised, reaching 39.1°C with almost 2 mol% of acrylic acid (Vernon et al., 2000). On the other hand, conjugation of hydrophobic comonomers to poly(NIPAAm) results in a decrease in the LCST. For example, when butyl methacrylate or propyl acrylic acid were conjugated onto poly(NIPAAm), the LCST was decreased, and similarly, the greater the amount of the hydrophobic comonomer, the greater the decrease in LCST (Feil, Bae, Feijen, & Kim, 1993a; Yin, Hoffman, & Stayton, 2006). Thus, poly(NIPAAm) has unique characteristics in that its phase transition temperature can easily be altered by copolymerization.

Due to its phase transition occurring around 31°C, poly(NIPAAm) has found a plethora of uses in various fields of science, particularly in fields involving biomedical applications. Because its LCST exists near physiological temperature (37°C), it has given it the advantage of being used *in vivo*. Poly(NIPAAm) is in solution state at room temperature, but once injected within the body, at a temperature higher than its LCST, it undergoes phase transition into a gel. Many studies have investigated using poly(NIPAAm) and its copolymers for biomedical applications. Combination of magnetic and thermoresponsive poly(NIPAAm) materials are on the rise. Magnetic hydrogel nanocomposites

based on poly(NIPAAm) and iron oxide have been investigated for remote heating for cancer treatment (Meenach, Anderson, Suthar, Anderson, & Hilt, 2009) and as magnetic resonance imaging contrast agents (Balasubramaniam et al., 2011). The thermoresponsive polymer has also been modified to contain or be coated magnetically for targeting and drug delivery (Guo, Yang, Wang, He, & Chen, 2006; Zhu, Kaskel, Ikoma, & Hanagata, 2009). Poly(NIPAAm) has also been used as a dual responsive material with pH dependence, either by conjugation with propylacrylic acid for delivery of angiogenic growth factors (Garbern, Hoffman, & Stayton, 2010) or as a semi-interpenetrating network with hyaluronic acid for therapeutic delivery (Santos, Alves, & Mano, 2010). Its temperature-sensitivity has also been combined with dependence on calcium content for drug and cell delivery (Kretlow, Hacker, Klouda, Ma, & Mikos, 2010); (Kretlow et al., 2010). Synthesized as shell cross-linked hybrid micelles (Wei et al., 2008), comb-shaped conjugates with hydroxypropyl cellulose (Xu et al., 2010) or in chitosan coated alginate beads (Shi, Alves, & Mano, 2008), poly(NIPAAm) can improve encapsulation efficiency and slow or sustain drug release rate. Surfaces modified with thin films of poly(NIPAAm) have been capable of tuning cell adhesion and detachment (Kong, Choi, Jeon, & Choi, 2009; Yu et al., 2010). Poly(NIPAAm) has also been encased in semiconductor quantum dots for specific targeting of growing neurons (GhoshMitra, Diercks, Mills, Hynds, & Ghosh, 2011), conjugated with methylcellulose to form a three dimensional extracellular matrix for cartilage tissue engineering (Sá-Lima, Tuzlakoglu, Mano, & Reis, 2011), thiol-terminated for intracellular triggered gene

and drug delivery upon reduction (Meng, Hennink, & Zhong, 2009), synthesized as a biodegradable, injectable hydrogel as a therapy to prevent remodeling of cardiac tissue after myocardial infaction (Fujimoto et al., 2009) and combined with graphene as sheets demonstrating high potency of killing cancer cells *in vitro* (Pan, Bao, Sahoo, Wu, & Li, 2011). These are just a few examples of recent studies using poly(NIPAAm), with many more novel applications underway or yet to be discovered.

Although poly(NIPAAm) has seen a diverse range of synthesis techniques and applications, the fascinating phenomenon of its phase transition and how it occurs is still widely debated. Heskins and Guillet first reported that there may be two different scenarios associated with the phase transition phenomenon. The first ascribes it to the association of the polymer molecules into larger aggregates due to the formation of intermolecular hydrogen bonds and nonpolar bonds (Heskins & Guillet, 1968). As the hydrogen bonds with water are broken, endothermic heat is released through the phase separation. The second case suggests that the polymer is more ordered in the solution state than in the collapsed state due to strong hydrogen bonds formed between water and the polymer. As temperature is increased, these hydrogen bonds become weaker making the solution unstable and causing the polymer to associate. Both may also be involved in the phase transition. Using a Flory-Huggins model, they noticed that the major factor leading to the phase transition is the entropy term which allows for the separation into two phases to be thermodynamically favored. Since then, various studies have been conducted on poly(NIPAAm) and its phase transition, to try to

elucidate how the event occurs. Schild and Tirrell noted that as precipitation of the polymer occurs above the LCST, the entropy of the system dominates over the enthalpy contribution to free energy, and the hydrophobic effect adds to the entropy domination. In their experiments, they observed different shapes and heights of calorimetric endotherms associated with different molecular weight distributions of poly(NIPAAm) (Schild & Tirrell, 1990a). Otake et al. also described the existence of cage-like structure of water molecules around the hydrophobic solute, resulting in the hydrophobic hydration of the polymer and allowing even nonpolar molecules to be soluble in water. As temperature is increased, the number of water molecules structured around the hydrophobic component decreases (Otake, Inomata, Konno, & Saito, 1990). Shibayama et al. have conducted several studies on the phase transition of this thermoresponsive polymer and were able to identify that 13 water molecules are released from the NIPAAm monomer unit but also that there are more water molecules which do not take part in the shrinking transition (Shibayama, Morimoto, & Nomura, 1994; Shibayama, Mizutani, & Nomura, 1996). In small angle x-ray spectroscopy (SAXS) studies performed by Dingenouts et al., it was similarly noticed that a poly(NIPAAm) shell on a core-shell particle shrinks in thickness as temperature is increased above LCST but that it does not fully associate since liquid-like fluctuations were still observed in the shrunken state (Dingenouts, Norhausen, & Ballauff, 1998). Wang et. al observed different stages which the polymer in coil form undertakes to reach the globule state with temperature increase. The coil forms a “crumpled coil” in which some clusters develop along the chain

backbone. This “crumpled coil” then further collapses into a molten globule and finally into a globule (X. Wang, Qiu, & Wu, 1998). Using infrared spectroscopy, Maeda et al. examined the shift in the C-H bands of the isopropyl groups on poly(NIPAAm) which indicated dehydration of hydrophobic groups during phase transition, but also noted that only a small amount of C=O groups become dehydrated above the LCST (Maeda, Higuchi, & Ikeda, 2000). Recently, studies have been conducted to analyze the structure of water molecules around the polymer and the changes that occur through the phase transition. Using dielectric relaxation techniques, Ono et al. found the presence of 11 water molecules per poly(NIPAAm) monomer unit and that 2 of these water molecules hydrate the amide through hydrogen bonding, leaving the remaining 9 water molecules to form hydrogen bonds amongst themselves and to the 2 water molecules (Ono & Shikata, 2006). This phenomenon only occurred in poly(NIPAAm), and not its monomer only, concluding that polymerization is necessary for the phase transition (Ono & Shikata, 2007). With molecular dynamics simulations, Deshmukh et al. calculated the radius of gyration to be around 16.6Å below the LCST and 10.2Å above the LCST, while also noticing a decrease in the number of water molecules (from 175 to 145 per poly(NIPAAm) chain) with an increase in temperature, indicating a coil-to-globule transformation (Deshmukh, Sankaranarayanan, & Mancini, 2012). This event was seen to take place only in poly(NIPAAm) chains with 30 mers or more (Deshmukh, Sankaranarayanan, Suthar, & Mancini, 2012). The scientific community has thus made many contributions to better understand the phase transition of this thermoresponsive

polymer, yet still more has to be uncovered with regards to various factors that can impact this polymer.

Our lab has conducted different studies employing poly(NIPAAm) and its copolymers for biomedical applications. Poly(NIPAAm) was conjugated with thiol and acrylate groups for dual gelling mechanisms via physical temperature sensitivity and chemical Michael-addition reaction for use as embolic agents for aneurysm occlusion (Bearat, Lee, Valdez, & Vernon, 2011; Bearat, Lee, & Vernon, ; Bearat, Preul, Bichard, & Vernon, ; B. H. Lee et al., 2006; Robb, Lee, McLemore, & Vernon, 2007a). Poly(NIPAAm) was conjugated with acrylic acid to investigate gel strength and viscosity for arteriovenous malformations (Vernon & Martinez, 2005) and poly(NIPAAm-HEMA-lactate) as an injectable bioerodible material for drug delivery (B. H. Lee & Vernon, 2005). A hydrolysis-dependent gel was developed by combining dimethyl-γ-butyrolactone acrylate for drug delivery applications (Cui et al., 2007; Cui, Lee, Pauken, & Vernon, 2010) and covalently bound radio-opaque moiety to poly(NIPAAm) for physiological x-ray visualization (Leon, Lee, Preul, McLemore, & Vernon, 2009). Aside for its application aspects, our lab has also modeled the local monomer activation for phase transition (Solis et al., 2005). In the latter paper, Solis et al. discuss two models which can be used for investigation of the LCST and phase transition of poly(NIPAAm), as seen in Figure 3.1.

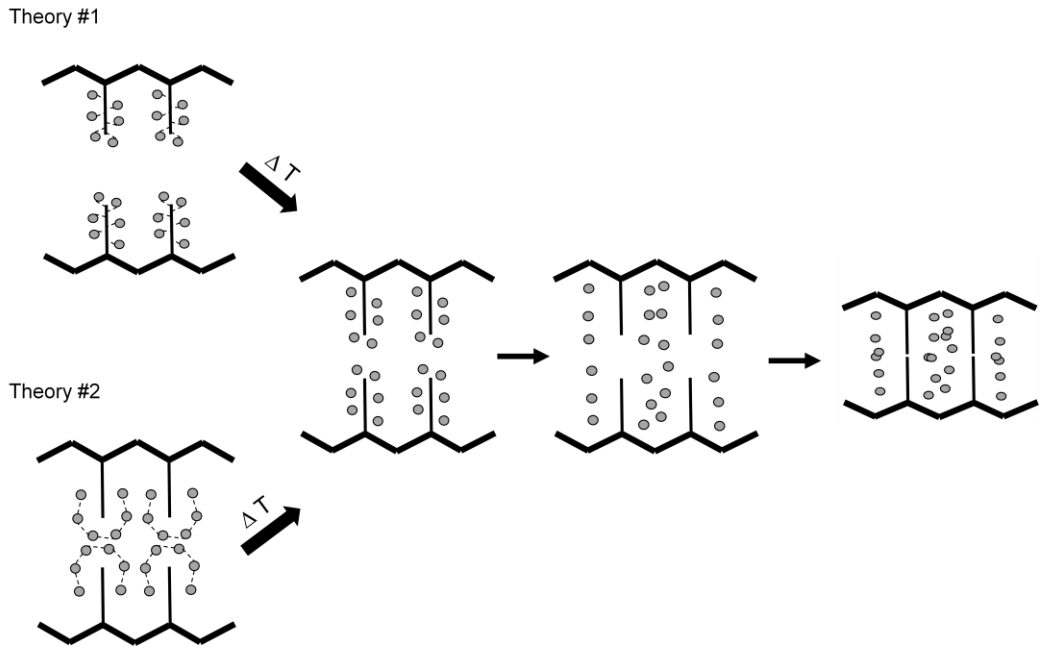

Figure 3.1 Representation of the two possible theories for the phase transition of poly(NIPAAm). The first involves the hydrogen bonding of water molecules to the hydrophilic portions of the polymer below LCST, while the second suggests that the water molecules form a clathrate structure around hydrophobic components due to repulsion forces at low temperatures. Both lead to the association of polymer chains above LCST.

The first involves the physical association via hydrogen bonds of water molecules and monomers below LCST, and as temperature is increased, these hydrogen bonds are lost. This allows for the polymer chains to collapse upon each other, forming a gel. The second model suggests that the water molecules below LCST are actually repelled by the monomers, instead of being associated with them, forming a clathrate structure. This causes the formation of strong hydrogen bonds

between the water molecules near the monomers, and above LCST, these bonds are broken and the polymer chains can then collapse or entangle to form a gel.

In this work, further analysis of the phase transition temperature and behavior of poly(NIPAAm) is conducted. It was hypothesized that a difference at the molecular level can be identified between the polymer in solution (below LCST) and in gel form (above LCST). By using thermal analysis techniques and x-ray scattering tools, data was collected regarding the phase transition and the polymer structure at the molecular level, with the results presented herein.

3.2 Materials and Methods

3.2.1 Differential Scanning Calorimetry (DSC)

Differential scanning calorimetry is an important tool in examining phase transition and the lower critical solution temperature (LCST). DSC studies were conducted on the 3 polymers (using a CSC 4100 multicell differential scanning calorimeter). Samples were dissolved in PBS pH 7.4 and prepared at 5 wt% to examine the LCST of each polymer and to infer information from their curve shapes. DSC measurements (n=3) were made from 0 to 50°C, at a heating rate of 1°C/min, with PBS as a reference. Additionally, poly(NHA) was investigated at concentrations of 20, 10, 0.31, 0.16 and 0.08 wt% to compare to the cloud point data. Plots of molar heat capacity vs. temperature were prepared to determine the LCST point and the phase behavior.

3.2.2 Cloud Point

Cloud point is also an important method to be used for better understanding of phase transition. Cloud point was conducted on poly(NIPAAm), poly(NIPAAm-co-cysteamine) (NC) and poly(NIPAAm-co-HEMA-acrylate) (NHA) at various concentrations. Polymers were synthesized as previously reported in (Bearat et al., 2011). The polymer samples were dissolved in PBS pH 7.4 in a concentration dilution series: 20, 10, 0.31, 0.16 and 0.08 wt%. These high and low concentrations were chosen to allow for differentiating the phase transition behaviors at concentrations where gels are known to form and at concentrations where no gels form. One milliliter of each sample (n=3 for each concentration) was loaded in cuvettes and placed in a temperature-controlled water bath. Temperature was increased by increments of 1°C, over a range of 5 to 40°C, and allowed to equilibrate for approx. 2 min. A UV spectrophotometer (Ultrospec 3000, Pharmacia Biotech) was used for absorbance measurements at 500nm. Absorbance (A) values served to determine the % transmission (%T) values using the following equation $A = -\log(\%T/100)$. Plots of % T vs. temperature were obtained for analysis of the phase behavior and phase transition temperature.

3.2.3 Small Angle X-Ray Scattering (SAXS) of Physical Gelation

Small Angle X-Ray Scattering (SAXS) is a highly useful technique for analysis of polymer interactions at the nano scale. Using a high energy X-ray

beam, generated by a synchrotron, directed at a polymer sample, the scattering of X-rays from the sample can infer about the macromolecular structure of the sample at the nano scale. To conduct SAXS experiments, the Advanced Photon Source of Argonne National Laboratory was visited, benefitting from SAXS capabilities on Sector 12-ID-C. SAXS was used to look at the interactions in the 3 polymers at the various concentrations, dissolved in PBS pH 7.4 and loaded in 1.5mm diameter Quartz capillaries. Temperature studies were performed using a custom-built Peltier heater/cooler system and an aluminum cell. Polymer temperature measurements were recorded at 10, 16-34 (in increments of 2°C) and 37°C, with shots taken after allowing 5min to reach thermal equilibrium at each temperature. Heating and cooling kinetic studies were also conducted by rapidly increasing the temperature from 4 to 32°C and rapidly decreasing it back to 4°C (below and above LCSTs) while taking 20 shots at each set of time intervals of 5s, 10s, 30s and 1min. The 5s shots looked at the quick transition from liquid to gel while the later shots explored the kinetics at the stable temperature. From the 2D image captured by the detector, a binary file can be generated which was used to obtain a spectrum of the scattering intensity (I) as a function of the scattering vector (q). Using the q value and the Bragg relation $d = 2\pi/q$, the characteristic distance in real space (d) was determined. This distance elucidates the structural characteristics of the polymers. SAXS was performed using a camera distance length of 1016mm, to capture the high-q domain, and incident energy of 17.9 keV.

3.2.4 Small Angle X-Ray Scattering (SAXS) of Chemical Gelation

Studies were conducted on the chemical gelation characteristics of the polymer system to examine any possible difference between physical and chemical gels of poly(NIPAAm). The polymers were first dissolved at 20 wt% in PBS at pH's of 6.4, 7.4 and 8.4. An automated mixing pump was used to mix the moieties and induce the chemical reaction for covalent cross-link formation. The poly(NC) solution was loaded in an Eppendorf tube with a tube connected to the quartz measuring capillary while the poly(NHA) solution was loaded in another tube connected to the mixing pump. The pump automatically mixed the two polymer components and injected the mixed sample into the measurement tube which receives the X-rays, as seen in Figure 3.1. Thiols on the cysteamine and vinyls on the acrylate react through a Michael-addition reaction to form covalent cross-links, thus resulting in a gel. This was done at 3 different pH's (6.4, 7.4 and 8.4) and at different mixing times (6s, 12s, 30s and 60s) at 20°C. One measurement was performed at 37°C for pH 7.4 and 60s of mixing to analyze the effects of both physical and chemical gelation on the molecular structure.

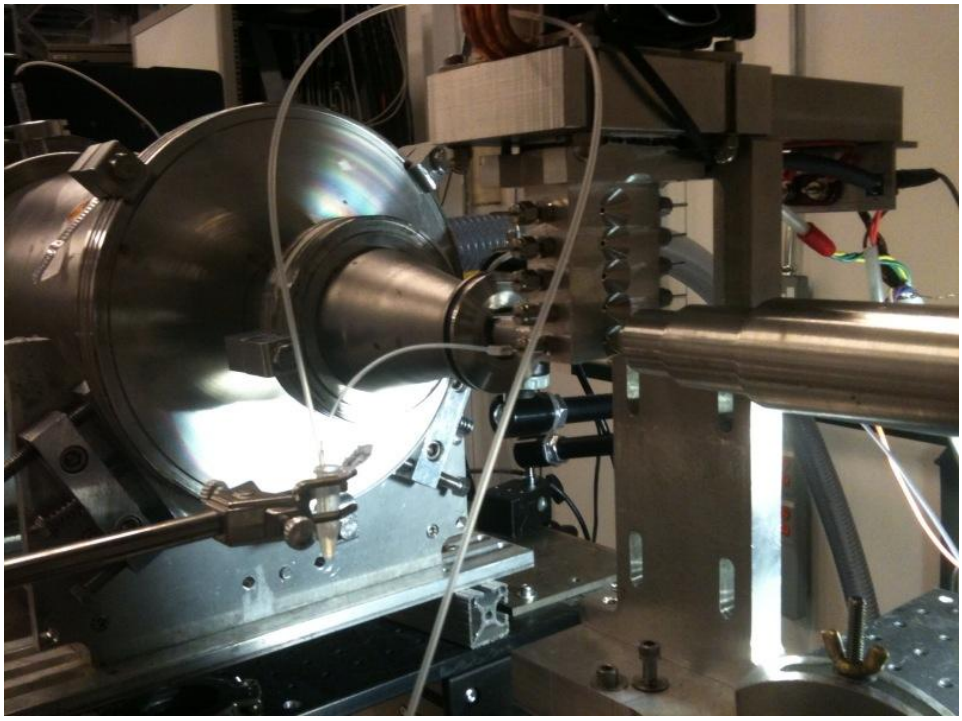

Figure 3.2 Picture of the set-up for the chemical gelation SAXS studies, with the pumps for mixing of components, quartz capillaries for injection of material and the beamline for high energy X-ray.

3.2.5 X-Ray Diffraction (XRD)

With X-ray diffraction, information about the crystalline nature and atomic structure of the material can be obtained. Here, powder XRD was used to infer about the crystalline state of the polymers. The information obtained from XRD was used to correlate and better interpret the data acquired from SAXS, specifically the significance and the relation of the *d*-spacing value(s) to the real state of the polymers. XRD (Rigaku D/MAX-IIB) was executed on the three polymers, as well as the chemical gel and the physical-chemical gel. The chemical and physical-chemical gels were prepared by stoichiometrically mixing poly(NC)

and poly(NHA), both dissolved at 20 wt% in PBS pH 7.4, in 3cc syringes and couplers for 1min. The chemical and physical-chemical gels were left to react and cure for 3 days, at room temperature and at 37°C, respectively. They were then frozen at -80°C and lyophilized. Each polymer/gel was ground into a fine powder which was then uniformly spread on a zero-background slide (a non-diffracting quartz slide cut off-axis). Using a diffractometer with Cu$K\alpha$ radiation and an average wavelength of 1.5418Å, scans were done first for $2\theta = 2$ to 65° with a scan speed of 10°/min and then specific areas of interest in the pattern (2-25° for the polymers and 2-45° for the gels) were performed at a much slower speed of 0.5°/min with steps of 0.02° to acquire higher resolution patterns. From the X-ray diffraction, a pattern can be obtained (intensity vs. 2θ), with peaks providing information about the crystallinity and spacing in the molecular structure. Data were processed using Jade software.

3.2.6 Rheology

Rheological studies were performed on the polymers and gels to investigate their mechanical and gelling properties, using a Physica MCR 101, Anton Paar rheometer, with a sandblasted measuring plate of a 25mm diameter and a gap of 0.5 mm. Frequency sweeps, conducted after time sweeps for gelation, measured the elastic modulus (G') as a function of a frequency ramp. Samples were prepared at 20 wt% in PBS pH 7.4. The time sweeps were conducted at controlled stress of 10Pa (linear viscoelastic region), a frequency of 1Hz and a normal force of 1N for 3600s. The frequency sweeps were performed

subsequently using a logarithmic frequency ramp from 0.01 to 100Hz, a controlled stress of 10Pa and a normal force of 1N. Physical gels (poly(NIPAAm), poly(NC) and poly(NHA)) were measured by injecting 0.6mL of each on the plate at 37°C. Chemical gels entailed mixing the copolymers (NC and NHA) for 1min and injecting 0.6mL of the mixture onto the rheometer plate at 22°C. Physical-chemical gels involved mixing the copolymers for 1min and injecting 0.6mL of the solution on the rheometer plate at 37°C. The time and frequency specifications outlined above were used for all runs.

3.3 Results and Discussion

3.3.1 Thermal Properties

When working with thermoresponsive materials, it is highly important to analyze their thermal properties, especially the temperature at which the phase transition occurs. Using DSC, the LCST values of homopolymer NIPAAm as well as its synthesized copolymers, poly(NC) and poly(NHA), were examined. As seen in Figure 3.3, the DSC curves, from 10 to 50°C, of the 3 polymers are presented, with their peaks indicating their corresponding LCSTs.

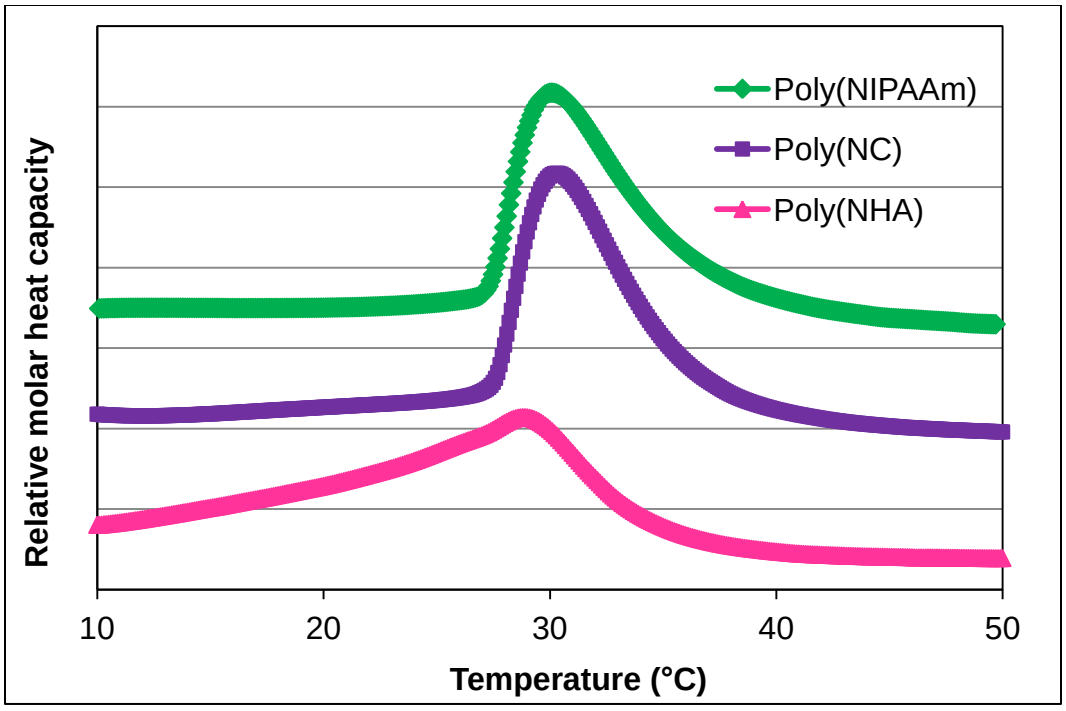

Figure 3.3 DSC endotherms of poly(NIPAAm), poly(NC) and poly(NHA) demonstrating LCSTs ranging from 28 to 31°C and various peak shapes corresponding to the homogeneity of polymer compositions.

Poly(NIPAAm) exhibits a peak around 30.1°C, with a peak curve that is broader and which tails off. A reason for this behavior may be due to a more polydisperse homopolymer which resulted from free radical polymerization. Studies have reported that by using reversible addition-fragmentation chain transfer (RAFT), a living free-radical polymerization method, more narrow polymer polydispersities and molecular weight distributions were obtained (Ganachaud et al., 2000). Monodisperse poly(NIPAAm) was also shown to undergo a more complete coil-to-globule transition (X. Wang et al., 1998). With the conjugation of cysteamine, the LCST of poly(NC) slightly increased to 30.5°C. Cysteamine being

hydrophilic allows for the increase in the LCST. Feil et al. explained that the effect of comonomers hydrophilicity on the LCST is due to the reduction of the amount of hydrophobic groups and to the increase in the overall polymer hydrophilicity because of the interaction between water and the hydrophilic groups. The LCST is increased because of the increased presence of water-polymer interactions, inhibiting the hydrophobic interactions which occur at higher temperatures and lead to the association of the polymer chains (Feil, Bae, Feijen, & Kim, 1993a). The shape of the poly(NC) DSC curve is similar to that of poly(NIPAAm). Poly(NC) was synthesized at molar feed ratios of 98:2 (NIPAAm to cysteamine). Thus, the NIPAAm content is very high and would result in a similar shape and peak as the homopolymer. On the other hand, with the incorporation of hydrophobic HEMA-acrylate, the LCST was decreased to 28.6°C. More hydrophobic monomers have been shown to result in lower LCSTs (Jeong et al., 2002). Having an overall more hydrophobic polymer decreases the water-polymer interactions and more readily increases the interaction between hydrophobic moieties, allowing the transition to occur at lower temperatures. The shape of the DSC curve for poly(NHA) portrays different properties of this polymer. As observed, the peak is very broad, starting to increase in slope early on (~ 15°C). The broad endotherm is related to the synthesis of the polymer at a molar feed ratio of 95:5 (NIPAAm to HEMA-acrylate). With larger content of the comonomers, the features of this polymer are further removed from the homopolymer and exhibit broad peaks (Y. H. Bae et al., 1991). With a higher

amount of copolymerization, more combinations of diverse polymer chains can result, leading to a less homogeneous and more polydisperse polymer.

Using cloud point method, the phase transition of the homopolymer and copolymers could be further analyzed. Cloud point data was collected for the samples of the copolymers by measuring the transmission via UV spectrophotometry. A clear solution will transmit at 100% while an opaque solution will transmit at 0% as UV light cannot pass through it. To identify any relationship of polymer concentration on the gelation behavior, various concentrations were used for all polymers. High polymer concentrations of 20 and 10 wt% and low polymer concentrations diluted down to 0.08 wt% were tested from 5 to 45°C, as seen in Figure 3.4.

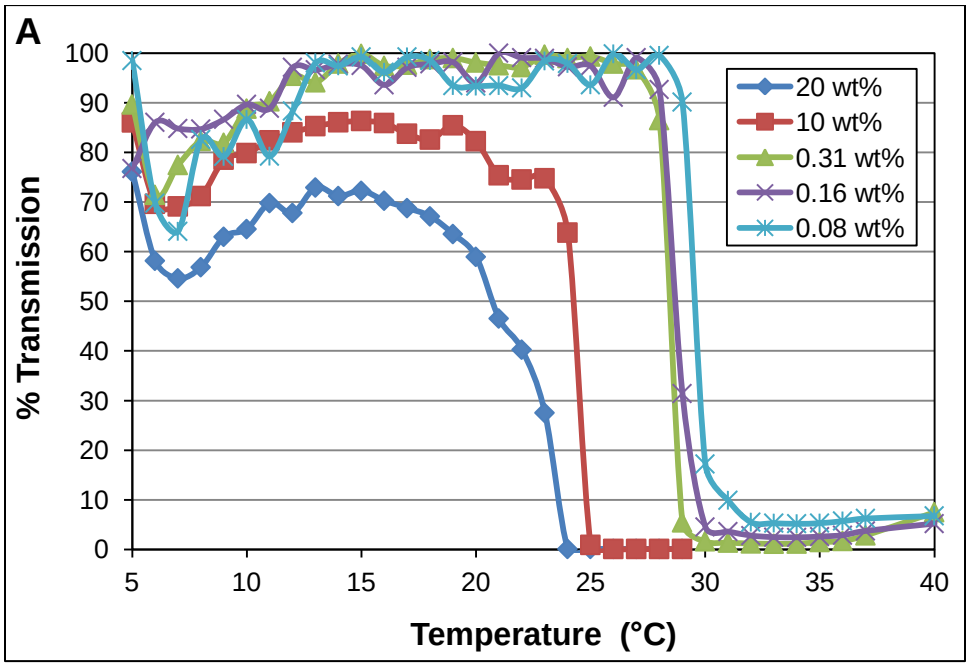

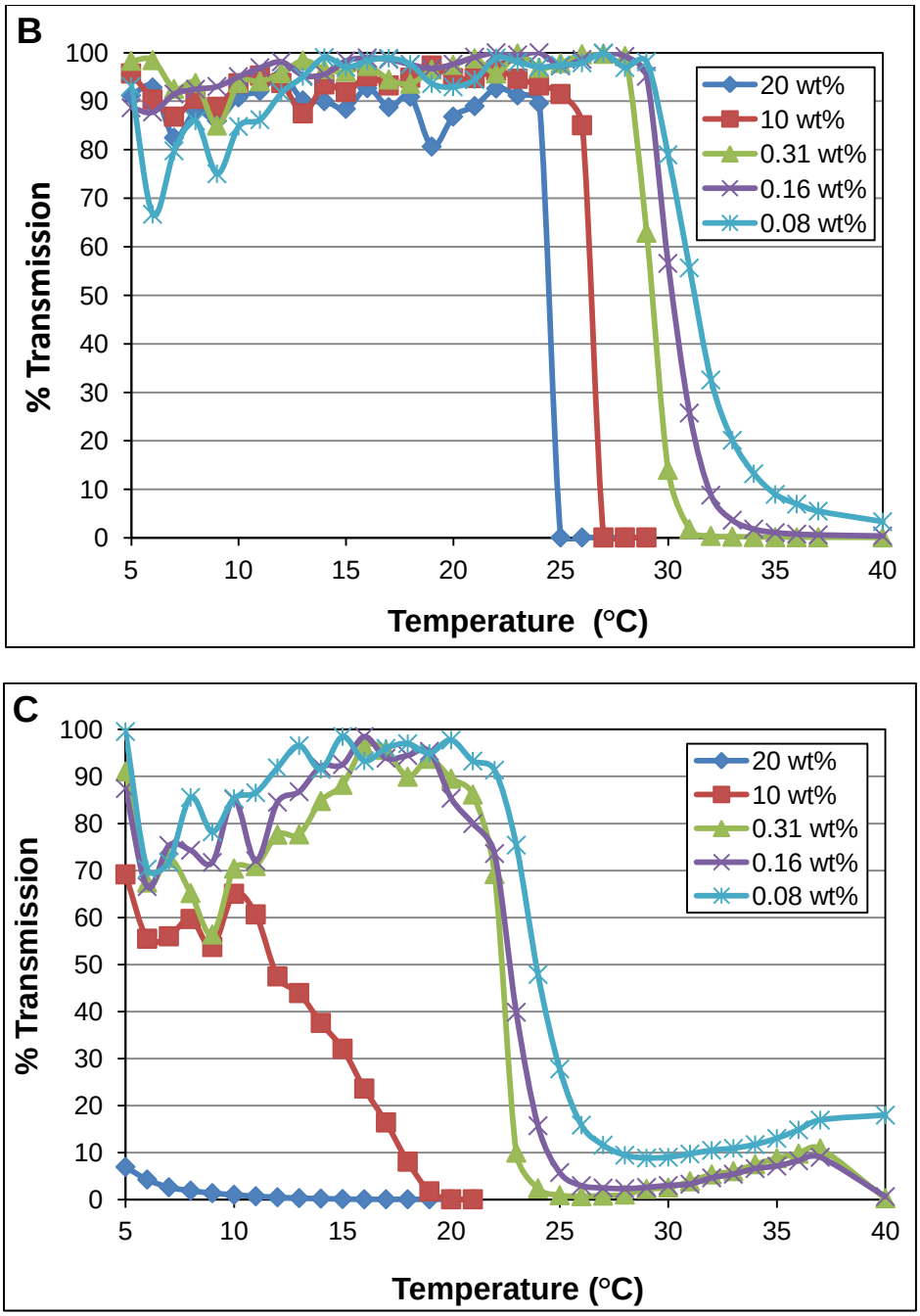

Figure 3.4 Cloud point data for A) poly(NIPAAm), B) poly(NC) and C) poly(NHA) demonstrating an increase in phase transition temperature with a decrease in concentration.

In Figure 3.4A, poly(NIPAAm) at 20 wt% undergoes phase transition at lower temperature, with cloud point (50% transmission) occurring around 21°C. As concentration is decreased to 10 wt%, cloud point occurs around 25°C and with further decrease in concentration, higher cloud point temperatures are recorded, with 30°C for the low concentration of 0.08 wt %. Thus, a trend is observed between polymer concentration and cloud point temperature. As concentration is decreased, the temperature at which cloud point occurs increases. In Figure 3.4B, poly(NC) demonstrates similar cloud point data as the homopolymer, in that as concentration is decreased, the cloud point temperature increases. With this polymer, however, the temperatures at which cloud point occurs are overall slightly higher than those of poly(NIPAAm). This is in correlation with the DSC data which illustrated a higher LCST for poly(NC) due to the more hydrophilic nature of cysteamine. Poly(NHA) also showed the familiar trend of increased cloud point temperature with decreased polymer concentration (Figure 3.4C). Although similar behavior was observed, the temperatures at which cloud point was reached were much lower than the two other polymers. In DSC, poly(NHA) was shown to possess a LCST around 28-29°C; however, the onset of the phase transition was seen to take place at very low temperatures, starting between 10-15°C. Because of the heterogeneous composition of this polymer and the greater amount of hydrophobic monomers, some chains can undergo phase transition at very low temperatures. This explains why at the high polymer concentration of 10 wt%, cloud point occurs around 12°C. By visual observation, poly(NHA) becomes opaque rapidly at room temperature. Since the cloud point technique

relies on opacity of the material to measure its transmission, it therefore explains why poly(NHA) is seen to possess low transmission at lower temperatures than its counterparts. The 20 wt% concentration of poly(NHA) shows low transmission at all temperatures. This may be due to the yellow tint in the polymer's color (originating from the yellow color of acryloyl chloride used during synthesis for conjugation of acrylate to HEMA), which interferes with the absorbance at that wavelength. For more conclusive information on the phase transition of poly(NHA) at various concentrations, DSC was run at a set of low polymer concentrations. In Figure 3.5, the DSC curves are plotted from 20 to 50°C for poly(NHA) in a concentration dilution series, ranging from 5 to 0.08 wt %.

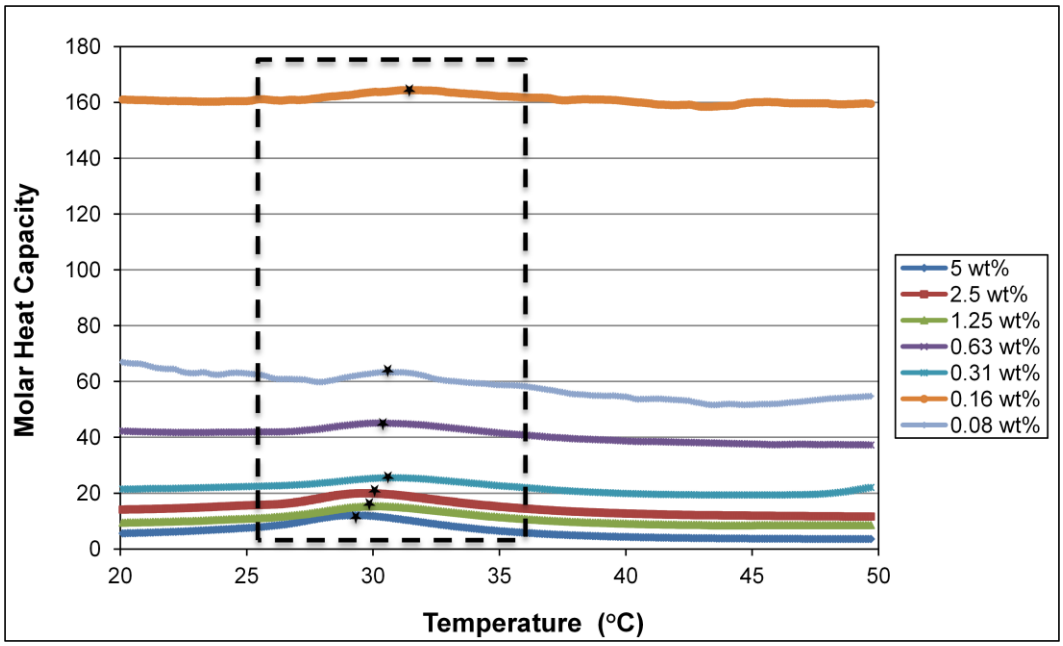

Figure 3.5 DSC measurements of LCSTs at various concentrations of poly(NHA), showing that as concentration is decreased, the LCST value is increased.

The boxed area highlights the peaks at the various concentrations and the LCST values are indicated by the stars. As was observed in the cloud point data, the LCSTs increased with decreasing concentration. Concentrations as low as 0.08 wt% still exhibited a phase transition and LCST. Additionally, higher enthalpies were recorded at higher concentrations and enthalpy decreased as concentration decreased. At low concentrations, less amount of polymer is present which requires less energy to break the hydrogen bonds formed between the water molecules and the polymer. Overall, from both thermal characterization techniques, it was determined that even at low concentrations, the phase transition can be detected.

3.3.2 SAXS Temperature and Kinetic Studies

In order to elucidate the mechanism behind the phase transition of poly(NIPAAm), a closer look into the macromolecular structure of the polymer is of great relevance. Because the phase transition involves the interaction of water molecules around the polymer groups and their displacement at higher temperatures to result in gel formation, it is crucial to be able to examine the effect temperature has on the polymer chains at the nanoscale. To do so, small angle x-ray scattering (SAXS) derived from synchrotron radiation was sought. With this technique, the changes occurring in the amorphous or semicrystalline polymer structure at very miniscule scales could be investigated (Chu & Hsiao, 2001), while performing the experiments *in situ*. The SAXS data plotted the scattering intensity (I) as a function of the scattering vector (q), from which the d-

spacing value could be determined. The three polymers, homopolymer poly(NIPAAm), poly(NC) and poly(NHA) were first analyzed as a function of temperature at 10 and 20 wt% concentrations. In Figure 3.6, the scattering data is displayed for poly(NIPAAm).

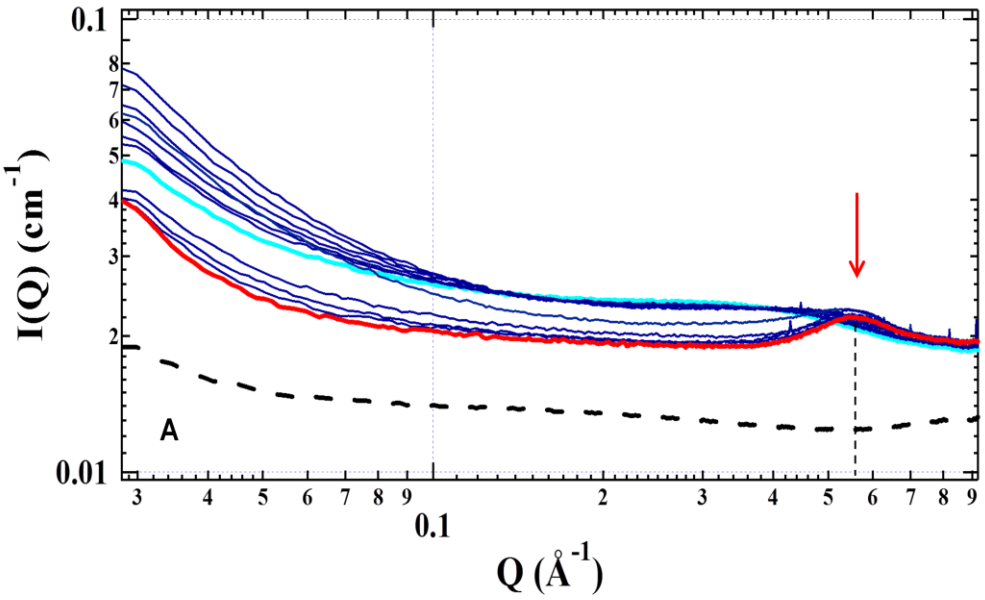

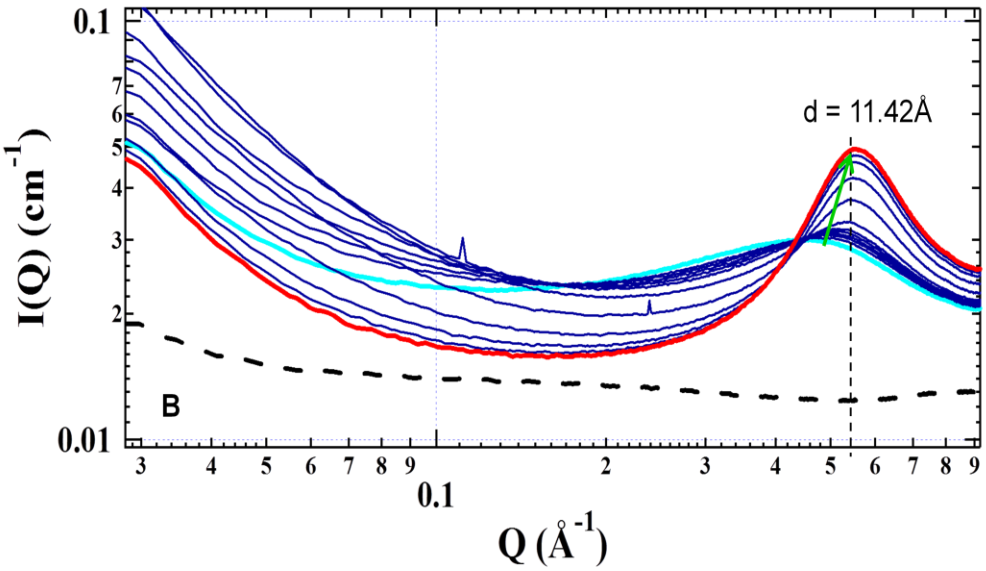

Figure 3.6 SAXS temperature studies from 10 (light blue) to 37°C (red) of poly(NIPAAm) at A) 10 wt% and B) 20 wt%, with peak forming as temperature is increased. Higher peak intensity at higher concentration indicates a peak at a d-spacing of 11.42Å. Dashed line represents background of solvent only.

At 10 wt% (Fig. 3.6A), it was seen that as temperature was increased from 10°C (light blue line) to 37°C (red line), a small peak developed at higher temperature. This peak is more pronounced at 20 wt% (Fig. 3.6B) and occurs at a *q* value of 0.55, corresponding to a *d*-spacing of 11.42Å. Mainly the intensity of the scattering increases with increased concentration; however, it occurred in the same *q* value. This indicates that because of the higher concentration of polymer in Fig. 3.6B, more scattering of that particular polymer structure can be captured. Although originally low concentrations were to be tested, it was observed that even at a high concentration of 10 wt%, a small peak could be detected. Thus,

lower concentrations would only result in undetectable peaks and therefore, 20 wt% concentrations were used for the subsequent experiments. It is also important to note from the evolution of the curves that the peak position moves to the right (higher *q*-value) as temperature is increased. Thus, the polymer structure causing the scattering intensifies and its d-spacing also becomes smaller as temperature is increased. What can be inferred from this peak is that it correlates to the distance between the polymer chains as they begin to associate. At low temperatures, water molecules interacting with the polymer via hydrogen bonds prevent the polymer chains from being in the vicinity of each other and therefore no feature appears in the scattering. However, as temperature rises and approaches LCST, the hydrogen bonds are weakened and the water molecules are expelled, which encourages association of polymer chains. These chains begin to close the gap between each other as they start associating, which correlates to the peak shifting from a *d*-spacing of about 14Å to 11.42Å. As more chains collapse on themselves to form a gel, the intensity of this peak increases. Similar *d*-spacing values were observed in studies using poly(NIPAAm) cryogels, from which the *d*-spacing value was also referred to as the distance between chains, since it is too large to be a distance between side groups on the backbone and not large enough to be the size of nanodomains (Chalal et al., 2010; Perez et al., 2007). When performing the same temperature studies on poly(NHA) and poly(NC) at 20 wt%, very similar evolution of a peak is witnessed with increasing temperature, as shown in Figure 3.7A and B. The peaks for poly(NHA) and poly(NC) also developed in the same region as the homopolymer, with *d*-spacing values of 11.02Å and 11.22Å,

respectively. This indicates that the major effect on the overall structural changes occurring through phase transition is the polymer chains associating as temperature is increased.

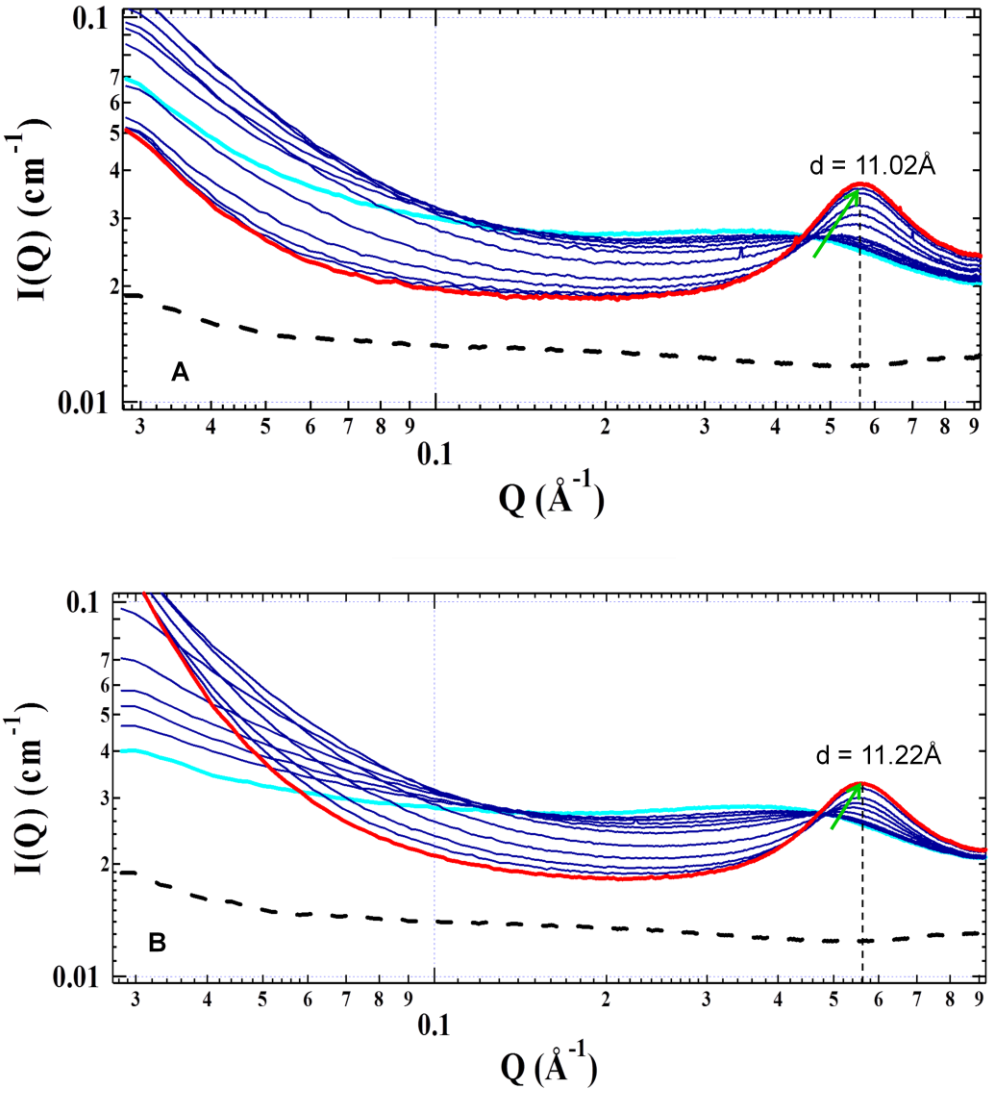

Figure 3.7 SAXS temperature studies from 10 (light blue) to 37°C (red) of A) poly(NHA) and B) poly(NC) at 20 wt%, indicating similar peak formation as temperature is increased, occurring between 11 and 12Å.

To investigate the possible effect of time on the phase transition of the polymers, heating (4-32°C) kinetic studies were performed on the three polymers. Measurements were taken very rapidly throughout the change in temperature as well as at the final constant temperature (32°C). The evolution of the curves and peak of poly(NIPAAm) occurred with the same shape and at the same *q*-value as in the temperature studies; however, the time of the phase transition could be tracked (Figure 3.8).

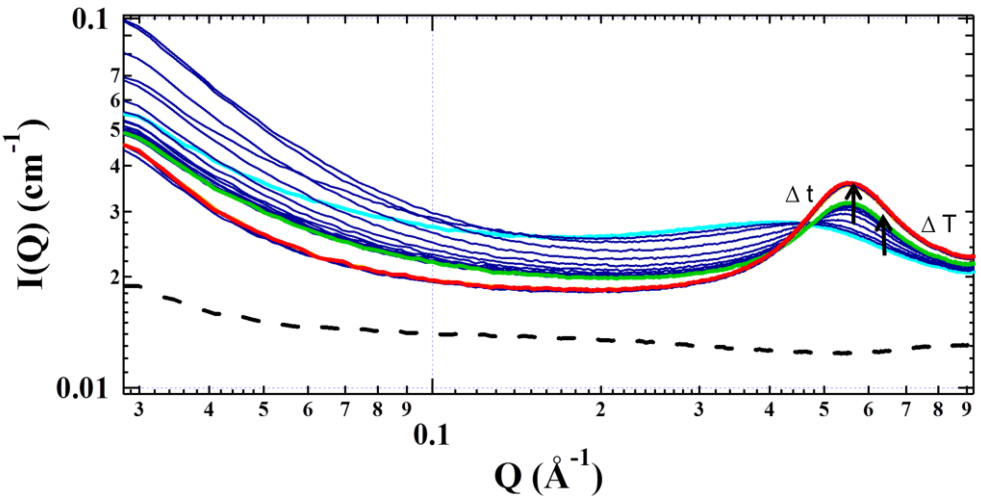

Figure 3.8 SAXS kinetic studies performed on poly(NIPAAm) indicating a rapid phase transition within 1min 40s (green) and extent of chain association reaching equilibrium within 15min (red).

The first 20 points taken every 5 seconds are shown, from the first point (light blue line) to the 20th point (green line). The sample was left at the constant temperature of 32°C for 20 minutes. The peak at 15 minutes is highlighted in

orange and the final measurement at 20 minutes is in red. As the temperature was quickly increased, the peak was seen to develop rapidly. Within the first 1 minute and 40 seconds (green line), the peak is fully formed, indicating that the chains are associating. After 15 minutes have lapsed, there is an increase in the peak intensity, indicating that more chains have collapsed. The 20 minute time point overlaps the 15 minute measurement which demonstrates that no difference can be observed and the intensity of scattering from chains associating remains the same. Thus, a fuller extent of the reaction seems to have been reached within 15 minutes, with no further increase in the peak beyond that time point. For poly(NC) and poly(NHA) (Figure 3.9A and B), the peak evolution and further extent of reaction (chains associating) were similar to those observed in the homopolymer.

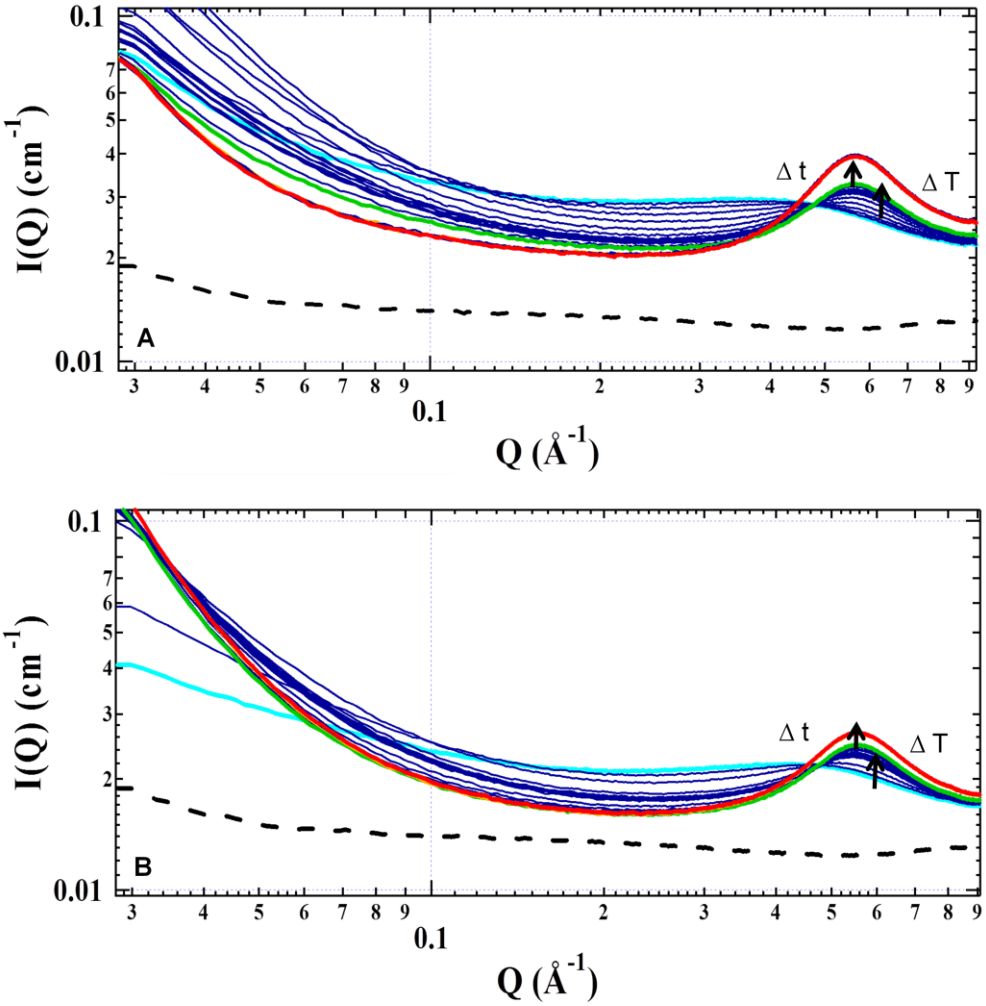

Figure 3.9 SAXS kinetic studies for A) poly(NHA) and B) poly(NC) with similar rapid association of polymer chains (green) and further completion of reaction (red).

The results exhibit a rapid phase transition, occurring within 1 minute and 40 seconds; however, the extent to which the association of the polymer chains reaches equilibrium is around 15 minutes. This indicates the rapid changes which occur at the structural level between water molecules and the polymer, but also

aids in better understanding the behavior of the gel once injected at 37°C *in vivo*. The kinetic studies elucidate on the time for gelation and the extent of the gelation reaction, which in turn, can be used to estimate specifications for *in vivo* use.

3.3.3 SAXS Chemical Gelation Studies

With the precision of measurement of structural changes, SAXS was also used to possibly investigate covalent cross-linking which occurs once the copolymers are mixed. Since the chemical reaction is dependent on many variables, studies were performed with different mixing times, pH's and temperatures. By mixing the copolymers, the chemical reaction between thiols and vinyls is instigated. The longer the copolymers are mixed, the more opportunities present themselves for the thiols to attack the vinyl groups and form cross-links. The pH also plays a role in the kinetics of the Michael-addition reaction. For the reaction to begin, the thiol must first be deprotonated, which is promoted in a more basic solution due to the high acidity of thiols. Once the thiolate anion is formed, it performs a nucleophilic substitution onto the vinyl of the other copolymer. The reaction rates thus increase with pH due to the greater amount of thiolate anions present (Mather, Viswanathan, Miller, & Long, 2006). Additionally, with increased temperature, two gelation mechanisms occur which trigger the association of chains: the chemical reaction and the physical gelation of poly(NIPAAm). Due to these factors, the mixing time (6s, 12s, 30s and 60s), pH (6.4, 7.4 and 8.4) and temperature (20 and 37°C) were tested employing SAXS. The scattering data obtained did not show any difference between the

various mixing times and neither between the use of different pH's of the PBS solutions in which the polymers were dissolved. There are several reasons for which no new peaks were detected. First, the runs in SAXS were conducted for 20 minutes on each sample. This duration is not long enough to observe the effect of chemical cross-linking. As was observed in subsequent kinetic studies, the reaction of thiols to vinyls in this particular system (NC with NHA) is very slow, with only about 15% of the thiols consumed in reaction after 5 hours at pH 7.4 ((Bearat et al.,). Since these runs were performed *in situ*, as the reaction was taking place over the course of 20 minutes, the extent to which the chemical cross-links would have formed is minute. Additionally, the *q* range of the SAXS experiments was limited for the runs. Thus, it is plausible that a peak may have formed in a higher q range, which could not be detected within this range. By running a much broader q scale, a more complete view of the system could be obtained.

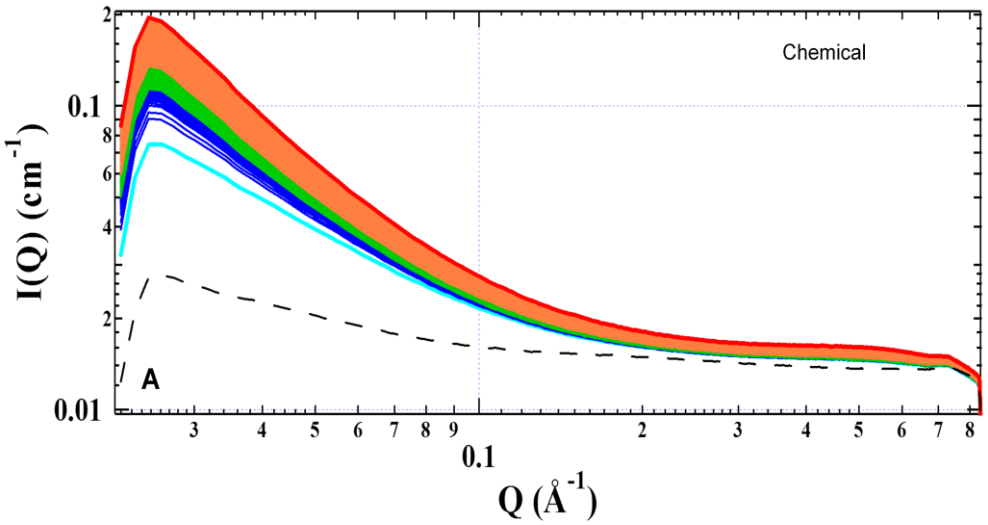

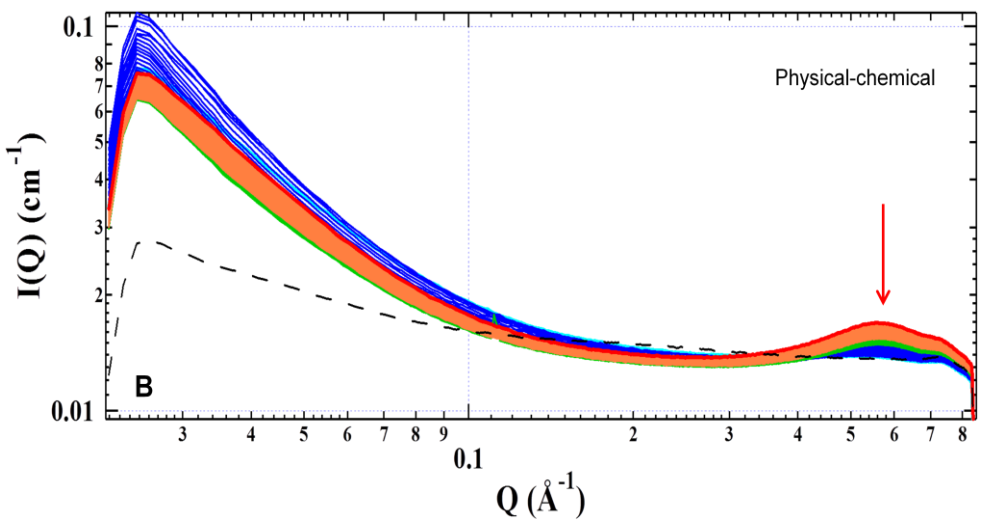

Figure 3.10 SAXS studies for chemical gelation by 60s of mixing of poly(NC) and poly(NHA) at pH 7.4 at A) 20°C and at B) 37°C for physical-chemical gelation. Peak detection occurred in physical-chemical gelation at the same location of 11-12Å.

Figure 3.10A portrays the SAXS data of the chemical gel, performed at 60s of mixing with a pH of 7.4 at 20°C, compared to Figure 3.10B illustrating the physical-chemical gel conducted at the same conditions as the chemical gel (60s mixing, pH 7.4) however at 37°C. When the temperature component was factored into the chemical reaction, a peak developed at a *q* value of 0.56, corresponding to a *d*-spacing around 11.2Å. This peak is the same as the one observed in the physical gelation studies, indicating that the effect of temperature on the physical-chemical gel could be detected.

3.3.4 XRD Analysis

To further analyze the structural features of the polymers and to verify what was detected in the SAXS studies, powder X-ray diffraction (XRD) was employed. The polymers alone as well as the chemical and physical-chemical gels were tested. In Figure 3.11, the XRD patterns of the homopolymer poly(NIPAAm), poly(NHA) and poly(NC) are stacked against the background.

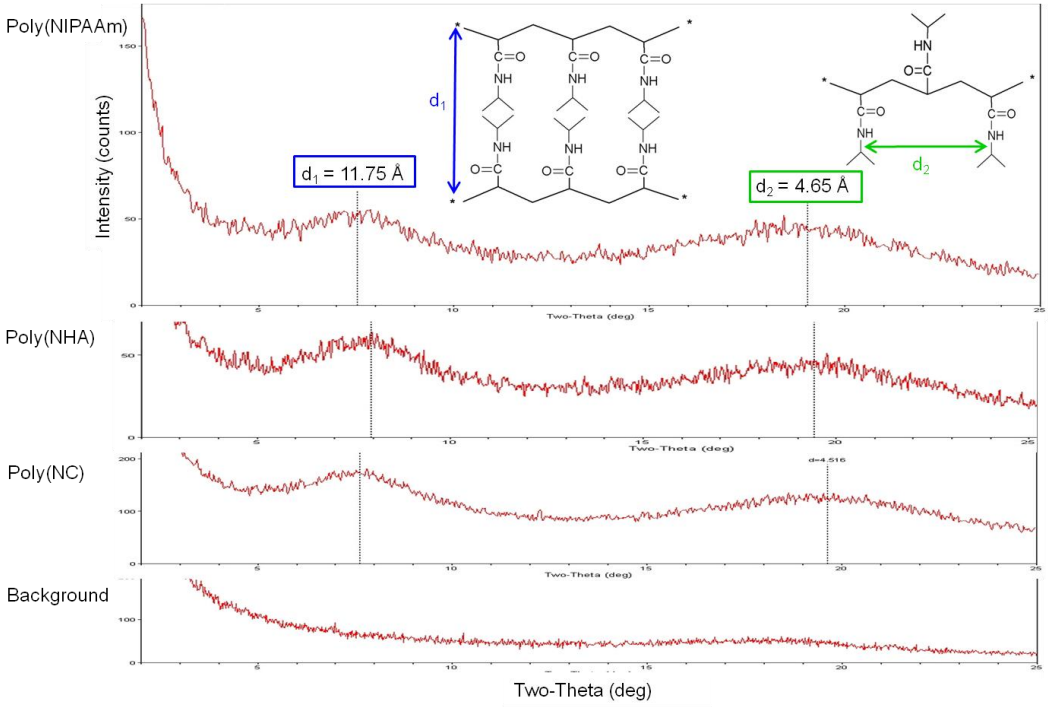

Figure 3.11 XRD patterns for the three polymers compared to background, with all polymers exhibiting peaks at 11-12Å, representing distance between polymer chains, and 4-5Å being the distance between every other side chain.

From the collected data, the diffraction peaks are detected in all polymers in the same 2θ regions. The narrower peak is detected at a 2θ value between 7 and 8°. This angle corresponds to a d-spacing between 11 and 12Å, which is identical to the peak observed from the SAXS studies. Thus, this peak corresponds to the interplanar distance between associated polymer chains. Since all the polymers are mainly composed of temperature-responsive poly(NIPAAm), it is expected that they exhibit peaks in the same vicinity which relates to the distance between polymer chains as they expel water and collapse at higher temperatures. The second broader peak is found between a 2θ value of 18 and 20°, corresponding to a *d*-spacing between 4 and 5Å. This peak cannot be a multiple of the diffraction peak observed at 11-12Å because of its value and therefore represents a structural feature of the polymers. By investigating the bond lengths of the backbone and between side chains, the nature of the peak could be explored. Since the -CH-CH_2- bond length is approximately 1.53Å (Allen et al., 1987) and the angle of the tetrahedral -CH-CH_2- bond is 109.5°, after some calculations, it was determined that the detected distance of ~4.6Å can correspond to the distance between every other side chain on the polymer backbone. Because of the orientation of the side chains and their free movement, the distance between every other side chain can be diffracted, as opposed to the non-constructive interference between adjacent side chains. Similar peaks were detected with wide-angle X-ray diffraction patterns of poly(NIPAAm) (Kim, Cho, Lee, & Kim, 2000) and cholesteryl-grafted poly(NIPAAm) (X. M. Liu, Pramoda, Yang, Chow, & He, 2004). The narrow shape of the peak at 7-8° indicates less variation in the interpolymer chain

spacing. With the chains less flexible because of their association, the distance between the chains is more restricted. On the other hand, the broad shape of the peak at 18-20° demonstrates that there is more variation in the spacing between the side chains, since they can more easily move freely, resulting in a wider range of distance at which these groups can diffract.

XRD studies were also performed on the chemical gel and the physical-chemical gel to observe any differences in the structure of both. For the chemical and physical-chemical gels, the XRD data, shown in Figure 3.12, portrays the two similar peaks previously observed, however, it does not show a difference in the location of peaks between either of the gels nor their polymer only counterparts (Figure 3.11).

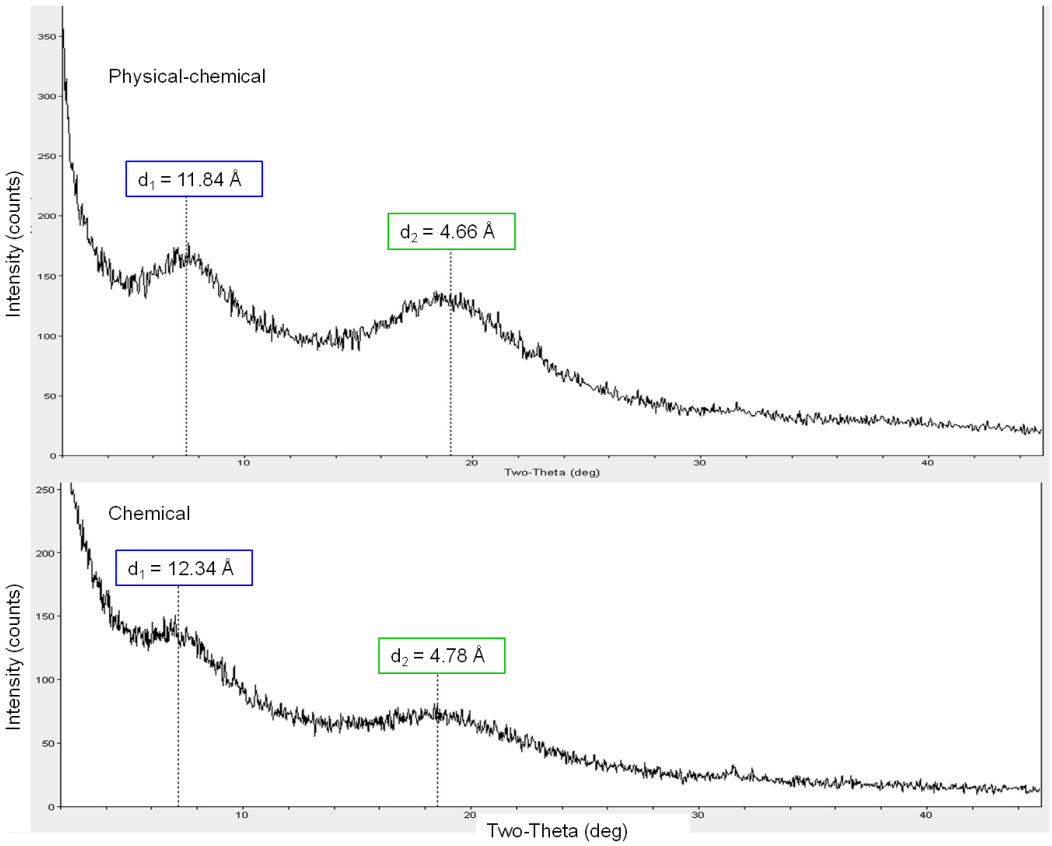

Figure 3.12 XRD patterns comparing chemical and physical-chemical gelation. Both gels indicated peak formation at 11-12Å and 4-5Å; however, difference in the ratio of peak intensities highlights more important effect of covalent cross-links in the chemical gel compared to both temperature and cross-links for the physical-chemical gel.

A difference that is observed however is the difference between the intensities of the two peaks. In the chemical gel, the peak found in the lower 2θ range is much higher in intensity than the peak found in the higher 2θ range. This indicates that the distance between polymer chains is of higher diffractive significance than the distance between side chains. In the chemical gel, the only contribution to this

distance between polymer chains is the covalent cross-links formed chemically between them. Therefore, the greater diffraction results from the proximity of the polymer chains covalently bound to each other. Since temperature is not involved, water molecules are still present around the side chains, making them less restrained. Thus, the diffraction from these side chains is much less important. In the physical-chemical gel, the difference of intensity between the two peaks is much less important. Here, both covalent cross-links and temperature contribute to the association of the polymer chains. Due to the temperature effect, the side chains have less water molecules near them and become more restrained, thus leading to greater diffraction from the side chains. It can also be noticed that the width of the side chain peak (18-20°) becomes narrower in the physical-chemical gel as opposed to the chemical gel. This additionally demonstrates less variation in the distance between the side chains, since they are now less mobile due to the temperature factor.

From the XRD and SAXS data, it can also be inferred that the structure of the polymers is mainly amorphous. The broad peaks observed in XRD and the diffuse scattering halo which arises in SAXS are indicative of amorphous regions in the material structure (Kakudo & Kasai, 1972). Although amorphous usually implies lack of regularity in the arrangement of atoms or molecules, the spatial orientation is not completely disordered, giving opportunity for scattering to exist in the material. The difference observed between the second peak (*d*-spacing of 4-5Å) manifesting itself in the XRD scattering and not witnessed in the SAXS scattering is again explained by the factors influencing the experiment. The XRD

samples of the chemical and physical-chemical gels were left to react and cure at 20 and 37°C, respectively, for 3 days prior to freeze-drying, whereas the SAXS samples were reacting *in situ* as the measurements were taken for 20 minutes. This resulted in different kinetics and structural detections. With longer reaction time (in the case of XRD), the chemical reaction was able to take place at a fuller extent in both gels. Additionally, the SAXS beamline could not be set to simultaneously measure at a higher *q* range. Nonetheless, the temperature and kinetic studies performed via SAXS and the wider range of scattering recorded using XRD elucidated the structural features of the polymers as well as their gelation behavior.

3.3.5 Rheological Sweeps

Examining the mechanical behavior of polymers can disclose indispensable information related to the changes occurring within their structures. Using rheology, the viscoelastic properties of hydrogels can be analyzed. In Figure 3.13, rheological frequency sweeps are plotted examining the elastic modulus (*G'*) over a frequency ramp (0.01 to 100Hz) for the polymers and the gels.

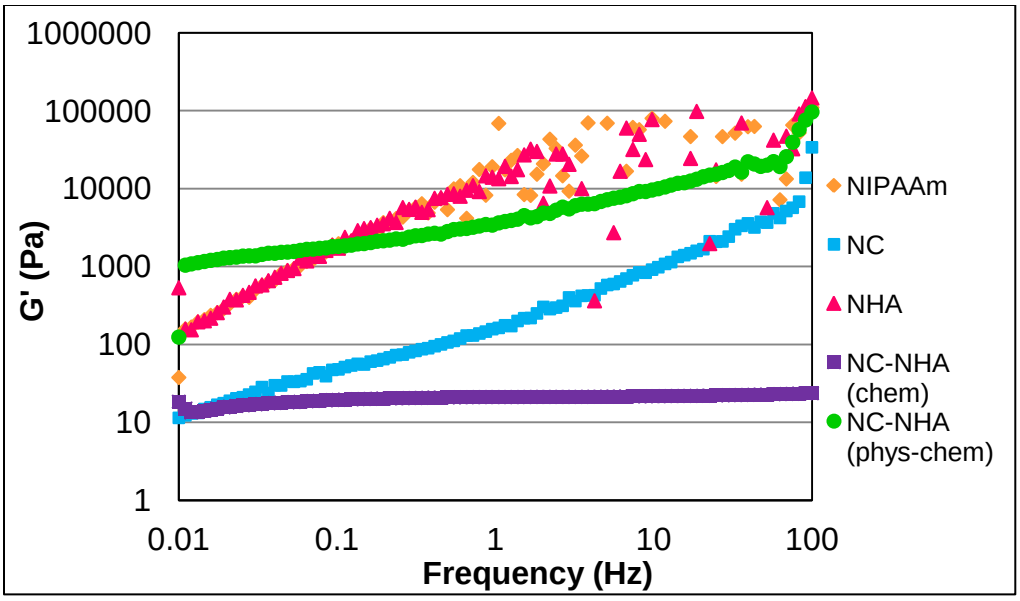

Figure 3.13 Rheological frequency sweeps comparing purely physical gels (NIPAAm, NC and NHA), purely chemical gel and physical-chemical gel demonstrating reduced frequency-dependence and increased strength in the latter.

Purely physical gels (NIPAAm, NC and NHA) are designated as the polymers injected on the rheometer plate at 37°C. Only physical gelation occurs via temperature-sensitivity of NIPAAm on the polymers. As observed in the figure, the sweeps for the purely physical gels exhibit frequency-dependence. Physical gels are reversible networks comprised of finite cross-links (Fuchs, Richtering, Burchard, Kajiwara, & Kitamura, 1998) and they possess an internal fluidity which allows each chain to diffuse through the network, despite its connection to the overall network structure (F. Tanaka & Edwards, 1992b). Because of this fluidity, the system can flow when an external force is applied for an extend time period. On most occasions, physical gels experimentally exhibit creep flow with

little recovery, even after gelation is reached (F. Tanaka & Edwards, 1992b). It is therefore expected for the NIPAAm, NC and NHA polymers to reveal some creep flow under purely physical gelation conditions. By stoichiometrically mixing poly(NC) and poly(NHA) together for 1 min, a chemical reaction is triggered between thiols on NC and vinyls on NHA via a Michael-addition reaction, forming covalent cross-links. Since the mixing, reaction and rheology measurements are performed at room temperature (22°C), the only factor contributing to the gelation of the system is chemical. In the figure, NC-NHA (chem) does not exhibit any frequency-dependence, contrary to physical gels, because of the infinite lifetime of the covalent cross-links (Fuchs et al., 1998). To form a chemical gel, Chambon and Winter describe that cross-linking reactions must occur to connect the macromolecules in the overall polymer network (Chambon & Winter, 1987). These reactions start by having some branched molecules formed, with their molecular weights increasing with further extent of the cross-linking reaction. As gel point is approached, weight average molecular weight diverges to infinity (theoretically) or a macromolecular cluster is formed which extends throughout the sample (experimentally) (Chambon & Winter, 1987). This macromolecular network subsists in the presence of unattached branched molecules, and once beyond gel point, network stiffness increases until complete chemical reaction is reached. In the case of the NC-NHA chemical gel, the 1 minute of mixing allows for as many cross-links to form during that time, allowing for the system to reach gel point rapidly. With the 56 seconds of delay between the injection of the polymer mixture on the rheometer plate at 22°C and

the beginning of the test run, further cross-linking occurs. Thus, the frequency sweep portrays a cross-linked network which does not experience flow. Nonetheless, the strength of the chemical gel is compromised, reaching a *G'* value of only 10 Pa at a 20 wt% concentration. By combining both gelation mechanisms, physical and chemical, one would expect changes in the creep flow and strength of the resulting gel. The NC-NHA (phys-chem) gel takes advantage of the temperature-sensitivity of poly(NIPAAm) present in large majority on both copolymers, as well as the chemical reaction which takes places between the thiols on NC and the vinyls on NHA to result in chemical cross-links. As illustrated in the figure, the NC-NHA (phys-chem) data demonstrates some reduction in the creep flow experienced by purely physical gels (NIPAAm, NC, NHA). The data shows less frequency-dependence, but it is not as reduced as in the chemical gel. However, the overall strength of the physical-chemical gel is highly increased when compared to the chemical gel. The *G'* values range from 1000 to almost 100,000 Pa, indicating an increase on the order of at least 100 times. During the initial 1 minute of mixing of the copolymers, the covalent cross-links are developing throughout the solution to form a chemical network structure. Once the mixture is deposited on the rheometer plate at 37°C, physical gelation takes place almost immediately. This almost instant effect of temperature sensitivity on the polymer causes the NIPAAm chains to associate forming a gel, but in the meantime, also immobilizing the functional groups, making it more difficult for further chemical cross-linking to take place. Thus, the degree of chemical cross-links formed prior to the effect of physical gelation allows for the

observed reduction in frequency-dependence. The added component of the physical gelation manifested at 37°C by the NIPAAm chains provides for the increased strength. A combination of both physical and chemical gelation assisted in the overall increased strength and decreased creep flow.

3.4 Conclusions

The phase transition properties and behavior of poly(NIPAAm) and copolymers were investigated in this work using various thermal, X-ray and rheological techniques. With DSC measurements, the homopolymer and copolymers exhibited LCSTs ranging from 28 to 31°C. The more hydrophobic copolymer (NHA) showed a decrease in the overall LCST and a broad DSC peak due to its greater molar feed ratio of HEMA-acrylate to NIPAAm. This led to a more diverse range of temperature at which NHA chains undergo transition, when compared to the narrower peaks of homopolymer and NC. Cloud point data demonstrated that the phase transition temperature is dependent on concentration; as concentration is decreased, an increase in the cloud point temperature occurs for all polymers. SAXS temperature studies illustrated that as temperature is increased, a peak develops at a d-spacing value of 11-12Å for the three polymers. At low temperatures, the polymer chains are interacting with water molecules. As temperature is increased and reaches LCST, the hydrogen bonds are broken and some of the water molecules are expelled, leading to the association of the polymer chains. The distance between these chains above LCST corresponds to

the peak generated in SAXS. Kinetic studies performed with SAXS indicated that the phase transition occurs rapidly, within 1 minute and 40 seconds. Over the course of 15 minutes, the polymers reached equilibrium intensity, demonstrating that full extent of polymer chains association occurs within that time period. XRD studies on the three polymers, the chemical gel and the physical-chemical gel exhibited two peaks generated in all samples. One of the peaks arose around 11-12Å, similar to the peak observed in the SAXS studies, which corresponds to the distance between polymer chains above LCST as they associate. Another peak developed around 4-5Å in all polymers. This peak represents the distance between every other side chain on the polymer backbone. It was also noticed that the greater difference in the intensity ratio between the peaks in the chemical gel indicates a more important effect of the chemical cross-linking. In the physical-chemical gel, less difference was observed in the ratio of peak intensities, demonstrating that both temperature and covalent cross-linking play roles in the association of the polymer chains. Lastly, rheological frequency sweeps evaluated the mechanical properties of the purely physical, purely chemical and physical-chemical gels. Purely physical gels demonstrated frequency-dependence whereas purely chemical gels achieved low strength. By combining physical and chemical gelation, a reduction in frequency-dependence was observed as well as an increase in the overall strength by a factor of 100. The data showed that a structural difference between a polymer in solution at low temperatures and in gel form at higher temperatures could be detected at the macromolecular level. The studies elucidated possible mechanisms of gelation between the various polymer

and gels. With further work examining a broader range of d-spacings in the polymers and gels, more information can be uncovered with regards to the phase transition of the thermoresponsive polymer, poly(NIPAAm).

CHAPTER 4

COMPARISON OF PROPERTIES BETWEEN NIPAAM-BASED DUAL-GELLING SYSTEMS FOR USE IN VIVO

4.1 Introduction

Stimuli-responsive materials have attracted much attention from scientists and engineers due to their ability to adapt to environments when presented with various cues. These materials have the advantage of changing their form according to the environment and applied stimuli. Amongst the different forms of stimuli which have been investigated, temperature-sensitivity has been widely researched. Thermoresponsive materials can undergo a phase transition change, either a gel-sol or sol-gel, at a specific temperature called the lower critical solution temperature (Klouda & Mikos, 2008). One particularly popular thermoresponsive material is poly(N-isopropylacrylamide) or poly(NIPAAm), due to its phase transition temperature being around 31°C (Heskins & Guillet, 1968). With a lower critical solution temperature (LCST) close to physiological temperature, this material has thus found prominent use in biomedical applications. This LCST can be altered by incorporation of various comonomers. Conjugation of hydrophobic monomers leads to a decrease in LCST, whereas addition of hydrophilic monomers results in an increase in LCST (Feil, Bae, Feijen, & Kim, 1993a; H. Y. Liu & Zhu, 1999; Ramanan, Chellamuthu, Tang, & Nguyen, 2006; Stile, Burghardt, & Healy, 1999). Groups have employed poly(NIPAAm) and its copolymers for different applications, including cell and

enzyme immobilization, controlled drug delivery and gene delivery, bioconjugation, protein dehydration process, and embolization (Bearat et al., 2011; Rzaev, Dinçer, & Piskin, 2007).

Poly(NIPAAm) undergoes gelation by physical cross-linking. At temperatures below its LCST, the polymer chains are hydrophilic and soluble in the aqueous environment. As the temperature is increased above its LCST, the polymer chains become hydrophobic, allowing for the expulsion of water molecules (Kuckling, Adler, Arndt, Ling, & Habicher, 2000). As the water present between chains is dispersed, the chains can then collapse upon themselves to form a gel at sufficient concentrations. The association of the NIPAAm chains is not fully understood; however, it can occur through various forces seen in reversible physical gels, such as molecular entanglement as well as secondary forces including van der Waals, dipole-dipole, hydrophobic interactions, and hydrogen bonding (Hoffman, 2002; Kavanagh & Ross-Murphy, 1998). Since the interactions by which physical gelation occur do not comprise of covalent cross-linking but mainly chain entanglement, an internal fluidity is observed in the network system, allowing for its reversible properties (F. Tanaka & Edwards, 1992a). This may also attribute to creep flow when exposed to an external force for a long duration. Creep flow can be undesirable, depending on the particular applications to which the gel is designed. For example, in the case of using a hydrogel for endovascular embolization of cerebral aneurysms, no creep flow should be observed in order to fully occlude the aneurysm and to not propagate further complications from material leaching into the blood circulation.

Hydrogels can also develop via covalent cross-links formed through chemical reactions between functional groups on copolymers. Different cross-linking densities result in different swelling properties of the hydrogel. In areas of low cross-linking density, high swelling is observed due to the formation of water-filled macropores. On the other hand, high cross-linking density regions demonstrate low swelling (Hoffman, 2002). Chemical gels which endure a large degree of swelling may not be feasible for applications requiring volume confinement. One method used to form chemical cross-links is through a Michael-type addition reaction. This reaction, sometimes referred to as conjugate addition, occurs between nucleophiles and activated olefins and alkynes, resulting in a nucleophilic addition across a carbon-carbon multiple bond (Mather et al., 2006). There are several advantages to the Michael-type addition reaction; these include its mild reaction conditions allowing the reaction to take place at physiological pH and temperature, its plethora of polymerizable monomers, and efficient conversion and reaction rates (Mather et al., 2006). Due to its fast curing and conversion, this reaction has been used for hydrogels (Lutolf & Hubbell, 2003a), thermoset resins (Can, Küsefoğlu, & Wool, 2001) and coatings (Scott et al., 2008).

Although purely physical gels and purely chemical gels possess some drawbacks, by combining both gelation systems, an improved gel network can result. Solely physical gels can experience creep flow under low frequency stress while solely chemical gels can undergo a large increase in swelling. With a combination of a physical and chemical gelling sytem, a physical-chemical gel

can be formed which can reduce creep flow observed with physical gels and decrease swelling while increasing strength. Several groups have investigated physical-chemical gels to be used for various applications. Censi et al. examined a block copolymer consisting of methacrylated NIPAAm cross-linked with hyaluronic acid. This system provides for an injectable, biodegradable, stable and biocompatible hydrogel for peptide and protein delivery (Censi, Fieten, di Martino, Hennink, & Vermonden, 2010). Cellesi et al. investigated an acrylate bearing tetronic and a thioacetate bearing tetronic for thermal and cross-linked gel formation. They noted rapid and biocompatible gel formation, which is feasible for cell encapsulation purposes (Cellesi et al., 2004). Hacker et al. looked into using NIPAAm macromers with methacrylation to result in a thermal and chemically cross-linked system, which provides hydrogel stability for use in tissue engineering and cellular delivery applications (Hacker, Klouda, Ma, Kretlow, & Mikos, 2008). Lin et al. employed a thiolated dextran with a vinylsulfone or acrylate functionalized pluronic to offer adjustable mechanical properties and low cytotoxicity for tissue engineering scaffolds (C. Lin et al., 2010). Using both gelation mechanisms, physical and chemical, not only provides for a greater variety of properties for the hydrogels but also with more feasible characteristics for particular uses in biomedical applications.

Here, a comparison is reported between two simultaneously physically and chemically gelling systems employing poly(NIPAAm) copolymers and a Michael-type addition reaction. Poly(NIPAAm) being a thermoresponsive polymer allows for physical gelation to occur at physiological temperature

(37°C), as the NIPAAm chains associate above the LCST. Chemical gelation occurs through a Michael-type addition reaction between thiol groups and vinyl groups on functionalized copolymers of NIPAAm. The advantage of this reaction is that the initial step of deprotonating thiols can be performed at a physiological pH of 7.4 and at body temperature. Additionally, this reaction benefits from the greater nucleophilic strength of thiols when compared to amino groups, for cross-link formation with acrylates (Friedman, Cavins, & Wall, 1965; Pratt, Weber, Schmoekel, Müller, & Hubbell, 2004). The physical-chemical gelling systems presented here are poly(NIPAAm-*co*-cysteamine) with poly(NIPAAm-*co*-HEMA-acrylate) and poly(NIPAAm-*co*-cysteamine) with poly(NIPAAm-cysteamine-*co*-vinylsulfone), as illustrated in Figure 4.1.

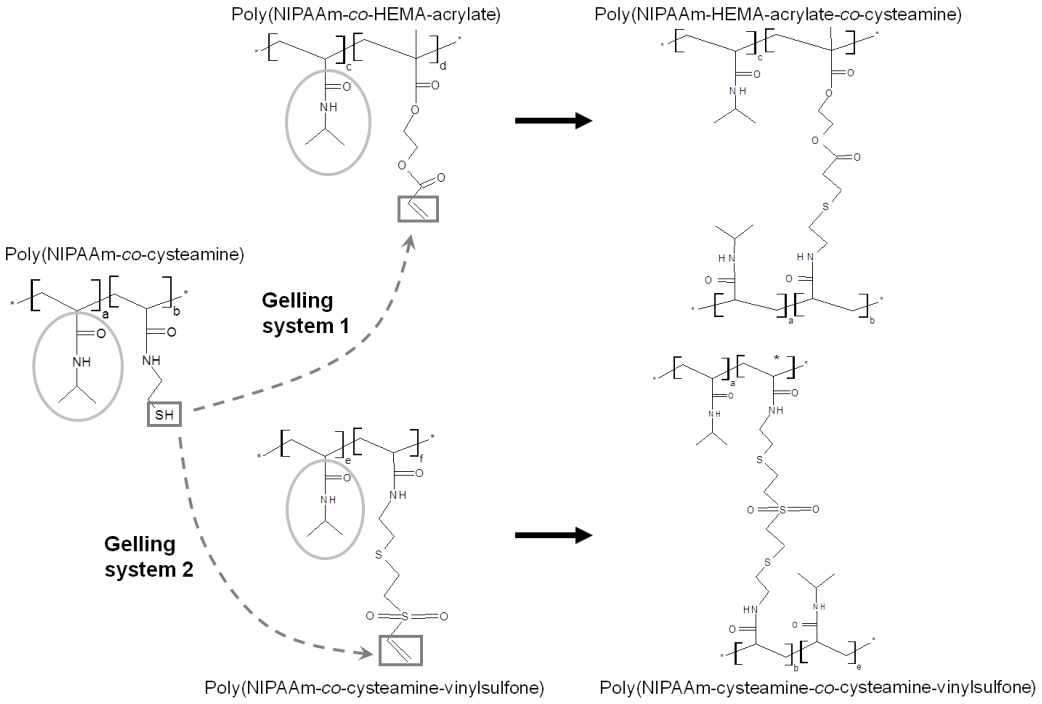

Figure 4.1 The two gelling systems addressed in this work; gelling system 1 comprises of poly(NIPAAm-*co*-cysteamine) with poly(NIPAAm-*co*-HEMA-acrylate) and gelling system 2 consists of poly(NIPAAm-*co*-cysteamine) with poly(NIPAAm-cysteamine-*co*-vinylsulfone). Both systems undergo dual gelation: physical gelation through the temperature-sensitivity of poly(NIPAAm) (circled) and chemical gelation via a Michael-type addition reaction between the functional groups on the copolymers (boxes and dashed arrows). Either system results in covalent cross-link formation between thiols and vinyls and gel formation above the LCST.

The use of different cross-linking copolymers is studied to determine which system possesses more feasible properties for use in endovascular embolization.

The different chemical structures of the cross-linking copolymers can result in differing reaction kinetics, degradation and swelling properties, as well as different thermal, mechanical and morphological characteristics. Studies performed using NIPAAm and various hydrophobic comonomers have shown that the more hydrophobic the monomer and the greater the amount of the hydrophobic monomer in the polymer, the lesser swelling is experienced. Additionally, it causes a decrease in the transition temperature while increasing the mechanical strength (W. F. Lee & Yeh, 2005). Incorporation of various hydrophobic moieties can also impact the kinetics of gelation through the control of the coil-to-globule transition (Jeong & Gutowska, 2002a; Jeong et al., 2002). Poly(NIPAAm-cysteamine-*co*-vinylsulfone) has no ester group, compared to two ester groups present on poly(NIPAAm-*co*-HEMA-acrylate), which can present more vulnerability to degradation since the ester groups have hydrolysable bonds (Bruice & Fife, 1962; Cui et al., 2007; Gopferich, 1996). Poly(NIPAAm-cysteamine-*co*-vinylsulfone) is also more hydrophilic than poly(NIPAAm-*co*-HEMA-acrylate) due to the presence of the sulfone, which presents polar covalent bonds between the sulfur and oxygen. The more hydrophilic nature of the former copolymer thus changes properties of the gelling system. Thus, when comparing the two gelling systems proposed here, differences in most aspects of their properties are witnessed and are reported herein.

4.2 Materials and Methods

4.2.1 Materials

N-isopropylacrylamide (NIPAAm; Aldrich 97%) was purified by recrystallization in hexanes and dried under vacuum for 4 days. 2,2'-Azobisisobutyronitrile (AIBN; Sigma-Aldrich 98%) was purified by recrystallization in methanol. Cysteamine hydrochloride (Fluka 98%), *N*-acryloxysuccinimide (NASI; Acros 99%), divinylsulfone (Oakwood Products, Inc. 97%) and 5,5'-dithiobis-(2-nitrobenzoic acid) (DTNB; G-Biosciences) were used as received. Tetrahydrofuran (THF; Sigma-Aldrich, HPLC grade 99.9%) was dried using sodium and triethylamine (TEA; Sigma-Aldrich 99.5%) was dried with barium oxide. Diethyl ether (Spectrum, anhydrous), hydrochloric acid (HCl; Mallinckrodt 37%), and anhydrous dichloromethane (MC; Sigma-Aldrich 99.8%) were used as received. Promega CellTiter 96® Cell Proliferation Assay was used as received.

4.2.2 Synthesis of Poly(NIPAAm-*co*-cysteamine) and Poly(NIPAAm-cysteamine-*co*-vinylsulfone)

Poly(NIPAAm-cysteamine-*co*-vinylsulfone) was synthesized from poly(NIPAAm-*co*-cysteamine), the latter previously reported in the literature (Bearat et al., 2011). Once poly(NIPAAm-*co*-cysteamine) (NC) was obtained, 20g of the batch was then dissolved in anhydrous MC, with addition of 2mL of TEA. Approximately 50 molar excess of divinylsulfone was added to the reaction

flask to prevent cross-linking. The reaction was allowed to take place for 16h at room temperature. The resulting copolymer, poly(NIPAAm-cysteamine-*co*-vinylsulfone), was precipitated in diethyl ether, filtered and dried under vacuum. The polymer was dialyzed for 5 days (at 4°C against 3,500 MWCO) in distilled water. After undergoing dialysis, the polymer solution was frozen and lyophilized. The copolymerization scheme for the synthesis of poly(NIPAAm-cysteamine-*co*-vinylsulfone) (NCVS) can be seen in Figure 4.2. To form the gel, the two synthesized copolymers (NCVS and NC) were stoichiometrically mixed. This combination (NCVS and NC) was then further compared to a previous gel formation (Bearat et al., 2011), NC stoichiometrically mixed with poly(NIPAAm-*co*-HEMA-acrylate) (NHA). The physical and chemical gelation mechanisms of the resulting gels are illustrated in Figure 4.2.

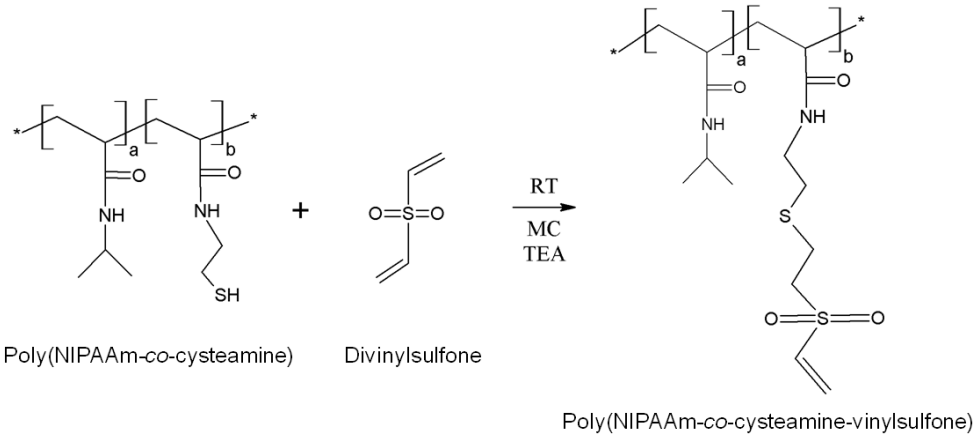

Figure 4.2 Synthesis of poly(NIPAAm-cysteamine-*co*-vinylsulfone) via conjugation of divinyl sulfone to poly(NIPAAm-*co*-cysteamine).

4.2.3 ^{1}H Nuclear Magnetic Resonance Spectroscopy (^{1}H NMR)

^{1}H NMR measurements were made using a Varian Gemini-400 spectrometer operating at 400 MHz in Fourier-transform mode. Samples were dissolved in D_2O and TMS was used as the standard.

4.2.4 Fourier Transform Infrared Spectroscopy (FTIR)

The chemical composition of the synthesized copolymers was determined using FTIR (Thermoelectron Nexus 470). ATR-FTIR was conducted on small pieces of the synthesized copolymers, enough to cover the diamond ATR crystal. Number of scans was set at 60.

4.2.5 Differential Scanning Calorimetry (DSC)

The thermal properties of the polymers were determined by measuring their lower critical solution temperature (LCST) using a CSC 4100 multicell differential scanning calorimeter. Samples were prepared with 5 wt% polymer solutions dissolved in 0.1M PBS at pH 7.4. Scans were run from 0 to 80°C at a scan rate of 1°C/min and in triplicates.

4.2.6 Free Thiol Determination and Kinetic Studies

To determine the content of free thiols present in the poly(NIPAAm-*co*-cysteamine) copolymer, Ellman's method was conducted (Ellman, 1958). To do so, polymer samples were dissolved at 1mg/mL in 0.1M PBS, pH 7.4 and 10mM DTNB [5,5'-dithiobis-(2-nitrobenzoic acid)] solution was added. For each 0.5mL

of the copolymer solution, 0.1mL of DTNB was added. Absorbance was measured at 412nm using a FLUOstar Omega microplate reader (BMG Labtech), with n = 4. A cysteine calibration curve of thiol content vs absorbance was used to evaluate thiol content. A kinetic study was performed on the copolymers, using the Ellman's method described above, to analyze the thiol content during gelation, as a function of molar ratios. Polymer samples were dissolved at 1mg/mL in 0.1M PBS at pH 7.4 for both gelling systems. The poly(NIPAAm-*co*-HEMA-acrylate) solution was added to the poly(NIPAAm-*co*-cysteamine) solution at a ratio of 1:1 and 1:10 (thiol:vinyl). Similarly, the poly(NIPAAm-cysteamine-*co*-vinylsulfone) solution was added to the poly(NIPAAm-*co*-cysteamine) solution at a ratio of 1:1 and 1:10 (thiol:vinyl). The control was taken with no vinyl content. Absorbance readings were taken at 412nm (n = 4) using the same microplate reader at time points of 1min, 15 min, 30 min, 1h, 2h, 3h, 4h, and 5h.

4.2.7 Gelation Properties

For analysis of the mechanical properties of the hydrogels, rheological studies were performed using a Physica MCR 101, Anton Paar rheometer, with a sandblasted measuring plate of a 25mm diameter and a gap of 0.5 mm. Measurements of the elastic (or storage) modulus (G') and the viscous (or loss) modulus (G'') were conducted and gelation point was identified as the crosspoint of G' and G''. Samples were prepared for each copolymer by dissolving in 0.1M PBS, pH 7.4 at 30 wt%. The physical, chemical and physical-chemical gelation properties of the copolymers were analyzed, as well as the gel point. Time sweeps

(3600 sec) of the copolymers mixed at 30 sec, 1 and 2 minutes were performed at 37°C with a frequency of 1Hz, a normal force control of 1N and a controlled stress of 10Pa. The copolymers were mixed stoichiometrically at a ratio of 0.48: 1 (poly(NIPAAm-*co*-HEMA-acrylate): poly(NIPAAm-*co*-cysteamine)) and a ratio of 3:2 (poly(NIPAAm-cysteamine-*co*-vinylsulfone): poly(NIPAAm-*co*-cysteamine)) in 3cc syringes via syringe couplers, at 2 strokes per minute, and 0.6mL of the solution was injected upon the rheometer plate. The copolymers were mixed at room temperature. The mixing of the components results in the chemical reaction between the vinyls and the thiols, and thus, cross-linking of the polymer network. Following gelation, frequency sweeps were conducted with a logarithmic ramp ranging from 0.01 to 100Hz at 20°C (for chemical gels) and 37°C (for physical gels), under similar conditions. For physical-chemical gelation, the copolymers were mixed as described above, loaded onto the rheometer plate (0.6mL) at 37°C, followed by measurements performed with time and frequency sweeps as described above. Temperature sweeps were also conducted on the gels after 1 minute of mixing at stoichiometric ratios, with a temperature range of 0-70°C, at a heating rate of 1°C/min, with a frequency of 1Hz and controlled stress of 10 Pa.

4.2.8 Swelling and Degradation Studies

Each copolymer was dissolved at 30 wt% in 0.1M PBS, pH 7.4, mixed stoichiometrically at a ratio of 0.48: 1 (poly(NIPAAm-*co*-HEMA-acrylate): poly(NIPAAm-*co*-cysteamine)) and a ratio of 3:2 (poly(NIPAAm-cysteamine-*co*-

vinylsulfone): poly(NIPAAm-*co*-cysteamine)) for 2.5 min at room temperature using 3cc syringes and a syringe coupler. The copolymer systems were placed in a hot room at 37°C for 24h to allow for further curing. The cylinder-shaped gels were then removed from the syringe, cut into 0.3cm long pieces (total of 9 pieces for each gelling system), weighed, and incubated in PBS, pH 7.4 vials at 4, 22 and 37°C. Samples (n = 3 for each temperature for each gelling system) were weighed (after dabbing with wet towel) at time intervals of 2, 4 and 7 days. The swelling ratio was defined as $[(W - (W_0 \cdot 0.3))/(W_0 \cdot 0.3)]$, where W is the weight of the swollen gel and $W_0 \cdot 0.3$ is the original weight of the gel multiplied by the ratio of polymer in the system. For the degradation study, those gel samples were measured at longer time points of 1, 30, 60, 90, 120, 150, 180 and 210 days.

4.2.9 Cytotoxicity

For sterilization purposes, the polymers were dissolved in a biosafety hood at 30wt% in sterile PBS pH 7.4. After allowing 24h to completely dissolve, the solutions were aspirated into 3cc syringes and mixed stoichiometrically for 2.5min in the biosafety hood. Mouse fibroblast cells (3T3 cell line) were seeded in a 24 well plate at 20,000 cells per well with 0.5mL of cell culture medium in each well. Cell culture medium consisted of Dubelcco's Modified Essential Medium (DMEM) with addition of 5% calf serum, 1% L-glutamine and 1% penicillin/streptomycin. Cells were incubated at 37°C with 5% CO_2 for 1 day prior to testing of materials. A standard curve was set up ranging from 500,000 down to 0 cells per well. While keeping the well plate on a hot plate at 37°C,

inserts (8μm pore Transwell) were placed in two rows (one row for each gel, n = 5 for each gel). The gels were then injected at 0.1mL per insert. The cells were incubated for 3 days with the gels to observe proliferation results. Control wells contained cells only. After 3 days, the inserts containing the gels were removed, the medium changed, wells washed with PBS and new medium was added to each well (0.5mL). Promega (Promega CellTiter 96® Cell Proliferation Assay) solution was added at a 1:5 ratio (per manufacturer recommendation), thus 0.1mL per well. The cells were allowed to sit with the Promega solution for 3 hours, after which, the absorbance was measured at 490nm using a FLOstar Omega microplate reader (BMG Labtech; Offenburg, Germany).

4.2.10 Scanning electron microscopy (SEM)

Polymer samples were dissolved at 30wt% and mixed stoichiometrically for 2.5min in 3cc syringes. The gels were cured at 37°C for 24h and removed from the syringes, cut into 0.3cm pieces with a razor blade and lyophilized. Gel samples were coated with gold, mounted on the stage, and placed in the FEI XL 30 SEM. Samples were imaged at a working distance ranging 6.2-6.7mm, using an accelerating voltage of 25kV and at magnifications of 500 and 2000, as well as other magnifications (not reported here) to obtain further information on the structures of the gels.

4.2.11 Statistical Analysis

The means and standard deviations of the swelling and cytotoxicity data were analyzed using a two-sided *t*-test, while a single-factor analysis of variance (ANOVA) test was performed for the degradation study, with a level of significance set at $p < 0.05$ for both tests.

4.3 Results and Discussion

4.3.1 Synthesis and Chemical/Structural Characterization of Copolymers

As demonstrated in Figure 4.1, two physical-chemical gelling systems were investigated. One involves poly(NIPAAm-*co*-cysteamine) (NC) and poly(NIPAAm-*co*-HEMA-acrylate) (NHA) while the second consists of poly(NIPAAm-*co*- cysteamine) (NC) and poly(NIPAAm-*co*-cysteamine-vinylsulfone) (NCVS). These two gelling systems were compared in order to determine the optimal properties of the gels. Both gelling systems undergo simultaneous physical and chemical gelation. All copolymers contain the thermoresponsive polymer poly(NIPAAm), which undergoes chain collapse at higher temperatures as it is subjected to a phase transition around 31°C (Heskins & Guillet, 1968). Additionally, the two gelling systems form covalent cross-links through a Michael-type addition reaction. The particular thiol and vinyl precursors for network formation are ideal in that the gelation properties can be controlled through addition of a basic catalyst. The advantage of these two gelling mechanisms is that they both can occur at physiological temperature and pH, and

that they are water-based which decreases the possible risk of damage or toxic effects seen with systems using organic solvents (Chaloupka et al., 1999; Dudeck et al., 2006; Murayama et al., 1998; Ruel-Gariepy & Leroux, 2004).

Figure 4.2 demonstrates the synthesis procedure for poly(NCVS). A 50-fold molar excess of divinylsulfone was used to minimize potential disulfide bonding in the system. TEA was used to assist in deprotecting the hydrochloride as well as the base catalyst to deprotonate the thiol on poly(NC), allowing the Michael-type addition reaction to take place between the thiol on poly(NC) and the vinyl on poly(NCVS) (Mather et al., 2006). The synthesis of poly(NCVS) was confirmed using ^{1}H NMR and FTIR. As seen in the ^{1}H NMR spectrum (Figure 4.3), characteristic vinyl sulfone peaks are found at 6.2, 6.4 and 6.8ppm (Seliktar, Zisch, Lutolf, Wrana, & Hubbell, 2004).

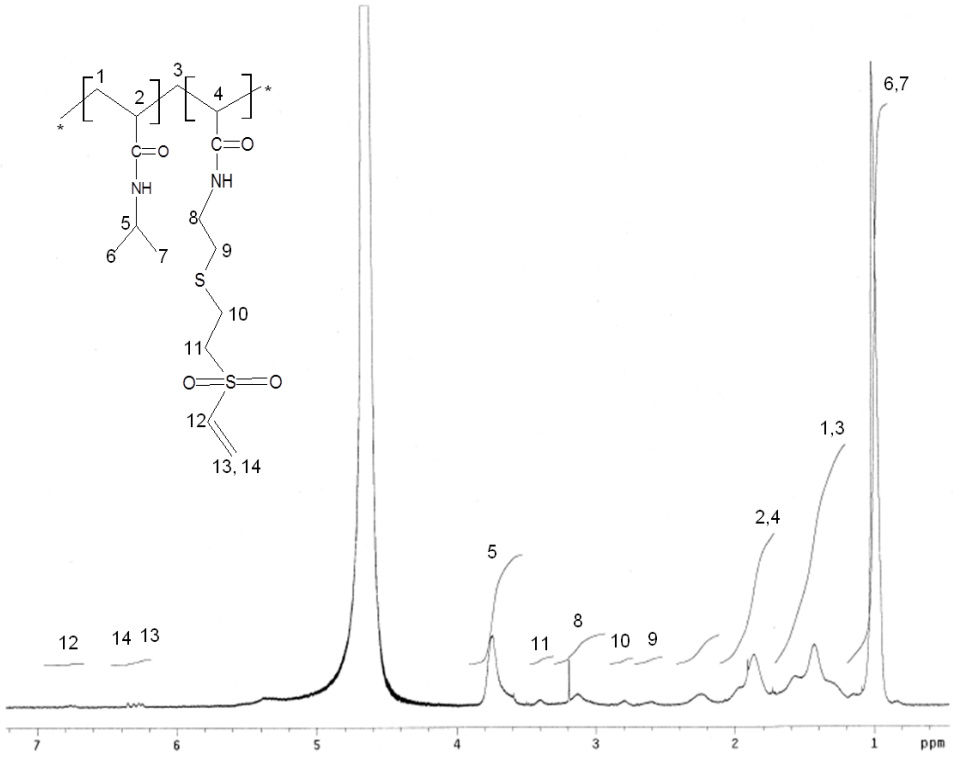

Figure 4.3 ^{1}H NMR spectrum of poly(NIPAAm-cysteamine-*co*-vinylsulfone), with labels of the respective H atoms identifying the corresponding peaks of its structure.

The methylene protons of the cysteamine are also shown around 2.6 and 3.2ppm, while the methylene protons of the newly formed covalent cross-link between the divinyl sulfone and the cysteamine are illustrated at 2.8 and 3.4ppm. The solvent peak for D_2O is observed at 4.79ppm. The remaining peaks on the spectra are depictions of the protons representative of the poly(NIPAAm) structure. It can be noted that the peaks characteristic of the cysteamine-vinylsulfone group are much smaller in amplitude than those of the poly(NIPAAm) structure as expected, due to the much larger ratio of NIPAAm in the copolymer than cysteamine-

vinylsulfone (molar ratio of NIPAAm:cysteamine-vinylsulfone being 98:2). FTIR was additionally used to verify the chemical and structural composition of the synthesized copolymer and the results are reported in Figure 4.4. The most important peak to notice on the spectrum, showing a strong absorption band at 1350-1300 cm^{-1}, depicts the sulfone group (Silverstein & Webster, 2006). The other peaks observed in the spectra are representative of the prominent NIPAAm structure.

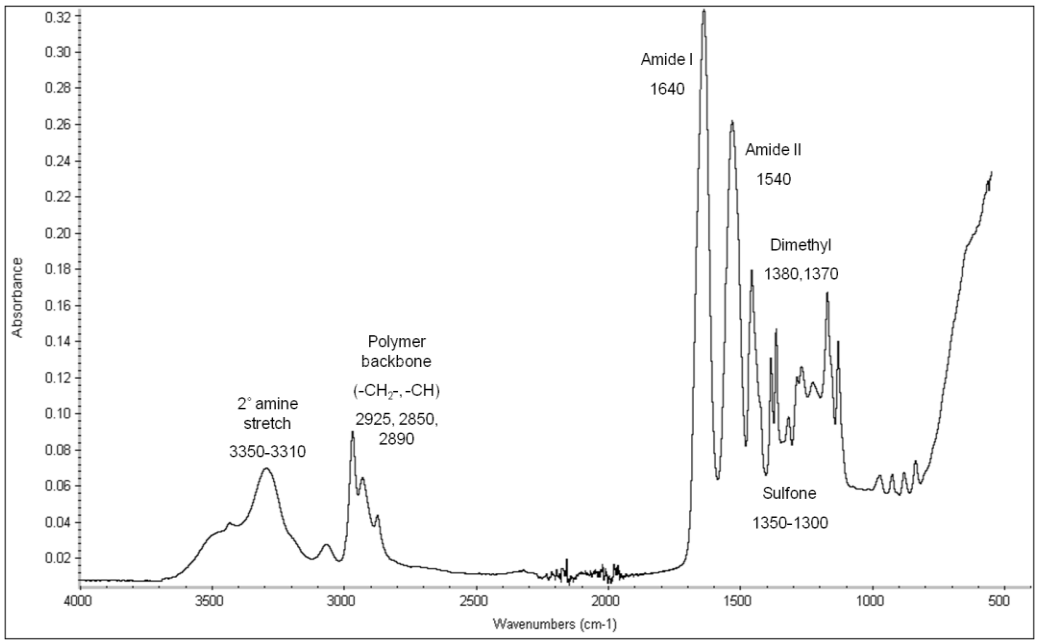

Figure 4.4 FTIR spectrum of poly(NIPAAm-cysteamine-*co*-vinylsulfone), verifying the structural composition of the copolymer.

4.3.2 Thermal Properties of Copolymers

For temperature-responsive polymers, determining their phase transition properties and temperature is crucial in understanding their behavior and to better tailor them for their particular applications. As reported in 1968 by Heskins, poly(N-isopropylacrylamide) shows a lower critical solution temperature (LCST) at 31°C in aqueous solutions (Heskins & Guillet, 1968). Using differential scanning calorimetry (DSC), the lower critical solution temperatures (LCST) of the copolymers were determined and reported in Figure 4.5.

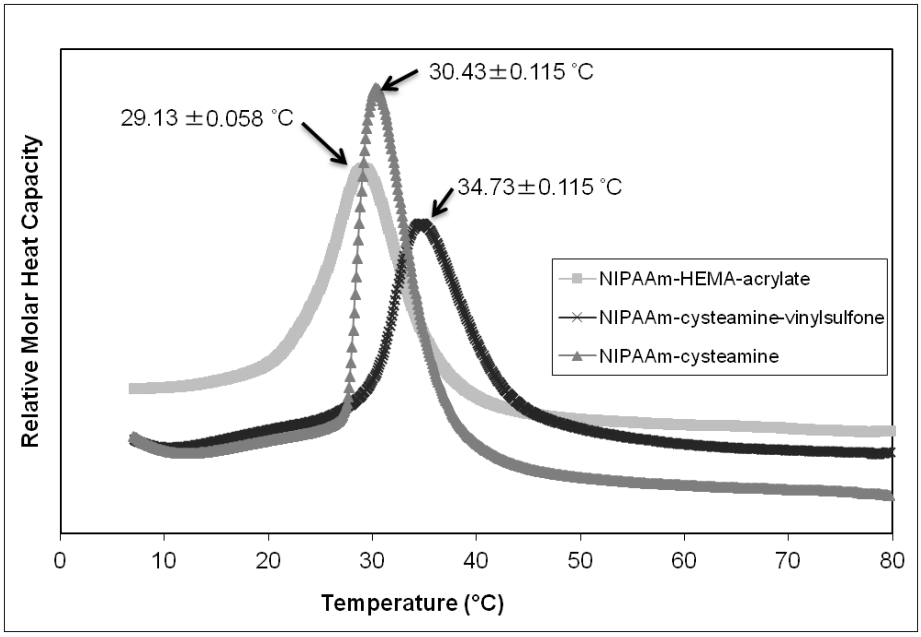

Figure 4.5 DSC curves of the various copolymers, with the peaks indicating their LCST point. All copolymers show LCSTs below physiological temperature, making them feasible for use *in vivo.*

As can be seen, the various copolymers have differing thermal curves. Poly(NCVS) shows a LCST around 34°C, when compared to poly(NC) with a LCST value at 30°C and poly(NHA) at 29°C. Poly(NCVS) has the highest LCST value amongst the copolymers due to the hydrophilic sulfone group present on the copolymer. It can be observed that the copolymer starts going through the phase transition around 30°C, close to the homopolymer NIPAAm's LCST. It has also been demonstrated that as more hydrophilic comonomers are added, there is a corresponding increase in the LCST observed, as it has also been shown that there is a decrease in LCST with more hydrophobic comonomers (Jeong & Gutowska, 2002a; Vernon & Martinez, 2005). The shift to the right is attributed to the added hydrophilic groups. The increase in LCST occurred as the hydrogel was better able to maintain its hydrated state at higher temperatures, due to the hydrophilic groups (Brazel & Peppas, 1995). Feil et al. proposed that this phenomenon occurs because the addition of hydrophilic comonomers diminishes the amount of hydrophobic groups and increases the overall hydrophilicity of the polymer, due to the strong interactions between water and the hydrophilic groups on the polymer (Feil, Bae, Feijen, & Kim, 1993a). The poly(NCVS) curve is also broader than that of poly(NC). Broader peaks demonstrate the less homogeneous nature of the copolymer. Since poly(NC) is mainly NIPAAm (98:2), it has a sharp peak around the poly(NIPAAm) temperature and does not possess as much inhomogeneity as poly(NCVS). Poly(NC) demonstrates that its chains experience a simultaneous collapse within a narrower range of temperatures. Poly(NCVS) has the potential to have more combinations from the outcome of polymerization,

for example, polymer chains with or without cysteamine and polymer chains with or without cysteamine-vinylsulfone. In a copolymer, there is a statistical distribution of the comonomers which leads to a different structure of the water bound to the polymer chain, when compared to the homopolymer (Kuckling et al., 2000). This different structure results in a broader distribution of transition temperatures, and thus, a broader curve. Additionally, the broad thermogram can be a result of the different chain lengths present in the copolymer (see polydispersity values in Table 4.1).

Table 4.1 Properties of the three copolymers, with their corresponding initial and actual molar feed ratios determined via ^{1}H NMR, LCSTs, molecular weights and polydispersities.

Name	Feed ratios		Monomer composition (mole ratio)		DSC (°C)	MW ($\times 10^4$ g/mol)	PDI
	NIPAAm	Cysteamine	NMR	Ellman method			
NIPAAm-*co*-cysteamine	98	2	99:1	98:2	30.4±0.12	3.694	1.660
	NIPAAm	HEMA-acrylate					
NIPAAm-*co*-HEMA-acrylate	95	5	97:3	-	29.1±0.06	6.103	1.541
	NIPAAm	Cysteamine-vinylsulfone					
NIPAAm-*co*-cysteamine-vinylsulfone	98	2	98:2	-	34.7±0.12	5.008	1.432

The higher molecular weight chains of the copolymer are represented in the sharp peak, whereas shorter chains cause the broadening of the curve (Schild & Tirrell, 1990a). An increasing content of comonomers, deviating from poly(NIPAAm)

homopolymer, also results in broader endotherms (Y. H. Bae et al., 1991). This can explain the broad endotherm also experienced by poly(NHA). Since both poly(NCVS) and poly(NHA) have to undergo more steps for copolymerization than poly(NC), there are more likely combinations and distributions for the polymer chains. With shorter and longer chains, the inhomogeneity in the chain lengths will initiate phase transition at different temperatures, resulting in broader thermograms. Poly(NC), on the contrary, has one less step of copolymerization than its counterparts, resulting in more homogeneous chains and a sharper and narrower peak. Since poly(NHA) has hydrophobic comonomers on its polymer chain (acrylates), a decrease in the LCST is noted.

4.3.3 Rheological Properties of Gelling Systems

The time it takes for a solution to transform from a liquid state to a gel state is crucial, especially for *in vivo* applications. Knowledge of the gelation mechanics is thus important in not only understanding the phenomena involved in the formation of the gel, but also in better comprehending the behavior of the gel as well as predicting its potential performance once injected in the body. To analyze the mechanics of gelation for the given physical-chemical gels, rheology was used. Rheology tests provide information on the in-phase, shear storage modulus and the out-of-phase, shear loss modulus of the gel when exposed to shear stress or strain (Kavanagh & Ross-Murphy, 1998). The former is often referred to as the elastic modulus, denoted as *G'*, and the latter as the viscous modulus, denoted as *G''*. Thus, in the liquid state, *G''* dominates and as the

solution evolves from a liquid to a solid, *G'* will start to take over *G''*, eventually surpassing it. Once *G'* has crossed over and has become the dominant factor, the elastic behavior marks the transition into the solid state. By analyzing the *G'* and *G''* output curves as well as the crossover between the two lines, one can infer about the viscoelastic behavior of the hydrogel as well as its time dependence. The results of the rheological time sweep of both gelling systems are presented in Figure 4.6.

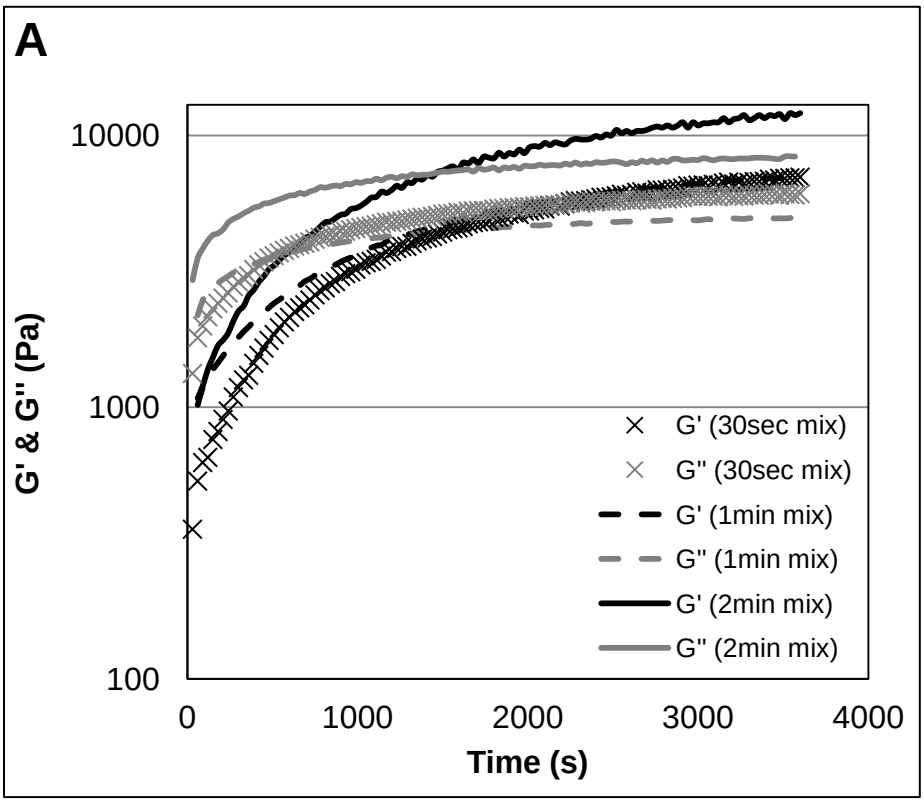

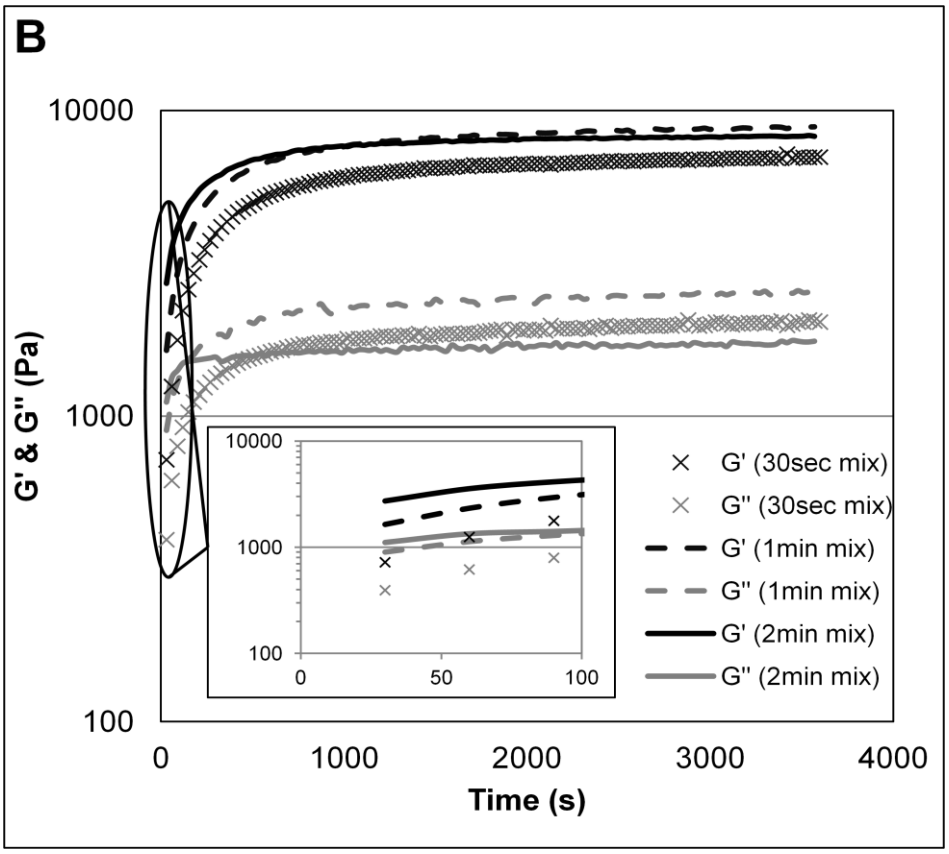

Figure 4.6 Rheological time sweeps demonstrating the difference in gel time of A) gelling system 1 (NC-NHA) compared to B) gelling system 2 (NC-NCVS) at varying mixing times of 30s (×), 1min (dashed line) and 2min (solid line) at 37°C. Black indicates *G'* values and gray indicates *G''* values.

Several differences can be noted when comparing the behaviors of the two hydrogels. For NC-NHA (Figure 4.6A), it can be observed that *G''* dominates over *G'* at the beginning of the time sweep, for the different mixing times. This demonstrates that the components are still in the liquid phase. At a certain time, *G'* starts to overtake *G''* and that time point varies, depending on the mixing time.

For the different mixing times, gelation occurs within 22 to 37 minutes. The longer the copolymers are mixed, the more the mixture becomes homogeneous and facilitates the covalent cross-link formation in the system, thus resulting in a gel at an earlier time. Overall, it appears that it takes time for the chemical gelation to take place in this system, as observed with the initial liquid-like characteristic which later develops into the solid phase of the system. On the contrary, for NC-NCVS (Figure 4.6B), it can be seen that at the different mixing times, a gel was formed immediately. As soon as the mixed components were injected on the rheometer plate and the first reading was taken, the mixture had already formed a gel. In the close-up box, one can notice that at the first point, the *G'* values are higher than the *G''* values, for all 3 mixing times. This not only indicates that it has already become a gel, but also that the gelling mechanics may not appear to be dependent on time because regardless of the duration of mixing, the components formed a gel rapidly. The reason for this difference in the gelation time between NC-NCVS and NC-NHA is attributed to the reactivity of the functional groups. NC-NCVS may have a higher cross-linking functionality than NC-NHA and the vinylsulfone groups on NCVS have a higher reactivity toward Michael-type addition reaction than do the acrylate groups on NHA; these characteristics have been observed in previous studies (Hiemstra et al., 2007; C. Lin et al., 2010).

Aside from time to gelation, one can also determine the mechanics of the hydrogels from rheological results. These hydrogels behave viscoelastically; going from a viscous liquid to an elastic solid during the gelation process. The

discussed hydrogels undergo two gelling mechanisms: physical and chemical. Ultimately, it is favorable that a combination of both physical and chemical gelation may render these hydrogels better materials for their applications by providing improved gelation kinetics and mechanical properties (Hacker et al., 2008). In Figure 4.7, rheological frequency sweeps are presented for both gelling systems for comparison of the mechanical properties and strength achieved. Physical gels entail the use of poly(NC) alone and poly(NHA) alone, after having gelled for 1hr.

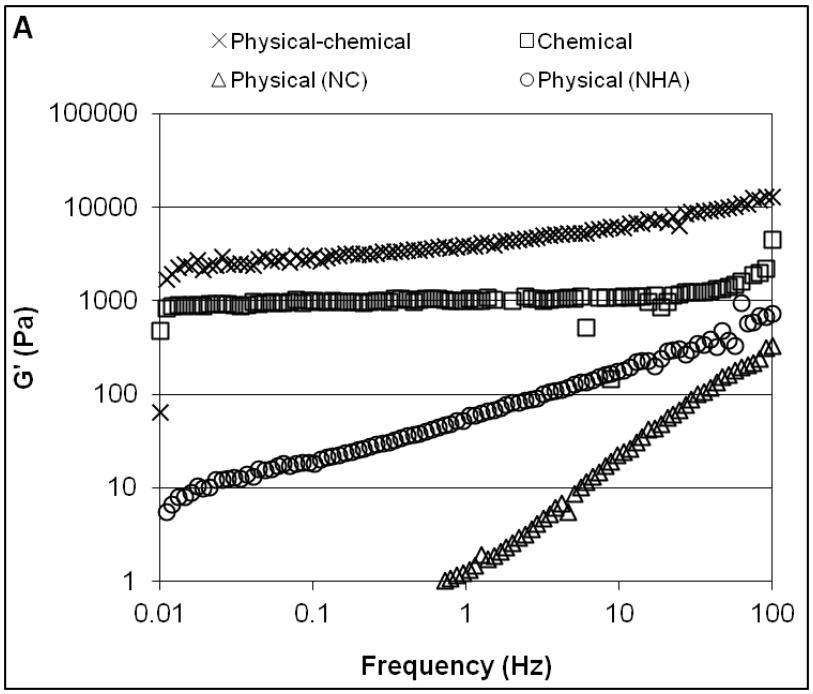

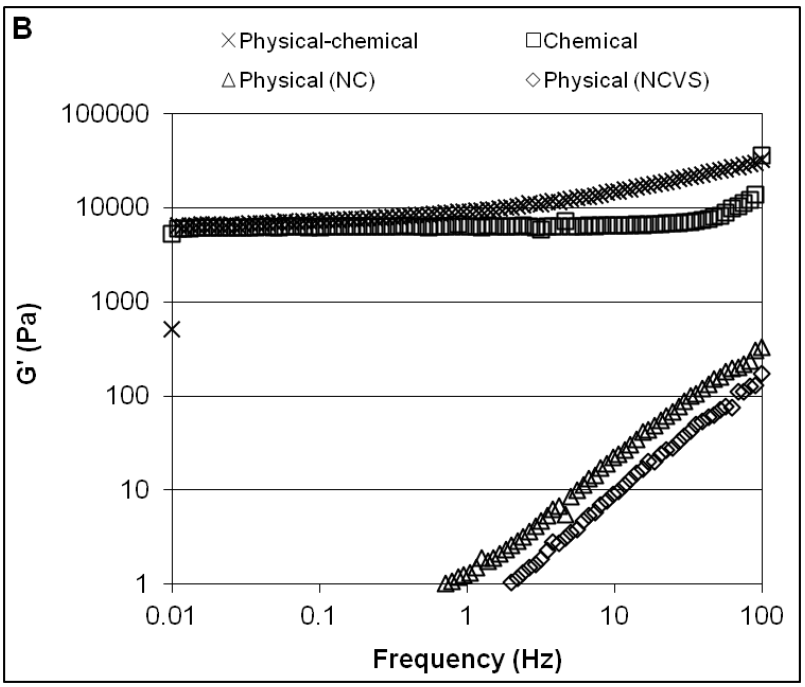

Figure 4.7 Analysis of mechanical strength using rheological frequency sweeps for A) gelling system 1 (NC-NHA) and B) gelling system 2 (NC-NCVS). The *G'* data show that the combination of physical-chemical gelation for either system results in decreased creep and increased strength, over purely physical and purely chemical gels.

In Figure 4.7A, one can notice that the purely physical gels, which are poly(NC) (Δ) and poly(NHA) (○), show frequency-dependent behaviors. The slope of the lines for the physical gels demonstrates vulnerability to viscoelasticity. At low frequencies, both copolymers have low *G'* values, indicating liquid-like behavior, and as the frequency is increased, the *G'* values of the physical gels increase as well, illustrating a more solid-like behavior. Nonetheless, this frequency-

dependence is not desirable for gels that will be used *in vivo*, as they would not form strong enough gels and would be less likely to withstand the low-frequency stress experienced in blood vessels. The chemical gel comprised of poly(NC) and poly(NHA) mixed together via 3cc syringes and a syringe coupler at room temperature for 1 min at 2 strokes/min. The mixing allows for the formation of the covalent cross-links through the Michael-type addition reaction, between the thiols on the cysteamine of poly(NC) and the acrylates of poly(NHA), prior to its deposition on the rheometer plate. After mixing, the gel was loaded onto the rheometer plate at 20°C and was exposed to the same stress and frequency sweep as mentioned above. The line for the chemical gel (□) does not illustrate frequency-dependence, thus overcoming the viscoelastic flow experienced by purely physical gels at low frequency stress. Additionally, an important observation is the higher *G'* values attained by the chemical gel, reaching a strength of 1000 Pa. For the testing of the physical-chemical gel, the components (poly(NC) and poly(NHA)) were mixed under the same conditions as previously stated and loaded on the rheometer plate at 37°C. Chemical gelation was achieved through the covalent cross-links formed by the chemical reaction as the copolymers are mixed and the physical gelation was undertaken as the polymer solution was heated to 37°C, or above the LCST. From the results, it can be seen that the combination of physical and chemical gelation (×) surpassed the strength achieved by the purely chemical gel, with *G'* values reaching 10,000 Pa. Furthermore, combining chemical gelation with physical gelation helped in reducing the frequency-dependence observed with purely physical gels under low

frequency stress. In Figure 4.7B, similar observations can be made for the second gelling system, poly(NC) with poly(NCVS). The purely physical gels, poly(NC) (Δ) and poly(NCVS) (◊) alone, show analogous frequency-dependence observed with the former gelling system. Of the three solely physical gels presented in Figure 4.7, one can notice the higher strength achieved by the poly(NHA) physical gel when compared to poly(NC) and poly(NCVS). The hydrophobic nature of the acrylates on poly(NHA) cause it to increase the mechanical strength of the overall gel (Qiu & Park, 2001a). An interesting observation with the chemical gel (□) (poly(NC) mixed with poly(NCVS) at 20°C) is that unlike the other gelling system, this one attains higher mechanical strength, with *G'* values almost reaching 10,000 Pa. The reaction between the thiols of the cysteamine on poly(NC) and the vinyls on poly(NCVS) happens more rapidly and at higher cross-linking completion than do poly(NC) with poly(NHA) due to the higher reactivity of vinysulfones than acrylates through the Michael-type addition reaction (refer to kinetic studies). The higher storage modulus (*G'*) values attained can also be attributed to the higher cross-linking density of the NC-NCVS hydrogel. The physical-chemical gel formed via NC-NCVS (×) seems to achieve higher strength than the former physical-chemical gel (NC-NHA), which may be ascribed to the faster and further extent of chemical reaction happening between the thiols and the vinyls of the NCVS.

Rheological temperature sweeps were additionally performed on the gelling systems to observe their thermal as well as swelling/shrinking behavior as a function of temperature. For the study, the *G'*, *G''* and δ values were recorded

for each gel mix from 0 to 70°C. Here, δ represents the phase angle (0 to 90°), which is the phase difference between the input variable and output variable ($\tan\delta = G''/G'$) (Stile et al., 1999). This variable assists in characterizing viscoelastic solids or liquids; for a purely elastic material, the stress wave is exactly in phase with the strain wave ($\delta \sim 0°$), while for a purely viscous material, the stress wave is out of phase with the strain wave ($\delta \sim 90°$) (Kuckling et al., 2000).

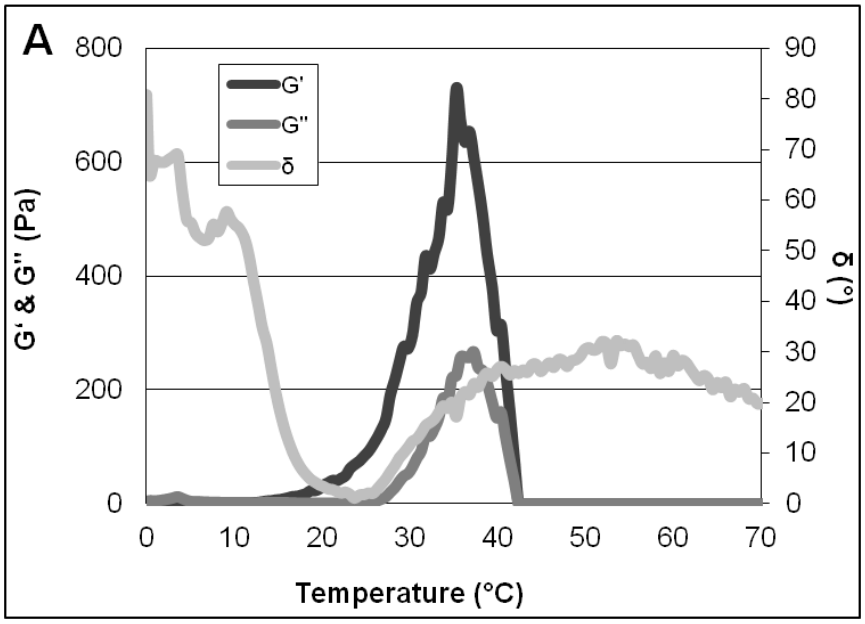

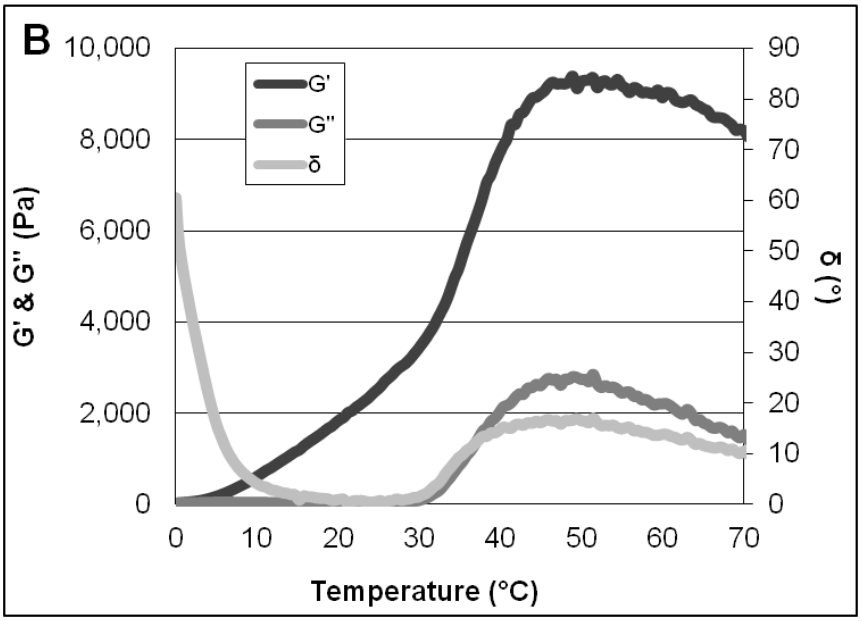

Figure 4.8 Temperature sweeps via rheology for A) gelling system 1 (NC-NHA) and B) gelling system 2 (NC-NCVS), with both systems demonstrating higher *G'* values when approaching LCST and undergoing gelation; additionally, both systems experience slight shrinking above LCST.

As can be seen in the temperature sweep of the NC-NHA system (Figure 4.8A), at low temperatures, the *G'* and *G''* values are low and δ decreases to reach 0°. This decrease in δ is indicative of the elastic behavior associated with chemical gelation and covalent cross-links formation. As the temperature approaches the LCST, *G'* starts to increase and overtake *G''* around 12°C. The moduli values increase dramatically near the LCST of the copolymers, while δ starts to increase from 0°. Thus, as the temperature approaches the LCST, physical entanglements are formed, resulting in viscoelastic cross-links which increase the overall

strength. These physical viscoelastic cross-links can rearrange themselves, and therefore, the increase in the phase angle is observed. The drop in the moduli and the slight noise observed at the high end of the temperature scale is result of the gel shrinking and releasing water. The rheometer head then loses contact with the gel and measures the water layer. Similar behavior is observed in the NC-NCVS system (Figure 4.8B); however, *G'* is seen to increase and overtake *G''* at lower temperatures, indicating that chemical gelation in this system is more important and leads to the formation of a gel rapidly after mixing. This gel then strengthens as physical gelation occurs near the LCST of the system. The δ value indicates that a gel is formed around 18°C. Due to a slight degree of shrinking experienced, the moduli and δ values slightly decrease with the presence of water on the gel. When comparing the two gelling systems, one can observe the higher *G'* values (by one order of magnitude) achieved by the NC-NCVS system when compared to the NC-NHA system. This correlates to the one order of magnitude difference witnessed in the frequency sweeps of the two systems.

4.3.4 Kinetic Rates of Chemical Cross-link Formation

Michael-type addition reaction, also termed conjugate addition, is a reaction between nucleophiles and activated olefins which leads to the addition of the nucleophile across the carbon-carbon double bond (Mather et al., 2006). Due to its mild conditions for reaction, it can occur at physiological pH and temperature. In the systems presented here, the Michael addition reaction takes

place between the thiol on the cysteamine and the vinyl on either the divinyl sulfone of NCVS or the acrylate of NHA. To better understand the mechanism by which each system undergoes Michael-type addition reaction to form covalent cross-links and the difference in time observed in the gel point, kinetic studies were performed. These kinetic studies investigated the rate of reaction between thiols and vinyls of the two gelling systems at different molar ratios. In one study, NIPAAm-*co*-cysteamine was combined with NIPAAm-*co*-HEMA-acrylate at molar ratios of 1:1 and 1:10 (thiol to vinyl) at physiological pH, while in the second study, NIPAAm-*co*-cysteamine was mixed with NIPAAm-cysteamine-*co*-vinylsulfone at the same molar ratios and pH. Each was compared to NIPAAm-*co*-cysteamine only (no vinyls present) as a control.

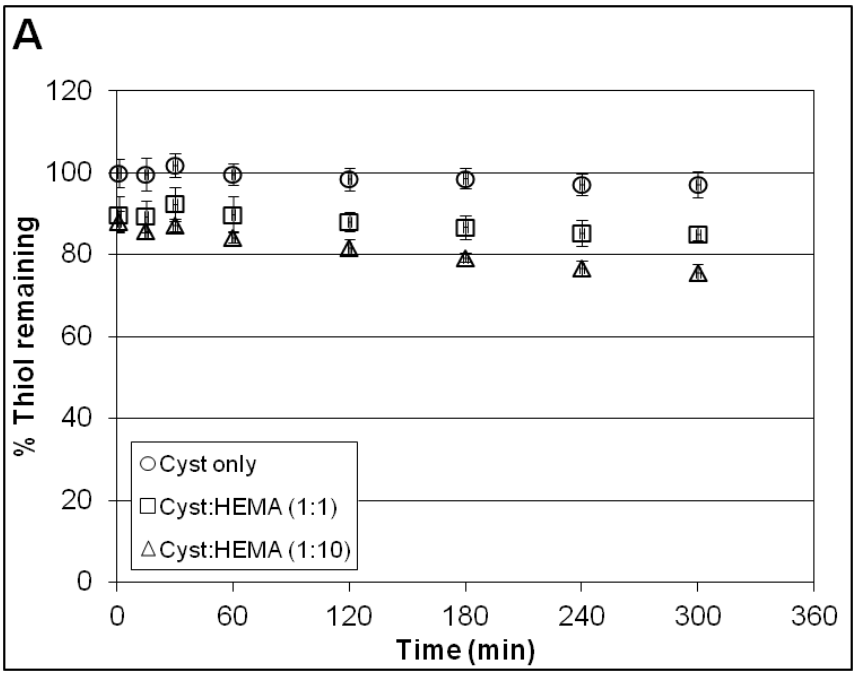

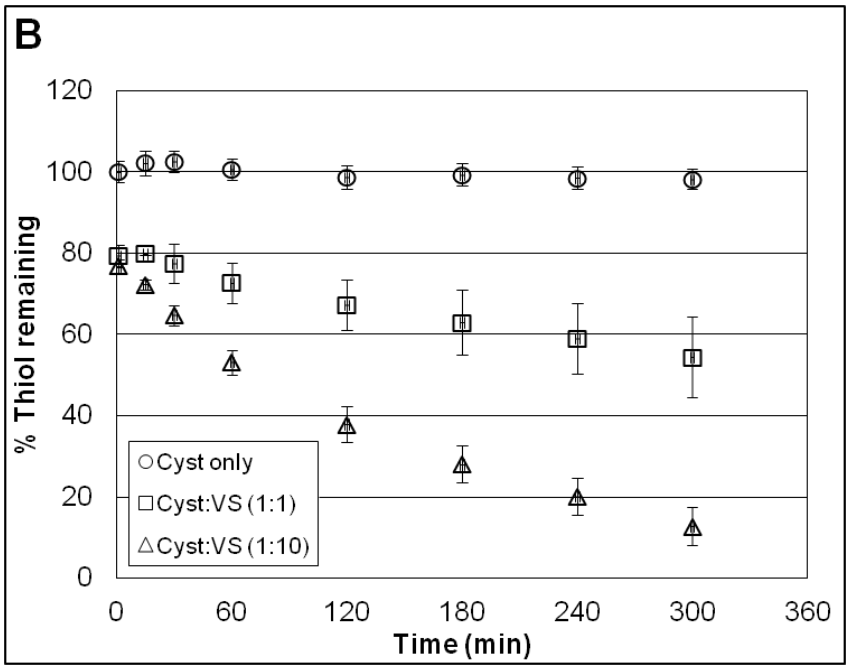

Figure 4.9 Kinetic studies performed using Ellman's reagent illustrating very different rates of reaction of thiols to vinyls between A) gelling system 1 (NC-NHA) and B) gelling system 2 (NC-NCVS) at the following molar ratios: thiols only (no vinyls) (○), 1:1 (thiol to vinyl) (□) and 1:10 (thiol to vinyl) (Δ).

As can be seen in Figure 4.9, the rate of reaction between thiols and vinyls differ significantly between the two gelling systems at the same pH of 7.4 and same molar ratios. For both gelling systems, the cysteamine only (○) curve shows relatively stable results over the course of the study, demonstrating that the number of thiols in the cysteamine only sample is not consumed over time. This in turn reveals that the formation of disulfide bonds is very slow. For the 1:1 molar ratios of thiols to vinyls (□), one can observe the difference in the slope of the curves for each gelling system. For the NC-NHA system (Figure 4.7A), thiols

are slowly reacting with the vinyls, having about 85% of thiols remaining after 5 hours. In the NC-NCVS system, the reaction at 1:1 is faster, with 54% of thiols remaining at 5 hours. As the molar ratio of thiols to vinyls is increased to 1:10 (Δ), the difference between the kinetics of the two gelling systems becomes more pronounced. When the molar ratio is increased from 1:1 to 1:10 in the NC-NHA system, the reaction is seen to happen faster; however, the difference in the rate of reaction between the two molar ratios is not very striking. The thiols remaining after 5 hours at a 1:10 molar ratio is 75%. On the other hand, this reaction is much faster at the 1:10 molar ratio for the NC-NCVS system (Figure 4.7B), with a rapid decrease in the number of thiols remaining with time, showing fast reaction of the two moieties to form covalent cross-links. After 5 hours, the number of thiols remaining in the NC-NCVS system is about 12%. The observations made from the kinetic studies of the two systems and the differences observed coincide with the results of the rheology time sweeps and help explain the different gel points of the systems. As was observed with the rheological time sweep, in which the copolymers were mixed for 30s, 1min and 2min, the NC-NHA system resulted in gel points ranging from 22 to 37 minutes. On the other hand, NC-NCVS demonstrated that a gel point was already developed within the first few seconds of the time sweep, regardless of mixing time. The kinetic studies reaffirmed that the chemical reaction in the gelling systems has an instrumental role in the overall gel formation of either system. As indicated with NC-NHA, the covalent cross-link formation of the chemical gel through the Michael-type addition reaction is very slow, thus taking a longer time for the gel point to be observed rheologically

due to this slow interaction between thiols and vinyls. The NC-NCVS system, which has a much faster reaction between thiols and vinyls and which thus rapidly forms covalent cross-links, results in the rapid creation of the gel while the components are mixed. Therefore, the gel point is detected within seconds of the rheology run. In the rheology experiments, the two components were mixed continuously for 30s to 2min before measurements were taken and were also exposed to room temperature. These conditions led to faster reaction of the thiols to vinyls for both cases, as opposed to the 5s of plate shaking and the 4°C temperature conditions of the kinetic studies, which slowed down the reaction for both cases. Nonetheless, the results of the kinetic studies correspond with the scenarios observed in the rheology runs. Mainly, faster reaction of the thiols to vinyls, thus faster gelation, in the NC-NCVS system when compared to the slower reaction and slower time to gelation observed in the NC-NHA system. The rate of chemical gelation primarily depends on how fast the double bond of the vinyl group can be broken, which is strongly influenced by the neighboring functional group. A possible explanation for the faster reaction of the vinyl on the NCVS than the vinyl on the NHA for reaction with the thiol may be due to the strong electron-withdrawing nature of the sulfonyl group on NCVS (Toru & Bolm, 2008). With a highly electron-deficient sulfonyl, compared to the ester, the bond of the sulfur atom to the α-carbon of the vinyl in NCVS becomes more polarized and thus destabilizes the double bond to a higher extent than the bond of the carbon atom to the α-carbon of the vinyl in NHA does. This in turn facilitates the breaking of the double bond and hence, the conjugate addition reaction.

4.3.5 Swelling and Degradation Behavior of Gelling Systems

The degree to which a hydrogel swells or shrinks can be a crucial factor in its potential applications. The degree of swelling can depend on various factors, which include pH, temperature, cross-linker, ionic strength, concentration, cross-linking density of the polymer network, polymerization conditions and polymer-solvent interaction parameter (Brannon-Peppas & Peppas, 1991; Elliott, Macdonald, Nie, & Bowman, 2004; Feil et al., 1992; Kabiri, Omidian, Hashemi, & Zohuriaan-Mehr, 2003). In Figure 4.10, samples of both gelling systems were analyzed for their swelling properties at different temperatures (4, 22 and 37°C) and various time intervals (2, 4, 7 days).

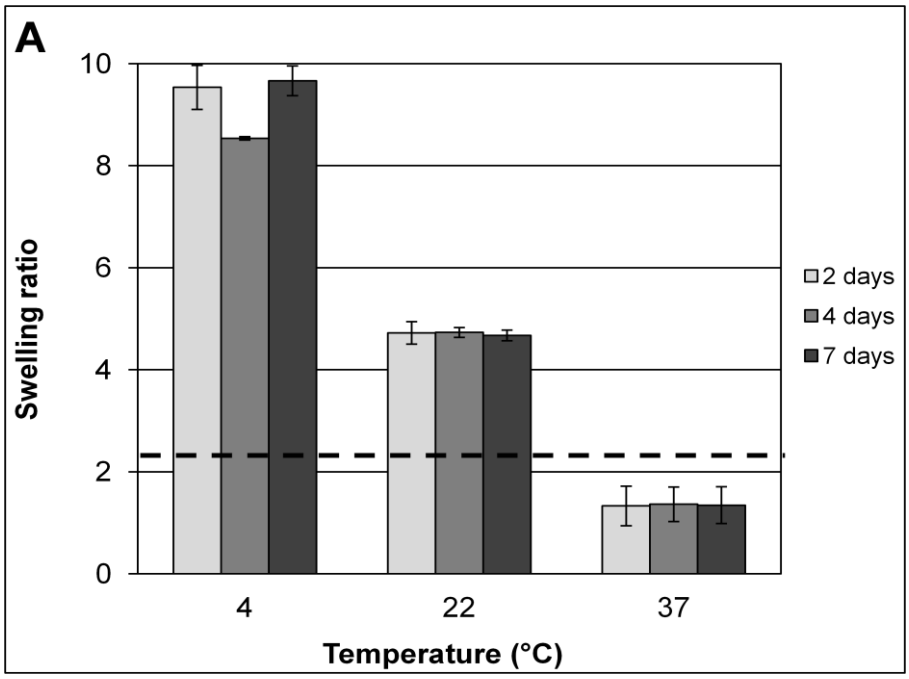

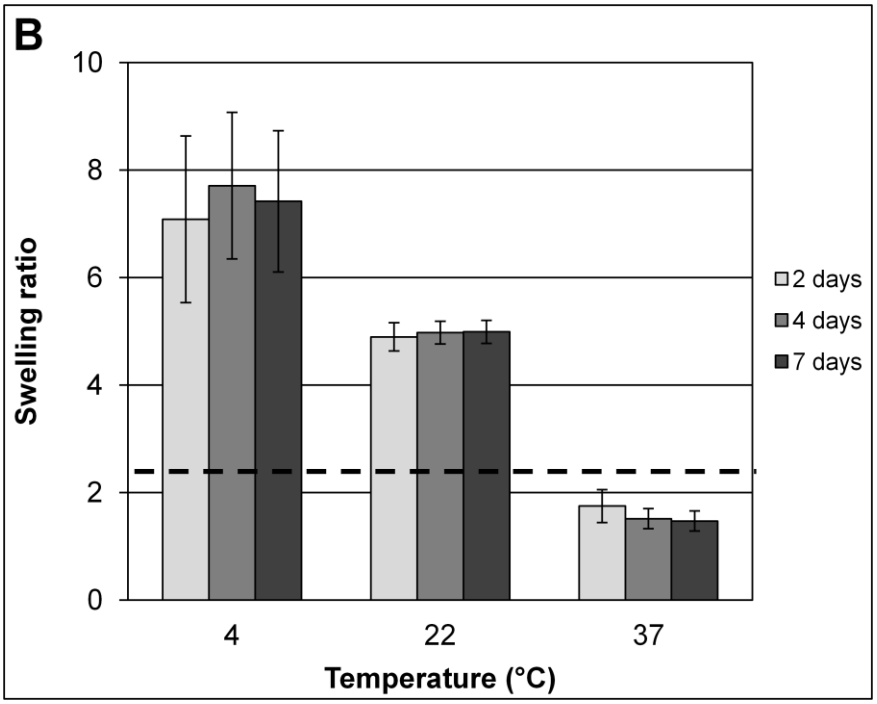

Figure 4.10 Swelling ratios of A) gelling system 1 (NC-NHA) and B) gelling system 2 (NC-NCVS) over the course of 2, 4 and 7 days at different temperatures (4, 22 and 37°C). Both systems show temperature-dependence of the swelling ratio, with a trend of increased swelling as the temperature is decreased. Dashed line indicates original swelling ratio.

By looking at the samples at the different temperatures, one can notice a decrease in the swelling ratio with an increase in the temperature, a trend previously reported with similar materials (Bearat et al., 2011; B. H. Lee et al., 2006; Robb, Lee, McLemore, & Vernon, 2007a). At low temperatures (4 and 22°C), the gel is influenced by chemical cross-links only. As the temperature is increased above the LCST, physical association of the NIPAAm chains is now also an influential

factor to the gel. With both forms of gelation occurring at 37°C, allowing for more cross-links and entanglements in the gelling system, less swelling is therefore experienced by both gels. At 37°C, both hydrogels demonstrated some degree of shrinking, when compared to the original swelling ratio of the gel samples (dashed line). At each temperature, both gelling systems did not show a difference over the course of the days (except for the NC-NHA samples at 4°C). Thus, most samples of either gel reached equilibrium swelling within the first 2 days. When comparing the swelling ratios between the two gelling systems, no difference was observed between samples at 4, 22 and 37°C over the time course; however, only one sample (4°C, 7 days) demonstrated a difference between the two gels. Although there was slight statistical difference observed between the degrees of swelling of the two gelling systems, it is interesting to note that at 4°C, the NC-NCVS samples appear to have lower swelling ratios than the NC-NHA samples. However, as temperature was increased, the NC-NCVS samples seem to possess greater swelling ratios than the NC-NHA samples. This indicates that temperature has a more important effect on the NC-NHA samples. Although the vinylsulfone present in the NC-NCVS gelling system is highly hydrophilic, chemical gelation played an important role in the formation of the gel. Thus, the chemical cross-links were formed rapidly, preventing the system from undergoing too much swelling.

Determining if a material degrades over time is highly important, especially if degradation would occur in the body and result in release of undesirable by-products which can be toxic in high concentrations. Polymer

degradation may occur through two processes: passively through hydrolysis or actively by enzymatic reaction (Gopferich, 1996). However, most biodegradable materials undergo degradation through hydrolysis. Passive hydrolysis is influenced by various factors, including the nature of the chemical bond, pH, copolymer composition and water uptake (Gopferich, 1996). Since the NC-NHA gelling system contains ester groups, which are vulnerable to hydrolysis, it is therefore crucial to analyze the degradation properties of the hydrogels. By measuring the swelling ratios over the course of 210 days, both hydrogels were compared for changes in their swelling ratios. In Figure 4.11, the data points at 30 day intervals over the period of 210 days are recorded for both NC-NCVS and NC-NHA gelling systems. By running an ANOVA test, it was determined that there is no difference in swelling ratio between all of the time points of the NC-NHA system as well as the NC-NCVS system. With the swelling ratio not showing any significant changes over time, the results indicate that both gelling systems do not undergo degradation over the 210 days.

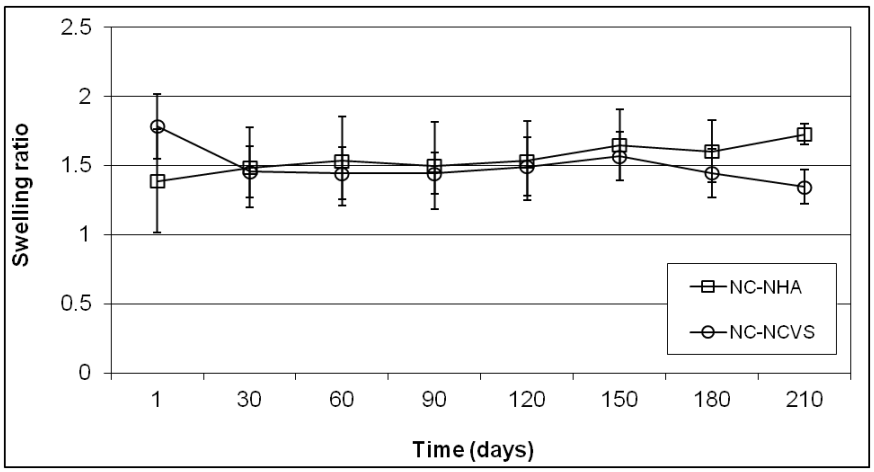

Figure 4.11 Degradation behavior of both gelling systems over the course of 210 days; both gels remain stable and do not show signs of degradation.

4.3.6 SEM analysis of morphologies of hydrogels

To further investigate the swelling behavior of the gels as well as their morphologies and structures, scanning electron microscopy (SEM) was used. After mixing the copolymers for 2.5 min and allowing them to cure at 37°C for 24h, it was interesting to observe that the NC-NCVS gel had shrunk in the syringe while the NC-NHA gel did not undergo any shrinking within these 24 hours. During curing, the NC-NCVS gelling system had experienced a 12% loss of water. The shrinking undergone by one of the gelling system and the lack thereof by the other gelling system explains the striking differences observed in the SEM images, reported in Figure 4.12 (A-D).

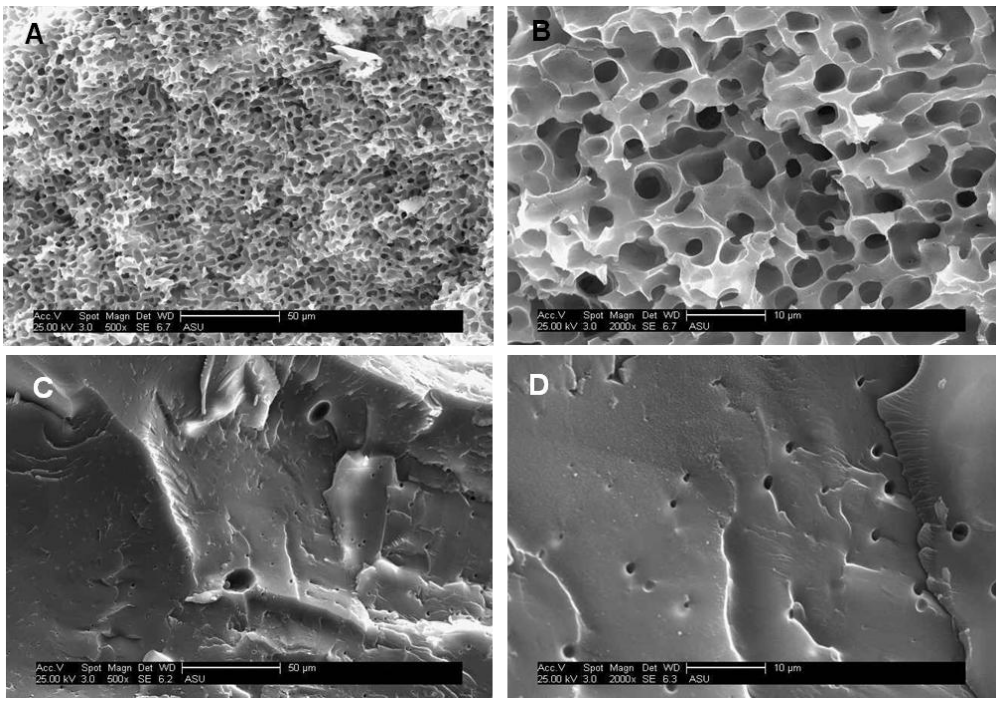

Figure 4.12 SEM images of the gels at various magnifications, A) NC-NHA at 500x, B) NC-NHA at 2000x, C) NC-NCVS at 500x and D) NC-NCVS at 2000x. The morphologies of the two gels differ greatly, with a channel-like, porous structure of NC-NHA compared to a dense, non-porous structure of NC-NCVS.

For the NC-NHA gel, a plethora of pores are observed at 500x (A), giving it a sponge-like structure. At 2000x (B), the pores have a much greater diameter, ranging from 2.9 to 9.4μm. This hydrogel appears to have the presence of interconnected channel-like pores. On the contrary, at a magnification of 500x (C), the NC-NCVS gel demonstrates a very dense polymer phase with very few pores, and at a higher magnification of 2000x (D), one can notice some scattered pores, ranging 0.6-2.4μm in diameter, but mainly a solid polymer phase. The

fundamentally different porous structure observed between the two gelling systems can be attributed to the degree of shrinking which each gel had experienced during curing. Since NC-NCVS shrunk drastically by 12% prior to freeze-drying, the water lost left behind a more dense polymer phase with little space for the remaining water. This remaining water was found concentrated in small pores. A different scenario was observed in the NC-NHA gel. Since no shrinking had occurred prior to freeze-drying, all the water in the system was trapped in the polymer system in the form of channel-like pores. As the gel sample was freeze-dried and the water was removed through lyophilization, the process left behind the pores in which water was dispersed throughout the polymer phase. It has previously been reported that with a greater swelling degree, bigger pores are observed, and as the the swelling degree decreased, the freeze-drying process would be less able to cause significant changes in the structure of the polymer network (Kato, Sakai, & Shibata, 2003).

4.3.7 Cell Viability Assay

A crucial parameter to how a hydrogel performs is its biocompatibility. It entails how the material interacts with cells and its ability to exist in the body, without causing damage to adjacent cells or altering the function of the physiological locale in question (K. Y. Lee & Mooney, 2001). Thus, determining the cytotoxicity and viability of cells when exposed to a hydrogel is highly critical to research for a particular physiological application. Synthetic polymers tend to

induce negative responses in terms of cytotoxicity and/or biocompatibility. NIPAAm monomers may possess some toxic effects; however, various NIPAAm copolymers have shown promising biocompatibility results (Wadajkar, Koppolu, Rahimi, & Nguyen, 2009). It was thus crucial to investigate the cytotoxicity and biocompatibility of the particular copolymers presented in this work. To test cell viability to exposure to the hydrogels, the two gelling systems were tested on mouse fibroblast cells (NIH 3T3). A sample size of 5 was used for each gel due to the variation which can be experienced with cytotoxic measurements of hydrogels. The cells were exposed to the gels for 3 days and cell viability was measured using a colorimetric proliferation assay with a Promega solution. This solution contains MTT, a tetrazolium salt, yellow in color. When active mitochondria react with it, they cleave the tetrazolium ring, reducing MTT to a formazan product, dark blue in color (Gupta & Curtis, 2004; Mosmann, 1983). This change in color can then be measured with a microplate reader. Since only live cells can do so, this method measures the number of living cells only. Thus, after reaction with the MTT solution and determining the absorbance via spectrophotometry and a standard calibration curve, the results of the numbers of live cells after 3 days of exposure to the two gelling systems are shown in Figure 4.13.

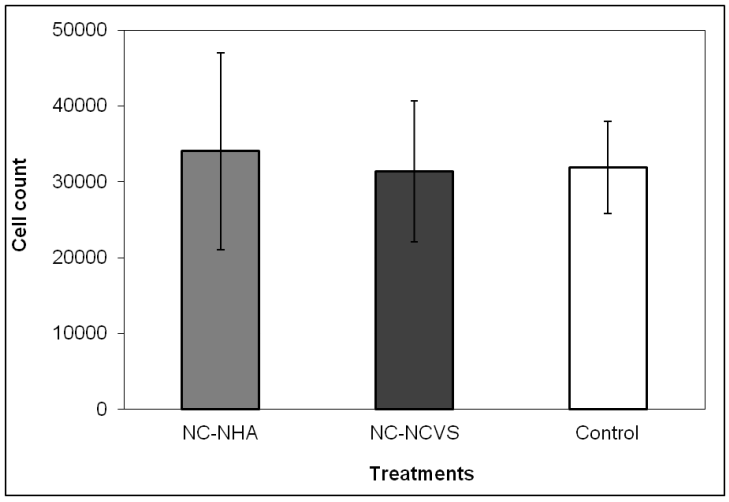

Figure 4.13 Cytotoxicity data (MTT proliferation assay) of the two gelling systems reveal that both gels possess good biocompatibility; mouse fibroblast cells proliferated normally (no significant difference with control $p<0.05$) when exposed to either gel.

As illustrated, both NC-NHA and NC-NCVS show cell proliferation after 3 days of exposure. When compared to the control, the statistics (via t-test, $p<0.05$) demonstrate no significant difference between either NC-NHA or NC-NCVS and the control. These results are promising since they affirm the normal growth of fibroblast cells while in contact with the hydrogels. Similar studies conducted by our group have also shown the favorable biocompatibility of various poly(NIPAAm) copolymer gels on 3T3 cells (Cheng, Lee, Pauken, & Vernon, 2007; Cui et al., 2010; B. H. Lee et al., 2006).

4.4 Conclusions

Two physical-chemical gelling systems were synthesized successfully using free radical polymerization and compared for their properties to be used *in vivo*. These gelling systems undergo gelation through two types of mechanisms: physical which consists of temperature-sensitivity due to the presence of the thermoresponsive polymer poly(NIPAAm) and chemical which takes place via a chemical reaction resulting in the formation of a covalent bond between thiols and vinyls between the copolymers. The chemical and structural identity of each copolymer was identified using H^1 NMR and FTIR, verifying the chemical composition of the copolymers. The thermal properties were analyzed using DSC and indicated that the copolymers had LCSTs ranging from 29 to 34°C. These temperatures prove to be feasible for use *in vivo* since they are below physiological temperature (37°C); thus, below the LCST, the polymers are in solution and when the temperature is increased above the LCST to body temperature, the polymer chains collapse and form gels. Rheology was used to examine the mechanical properties, time to gelation and temperature behavior. The time sweeps demonstrated that the NC-NCVS gelling system has much faster gelling properties. At all mixing times (30sec, 1min, 2min), the gel point is already reached within the first few seconds of the run, indicating that the gel forms rapidly. On the other hand, the NC-NHA gelling system has much slower gelling properties. A decrease in time to gel point was observed as mixing time was increased, which elucidates on the more homogeneous mixture developed and more cross-links formed, the longer the components are mixed. The faster

gelation of the NC-NCVS system was found to correspond with the results witnessed in the Ellman kinetic studies which demonstrated a faster reaction of the thiols to the vinyls on NCVS than to the vinyls on NHA. The frequency sweeps for both gelling systems indicate that the physical-chemical gels are stronger (higher *G'* values) and experience less creep than the purely physical or purely chemical gels. The NC-NCVS gel attains slightly higher *G'* values, presenting it as slightly stronger than the NC-NHA gel. Additionally, the temperature sweeps informed about the shrinking behavior of the gels as well as the greater influence that temperature has on the gelation of the NC-NHA system when compared to the NC-NCVS system. Both gels demonstrated a decrease in swelling ratio with an increase in temperature; however, this behavior is more accentuated with the NC-NHA system due to its greater influence by temperature. A similar behavior was encountered in the DSC results, showing a broad peak for NHA that has a range in lower temperatures. This leads to an early onset of phase transition, at low temperatures (as low as 15°C). The degradation studies did not show any difference over time, indicating both gels remained stable over the duration of the 210 days. Using SEM, the gels were shown to possess different morphologies, with many channel-like pores in the NC-NHA system and very few pores in the NC-NCVS system, signifying that the shrinking differences between the gels result in different gel structures. With NC and NCVS having similar LCSTs, it can contribute to a more homogeneous solution, as seen with the NC-NCVS images.When tested for cytotoxic effects, neither gel showed signs of cytotoxicity. Instead, cells exposed to either gel underwent normal growth, an

important characteristic for use *in vivo*. Some of the studies presented here have shown similarities between the two physical-chemical gelling systems, such as no difference in the swelling, degradation or cytotoxic properties. However, some differences were noted between the two gelling systems, especially in terms of the rheological and kinetic studies. The NC-NCVS system had a faster reaction of thiols to vinyls and thus faster gelation kinetics, with a gel formed almost immediately, regardless of mixing time. The NC-NHA system recorded longer time to gelation, with a decrease in gelation time with an increase in mixing time. The difference in the chemical gel formation may be due to different cross-link densities in the various gels. Rheological studies also demonstrated that the NC-NCVS system achieved more stable and more mechanically strong gels than the NC-NHA system. The morphology of the gels also differed, with a heavily porous structure observed in the NC-NHA system, allowing for the capture of water in these channels. The NC-NCVS system has very few pores, as a result of the immediate shrinking which occurs in the gel, giving it a dense polymer phase. With faster gelation, higher strength and stability, and more dense morphology than the NC-NHA gel, the NC-NCVS gelling system may have more appropriate properties for use *in vivo* in endovascular occlusion of aneurysms. Although both hydrogels require further optimization to achieve the desired properties, the physical-chemical gels presented here have shown the potential to be used *in vivo* for endovascular embolization applications.

CHAPTER 5

CYTOTOXICITY, IN VITRO MODELS AND PRELIMINARY IN VIVO STUDY OF DUAL GELS FOR ENDOVASCULAR EMBOLIZATION OF CEREBRAL ANEURYSMS

5.1 Introduction

An aneurysm is the dilation, bulging or ballooning-out part of a blood vessel, ranging from less than 5mm to greater than 25mm in diameter (Forget Jr et al., 2001; National institute of neurological disorders and stroke, 2012). Aneurysms can occur in different blood vessel locations, but are most common in the brain, often referred to as intracranial or cerebral aneurysms. Approximately 6 million people in the United States, or 1 in 50 people, have an unruptured cerebral aneurysm (Brain aneurysm foundation, 2012). Intracranial aneurysms are dilatations or acquired lesions of an intracranial artery which occur at branching points of major arteries, more often in the subarachnoid space at the base of the brain, an area known as the Circle of Willis (Peters et al., 2001; W. I. Schievink, 1997). They form in one of 3 shapes: saccular, fusiform and mycotic; however, saccular aneurysms account for 90% of intracranial aneurysms (Keedy, 2006). A saccular aneurysm consists of a rounded, pouch-like sac of blood with a neck which attaches it to the artery or branch of a blood vessel (National institute of neurological disorders and stroke, 2012.). The exact circumstances which lead to the formation of aneurysms have, until this day, been debatable. Studies have demonstrated the range of factors which may play a role in triggering aneurysm

formation, ranging from genetic to environmental (W. I. Schievink, 1997; Wiebers, Whisnant, & O'Fallon, 1981). Heritable connective-tissue disorders have been associated with intracranial aneurysms, such as autosomal dominant polycystic kidney disease, Ehlers-Danlos syndrome type IV, neurofibromatosis type 1 and Marfan's syndrome (Clarke, 2008; Keedy, 2006; Rinkel, Djibuti, Algra, & Van Gijn, 1998; W. I. Schievink, 1997; W. Schievink, 1998; Wiebers et al., 1981). Additionally, environmental factors including age, hypertension, sex, cholesterol as well as smoking, drug abuse, and excessive alcohol consumption, have been identified in possibly increasing the risk of developing intracranial aneurysms (Clarke, 2008; Keedy, 2006; Rinkel et al., 1998; W. I. Schievink, 1997; W. Schievink, 1998; Wiebers et al., 1981). Saccular aneurysms form when there exists a collagen deficiency in the internal elastic lamina (elastic layer between the innermost layer of the blood vessel adjacent to the lumen-tunica intima- and the muscular middle layer-tunica media) and a breakdown of the tunica media (Keedy, 2006). This in turn causes the protrusion of the tunica intima and adventitia (outer layer consisting of mostly connective tissue) through the defect in the internal elastic lamina and tunica media, forming an aneurismal sac (Keedy, 2006). With the damage already present in the blood vessel wall, further weakening of the wall occurs with hemodynamic stress (Parkinson, Eddleman, Batjer, & Bendok, 2006). Once an intracranial aneurysm ruptures, bleeding occurs in the brain, most commonly in the subarachnoid space at the base of the brain, leading to a subarachnoid hemorrhage (SAH) (Keedy, 2006). The effects of the rupture of an intracranial aneurysm are devastating; with more

than 30,000 people in the United States suffering from a severe form of stroke. Upon rupture, 50% of those individuals die at the instant of rupture or shortly following it, and 25% experience permanent disability, which include paralysis and loss of speech, vision and motor coordination (Peters et al., 2001). Even with medical and surgical intervention, the rate of morbidity and mortality due to rupture remain at a high of 60% (Forget Jr et al., 2001). Intracranial aneurysms present a significant public health problem not only due to their traumatic effects, but also due to the increasing age of the population (Wiebers et al., 1981).

The current methods approved by the FDA for treatment of aneurysms involve surgical clipping and endovascular embolization using coils. Two aims are aspired for with surgical clipping; the first is to permanently exclude the aneurysm from the blood circulation in the parent vessel by inserting a clip between the neck of the aneurysm and the healthy artery, while the second is to relieve the effect that the mass of the aneurysm has on surrounding brain tissue (Parkinson et al., 2006). The first attempt at surgical clipping of an intracranial aneurysm was performed by Dandy in 1938, in which a silver clip was placed over the neck of the sac and tightly secured to completely eradicate it (Figure 5.1) (Dandy, 1938). After applying the clip to the aneurysm, Dandy remarked that it ceased to pulsate, indicating a stop of blood flow to the sac. By clipping the aneurysm, blood flow to the aneurysm can theoretically be deterred and will resume to the normal parent vessel flow. Some studies, which report use of surgical clipping, have proven that it indeed blocks off blood flow to the aneurysm and upon post-operation angiography, no re-bleeding is witnessed

(Solomon, Fink, & Pile-Spellman, 1994). However, it is also commonly found that re-bleeding does occur in already clipped aneurysms due to portions of the neck or aneurysm sac remaining after clipping (T. Lin, Fox, & Drake, 1989). In such a case, either reoperation is required or a regrowth of the aneurysm may present itself by dilation of the neck remnant over time. Additionally, due to the high invasiveness associated with surgical clipping, higher risks of complications are witnessed (Keedy, 2006). Studies have reported relatively high morbidity rates resulting from craniotomy and adverse effects which include minor and major strokes as well as nerve damage and deficits (Khanna, Malik, & Qureshi, 1996; Solomon et al., 1994; Wirth, Laws Jr, Piepgras, & Scott, 1983). Aneurysm size, location, age have been identified as key factors for poor surgical outcomes (Keedy, 2006; Khanna et al., 1996; Solomon et al., 1994; Wiebers, 2003).

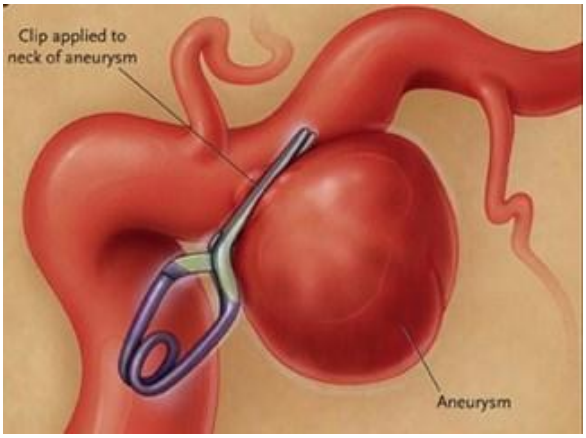

Figure 5.1 Surgical treatment of aneurysm using metal clip to close off the neck. Image reproduced from: http://chicago.medicine.uic.edu/departments___ programs/departments/anesthesiology/residency/subspecialty_training/neuroanesthesia.

To circumvent the highly invasive procedure used by surgical clipping, a new endovascular method for embolization of aneurysms was developed by Guglielmi in 1991 (Figure 5.2). A guiding catheter inserted in the femoral artery is directed using fluoroscopy through the cerebral vasculature to the site of the aneurysm. Once at the location, small soft platinum coils are deployed in the aneurysm sac via application of low direct current (0.5-2mA) which leads to electrolysis, which detaches the coil from the steel wire, and electrothrombosis, which attracts negatively charged blood components (Guglielmi, Vinuela, Dion, & Duckwiler, 1991). These blood components, which consist of white blood cells, red blood cells, platelets and fibrinogen, start the formation of a thrombus, or blood clot, within the aneurysm. The clot now present in the aneurysm acts as an emboli, preventing blood from entering the sac. A multitude of studies have used Guglielmi Detachable Coils (GDC) since their appearance. Use of GDCs is determined by the endovascular accessibility, aneurysm neck size and overall aneurysm size (Regli, Uske, & de Tribolet, 1999). While they have at times been reported to be safe relative to surgical clipping and preferred for treating aneurysms in areas difficult to approach via surgery (Keedy, 2006), some challenges have been presented. One of the most significant challenges identified has been recanalization due to incomplete occlusions reported by Guglielmi himself (Brilstra, Rinkel, van der Graaf, van Rooij, & Algra, 1999; Byrne, Sohn, & Molyneux, 1999; Guglielmi et al., 1991; Hayakawa et al., 2000; Keedy, 2006; Murayama et al., 2003; Parkinson et al., 2006). One study reports up to 24% of patients presented with intracranial unruptured aneurysms undergoing incomplete

occlusions and 18% with no occlusion (Wiebers, 2003). Additional to recanalization, several other complications were observed with use of GDCs, including perforation of aneurysm sac, neck remnants, technical difficulties in placement of coils, parent artery occlusion, coil migration and neurological deficits (Brilstra et al., 1999; Byrne et al., 1999; Guglielmi et al., 1991; Hayakawa et al., 2000; Murayama et al., 2003; Viñuela, Duckwiler, & Mawad, 1997).

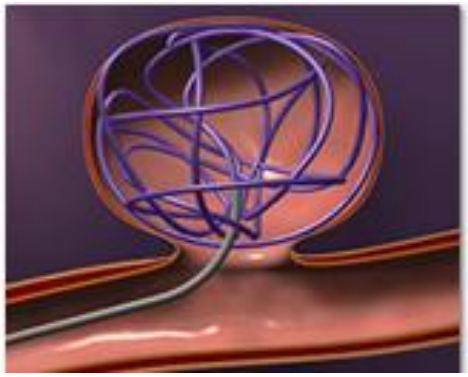

Figure 5.2 Endovascular embolization of aneurysm via detachable coils. Image reproduced from: http://www.brainaneurysm.com/aneurysm-treatment.html.

Recently, other endovascular devices have been developed and tested for occlusion of aneurysms. These consist of flow-diverting devices, such as self-expandable stents, with Pipeline and Silk stents having been tested in recent studies. The flow-diverting stents can allow for aneurysm occlusion via flow disruption. Once expanded, the mesh of the stent provides high coverage of the aneurysm neck and triggers thrombosis within the aneurysm sac while maintaining flow throughout the parent vessel (Lubicz et al., 2010). They can be

particularly helpful in challenging situations, such as wide-necked and fusiform aneurysms. Studies using a combination of particle image velocimetry and computational fluid dynamics have shown that the positioning of a stent across the neck of an aneurysm can significantly reduce the velocity magnitudes within the aneurysmal sac (Babiker et al., 2012). The Pipeline stent has provided good occlusion properties in patients treated with the device, with minor rates of complications experienced (Fiorella, Woo, Albuquerque, & Nelson, 2008; Lylyk et al., 2009; Szikora et al., 2010). Few studies have been reported on the Silk stent in patients; however, the few available demonstrate that although a majority of aneurysms demonstrated complete occlusion, difficulties were experienced (Kulcsár et al., 2010). The main limitations include the unpredictable aneurysm occlusion process, higher complication rates than conventional treatments and significantly high rates of parent artery stenosis (Lubicz et al., 2010).

Due to the many reports involving complications with endovascular embolization using coils, groups diverted their attention to liquid embolic agents. Unlike coils, liquid embolics have the advantage of conforming to the exact shape of the aneurysm and the possibility of better sealing large and giant aneurysms (Lanzino, Kanaan, Perrini, Dayoub, & Fraser, 2005; Lubicz, Piotin, Mounayer, Spelle, & Moret, 2005). Nonetheless, some *in situ* gelling polymeric systems require use of organic solvents to dissolve hydrophobic and water-insoluble polymers. These organic solvents can cause toxicity when injected intra-arterially. Onyx®, a liquid embolic material consisting of ethylene vinyl alcohol copolymer and dimethyl sulfoxide (DMSO), has been widely researched and tested for

occlusion of aneurysms (Figure 5.3) (Molyneux, Cekirge, Saatci, & Gál, 2004). However, this commonly used organic solvent, dimethyl sulfoxide (DMSO), shows signs of a local dose-related toxic effect on vessel and brain tissue when injected intravascularly in pigs (Mottu et al., 2000). Although *in vivo* testing of Onyx® demonstrate better morbidity and mortality rates than clipping or coiling, recanalization, parent artery occlusion, neurological deficits and procedure-related deaths occur nonetheless (Cekirge et al., 2006; Lanzino et al., 2005; Lubicz et al., 2005; Molyneux et al., 2004; Weber, Siekmann, Kis, & Kuehne, 2005). Additionally, the slow injection associated with the material and time for curing results in a long procedure. Cyanoacrylate glues have also been used as embolic liquids for aneurysm occlusion; however, their aggressive adhesive properties can result in 'gluing' of the catheter to the blood vessel (Debrun, Aletich, Ausman, Charbel, & Dujovny, 1997; Farhat, Elhammady, & Aziz-Sultan, 2010). Calcium alginate gels have likewise been utilized for aneurysm occlusion. By simultaneously injecting alginate and calcium chloride into the aneurysm sac, a calcium alginate gel is formed immediately upon contact of the two solutions (Becker, Preul, Bichard, Kipke, & McDougall, 2007). While this gelling system shows good biocompatibility and mechanical strength properties, emboli from unstable calcium alginate may be formed in the parent artery, incomplete embolization may occur and its instability caused some fractures in the gel (Raymond et al., 2003). Furthermore, use of a double-lumen catheter for simultaneous injection of the alginate and calcium chloride requires a larger diameter catheter and coordination in synchronized injection of both materials

into the aneurysm sac. Thus, further developments in the field of liquid embolics for aneurysm occlusion are in need.

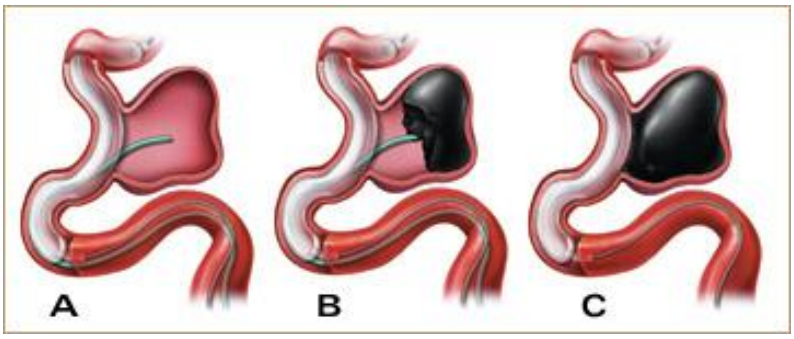

Figure 5.3 Use of Onyx® gelling system for endovascular occlusion of aneurysm. Image reproduced from: http://www.neurosurgery.pitt.edu/news/2008/onyx.html.

The use of a waterborne *in situ* gelling polymer system for endovascular embolization techniques was proposed, consisting of copolymers of poly(N-isopropylacrylamide) (NIPAAm) that undergo simultaneous physical and chemical gelation. Poly(NIPAAm) is ideal in that it is soluble in aqueous solutions and would thus circumvent use of organic solvents for preparation of gels, minimizing toxic effects. By mixing poly(NIPAAm-*co*-HEMA-acrylate) with poly(NIPAAm-*co*-cysteamine) or poly(NIPAAm-*co*-cysteamine-vinysulfone) with poly(NIPAAm-*co*-cysteamine), chemical gelation occurs through a Michael-type addition (MTA) reaction between the thiol group on the cysteamine and the vinyl group on the acrylate or the vinylsulfone, resulting in a covalent cross-link. The advantage with the Michael-type addition reaction is that the initiation step, which involves the deprotonation of the thiol, can be done at

the physiological pH of 7.4 (Lutolf & Hubbell, 2003a). Additionally, this reaction is highly selective, allowing thiols to react with acrylates at orders of magnitude faster than acrylates would react with amines or nucleophilic molecules in the body (Vernon et al., 2003). Aside from the cross-links formed through the chemical reaction, further cross-linking in the polymer system occurs due to the thermoresponsive properties of poly(NIPAAm). Poly(NIPAAm) undergoes phase transition from a liquid to a solid, known as the lower critical solution temperature (LCST), around 31°C (Heskins & Guillet, 1968). As the gel is exposed to body temperature (temperature above the LCST of the copolymers), NIPAAm chains on the copolymers become more hydrophobic and expel water molecules. This leads to the collapse of the polymer chains upon each other, referred to as chain entanglements, which results in the formation of a gel. The temperature at which this phase transition occurs can be altered by conjugating various hydrophobic or hydrophilic monomers. The benefits of the proposed system are that by simultaneous chemical and physical gelation, improved mechanical properties can be developed for the *in situ* gel. Whereas solely chemical gels experience a large extent of swelling in aqueous solutions, unless they are highly cross-linked (Metters & Hubbell, 2005), and solely physical gels show signs of creep at low frequencies due to their viscoelastic properties (F. Tanaka & Edwards, 1992b), a chemical-physical gel will attain a more creep-resistant system when exposed to constant stress and provide better mechanical properties for the gel to be used endovascularly for embolization. Our group has also investigated physical-chemical gels, however, employing poly(NIPAAm). Bearat et al. used

poly(NIPAAm-*co*-HEMA-acrylate) mixed with poly(NIPAAm-*co*-cysteamine) to form a physical-chemical gel, as shown in Figure 5.4 (Bearat et al., 2011).

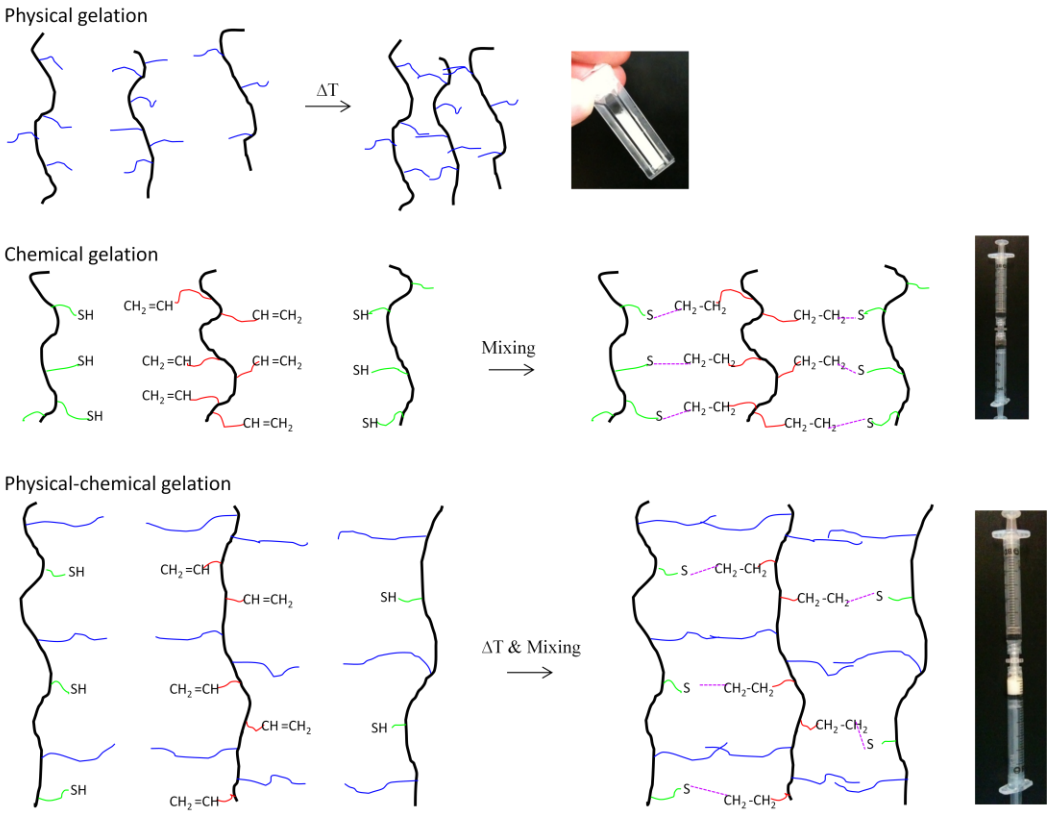

Figure 5.4 Representation of the separate and combined gelation mechanisms. In physical gelation, polymer chains entangle as temperature is increased, forming a physical gel. In chemical gelation, a reaction occurs between thiols (SH) and vinyls (CH_2=CH-) when mixed to form covalent cross-links. By combining physical and chemical gelation, both modes of gelation are employed to improve gel properties.

In this work, the properties of the components of the gelling systems can be altered as needed by conjugating different monomers to poly(NIPAAm) at various

ratios through free radical polymerization. This allows for more flexibility in the obtained gel properties, as an array of copolymers can be developed, stemming from poly(NIPAAm). An additional benefit of utilizing poly(NIPAAm) for biomedical applications is the biocompatible properties it expresses (Vihola, Laukkanen, Valtola, Tenhu, & Hirvonen, 2005; Wadajkar et al., 2009). An important aspect of this *in situ* gelling system is that it can be performed at physiological conditions, mainly at a pH of 7.4 and body temperature of 37°C, with the simultaneous use of a Michael-type addition reaction and the thermoresponsive properties of poly(NIPAAm). The mixed copolymers, once exposed to body temperature, can undergo physical gelation instantly, while further curing can occur through the chemical reaction between the thiol and vinyl functional groups on each copolymer. These biocompatible hydrogels can potentially be used as liquid-to-solid embolic agents for endovascular embolization of cerebral aneurysms.

5.2 Materials and Methods

5.2.1 Live/Dead Assay

Cell viability was assessed using a two-color fluorescent live/dead viability/cytotoxicity assay. Mouse fibroblasts (NIH 3T3) were seeded at 20,000 cells per well. Cell media comprised of Dubelcco's Modified Essential Medium (DMEM) supplemented with 1% penicillin/streptomycin, 1% L-glutamine and 10% calf serum. A standard curve was also seeded in a series dilution from

320,000 to 0 cells per well. Polymers (NHA, NC and NCVS) were prepared at 30wt% in sterile PBS pH 7.4 in a biosafety hood for sterilization purposes. The polymers were mixed stoichiometrically for 2min using 3cc syringes and couplers. The 24-well plate were placed on a hot plate at 37°C in the biosafety hood and 8-µm Transwell® inserts were added to the wells which contained the gels. After mixing the polymers, 0.1mL of the gel was injected in the inserts (n=4). Cells were left to incubate with the gels for 3 days at 37°C with 5% CO_2. A 10mL volume of the live/dead solution was prepared by adding 20µL of 2mM ethidium homodimer-1 and 5µL of 4mM calcein AM (LIVE/DEAD® Viability/Cytotoxicity Kit for animal cells, Molecular Probes) to 10mL of sterile PBS. Controls consisted of wells containing cells in media only and cells treated with 70% ethanol prior to staining. After 3 days of incubation (control and gels), wells were washed with PBS and 400µL of the fluorescent solution was added to each well and allowed to incubate for 45-60 min. A fluorescent microscope (Leica Microsystems DM IRB) was used to image the cells at a magnification of 20x. The appropriate excitation and emission filters for calcein AM and ethidium homodimer-1 were used. Image J Cell Counter was used to count the number of live and dead cells for the live control, NC-NCVS and NC-NHA with n=3, and to calculate the percent cell viability.

5.2.2 MTT Proliferation Assay

To determine the cytotoxic effects according to polymer concentration, an IC_{50} test was used. A similar procedure as outlined above was followed for cell

seeding, incubation, gel preparation and exposure; however, polymers were dissolved at 15 and 60 wt%. Control was designated as cells in media without gels. At 3 days, inserts were removed and wells were washed with PBS and new media added (0.5mL). Approx. 0.1mL of Promega solution (Promega CellTiter 96® Cell Proliferation Assay) was added to each well at a 1:5 ratio (Promega:media) and allowed to sit for 3-5 hours. The solutions were then assessed using a FLOstar Omega microplate reader set to measure absorbance at 490nm. Using the standard curve and the absorbance values, the number of live cells after 3 days of incubation with and without gels was quantified.

5.2.3 Preliminary *In Vivo* Swine Study

The animal study reported in this work was approved by the Institutional Animal Care and Use Committee at Barrow Neurological Institute and is in line with guidelines as set forth by the U. S. Department of Agriculture, National Institutes of Health, and AAALAC. Preliminary acute swine *in vivo* testing of the physical-chemical gels was conducted to test 'proof-of-concept' and feasibility of the dual-gelling system for endovascular embolization. Saccular sidewall aneurysms were surgically created in the right and left common carotid arteries (CCA) of the Yorkshire swine using a piece of the external jugular vein (EJV). One end of the EJV was sewn to the incision made in the CCA while the distal end of the EJV was sewn closed to form the oval shaped aneurysm sac. The resulting aneurysm sacs had heights of 8-9mm, longitudinal dome widths of 8-9mm and longitudinal neck diameters of 6mm. The animal was anesthetized and

maintained on 2% isoflurane and oxygen during the procedure. The copolymers were previously dissolved at 40wt% in PBS pH 7.4 in a biosafety hood for sterile purposes. The polymer components were mixed stoichiometrically via syringe and coupler for 3min for NC-NHA and 30sec for NC-NCVS. A guide catheter (X-pedion, ev3), a 135cm, 3-French outer diameter microcatheter (Renegade Hi-Flo Microcatheter Kit, Boston Scientific) and a balloon catheter (HyperGlide, ev3), were introduced through the right femoral artery and guided through the vasculature to the aneurysm site. The tip of the filling catheter was inserted in the sac, after both catheters were primed with saline. The balloon catheter was inflated to prevent migration of the gel into the parent vessel. The gel was injected with the appropriate volume calculated using the equation $V = \pi \cdot h \cdot w \cdot d/6000$, where *V* is aneurysm volume, *h* is aneurysm height, *w* is aneurysm width and *d* is aneurysm cross sectional depth, which were all measured before embolization (Becker et al., 2007). After injection, the balloon was deflated and all catheters were removed. Angiography was used during and after injection to monitor the extent of embolization and blood flow redistribution. Assessments were made immediately after injection and 1 hour after the procedure.

5.2.4 *In Vitro* Aneurysm Glass Models

Delivery of the polymer system *in vitro* into an aneurysm glass model was performed to determine the feasibility of injecting the material as well as its embolization characteristics. Additionally, testing of the gel in glass models prior to animal models is a cost-effective method to conduct preliminary work. Using a

flow system which imitates physiological conditions and an aneurysm glass model, more accurate assessment of the feasibility can be done while providing visualization of the material as it fills the aneurysm. The aneurysm glass models were designed as sidewall aneurysms with a neck width of 4mm and a diameter of 8mm, with a parent vessel diameter of 5mm. These models were tested in a temperature-controlled flow system at Barrow Neurological Institute (BNI). A schematic of the aneurysm flow system can be seen in Figure 5.5.

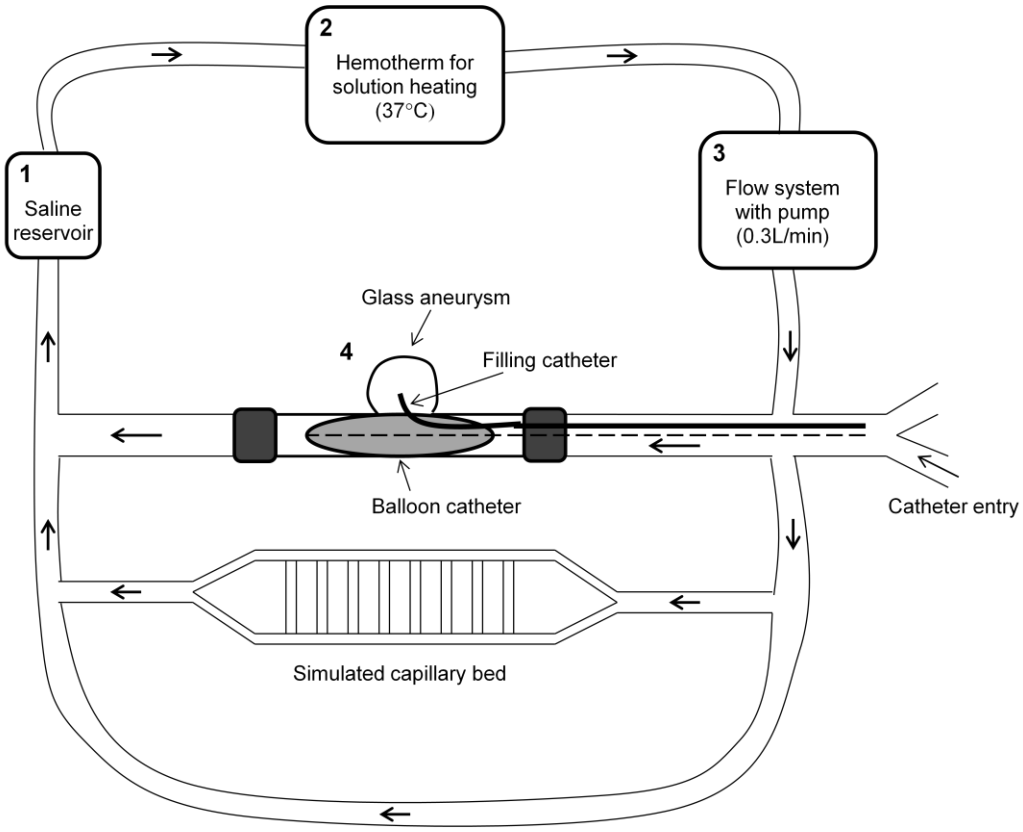

Figure 5.5 Depiction of the flow system set-up for the testing of the hydrogels *in vitro* in aneurysm glass models. Numbers note the order of steps and thick arrows indicate direction of flow.

A saline reservoir served as the fluid flow throughout the system, with the ambient temperature set at 37°C to simulate physiological temperature and a pulsatile flow was introduced at approximately 0.3L/min to match physiological carotid artery blood flow (Ford, Alperin, Lee, Holdsworth, & Steinman, 2005). The copolymers for gelling system 1 (NC & NHA) were dissolved in PBS pH 7.4 at 40wt% and mixed stoichiometrically for 3min via 3cc syringes and syringe couplers. The copolymers for gelling system 2 (NC & NCVS) were dissolved in PBS pH 7.4 at 30wt% and mixed stoichiometrically for 30sec using 3cc syringes and syringe couplers. The surgeon used a filling catheter (Fastracker 18 MX, Boston Scientific), a balloon catheter and guidewire (HyperGlide/X-pedion, ev3) to deliver the physical-chemical gel in the aneurysm sac and fully pack it for optimal occlusion. Prior to using the filling catheter, the surgeon primed it with saline. A very small amount of red food dye was added to monitor the expansion of the balloon during the procedure and to enhance visualization during video recording. The balloon was left up for 10 minutes to ensure proper time for the physical gelation to occur at 37°C. Once the balloon was taken down, the flow was allowed to resume and the occlusion status of the aneurysm with the gel was observed. Images were captured at various points of the procedure for analysis.

5.2.5 Rheology Creep Study

Rheological sweeps were performed to examine the creep behavior of the hydrogels using a Physica MCR 101, Anton Paar rheometer with a sandblasted measuring plate of 25mm diameter and 5mm gap. The creep test measures the

shear strain under constant shear stress. To do so, polymer samples (NC, NHA and NCVS) were dissolved at 30wt% in PBS pH 7.4. The copolymers were mixed stoichiometrically, as described above, for 30s, 1min and 2min. The run was set using a creep and recovery test with a rotational constant stress of 1Pa and temperature set at 37°C. The creep compliance was then plotted against time.

5.2.6 Degradation Study

Each copolymer was dissolved at 30 wt% in 0.1M PBS, pH 7.4, mixed stoichiometrically at a ratio of 0.48: 1 (poly(NIPAAm-*co*-HEMA-acrylate): poly(NIPAAm-*co*-cysteamine)) and a ratio of 3:2 (poly(NIPAAm-cysteamine-*co*-vinylsulfone): poly(NIPAAm-*co*-cysteamine)) for 2.5 min at room temperature using 3cc syringes and a syringe coupler. The copolymer systems were placed in a hot room at 37°C for 24h to allow for further curing. The cylinder-shaped gels were then removed from the syringe, cut into 0.3cm long pieces, weighed, and incubated in PBS pH 7.4 vials at 37°C. Samples (n = 3 for each gelling system) were weighed (after dabbing with wet towel) at time intervals of 1 day, 3mo, 6 mo, 1 yr and 1.5 yr. The swelling ratio was defined as $[(W - (W_0 \cdot 0.3))/(W_0 \cdot 0.3)]$, where W is the weight of the swollen gel and $W_0 \cdot 0.3$ is the original weight of the gel multiplied by the ratio of polymer in the system. ANOVA single factor tests were performed to determine the statistical significance of the points measured.

5.3 Results and Discussion

5.3.1 Cell Viability Assays

Interaction of hydrogels with the body is crucial in understanding the potential effects of an injected foreign material on the body. It is therefore desirable that the hydrogel, or material in question, does not have adverse effects on the nearby cellular environment and tissues. To determine cytotoxicity of the material, two different assays were used. In the first, a live/dead assay was used to determine live and dead cells. Calcein AM is enzymatically converted by live cells to a green fluorescent calcein, while ethidium homodimer-1 enters cells with damaged membranes and causes bright red fluorescence upon binding to nucleic acids. Here, the two different gels were tested on murine fibroblasts and compared to the control (cells only) (Figure 5.6).

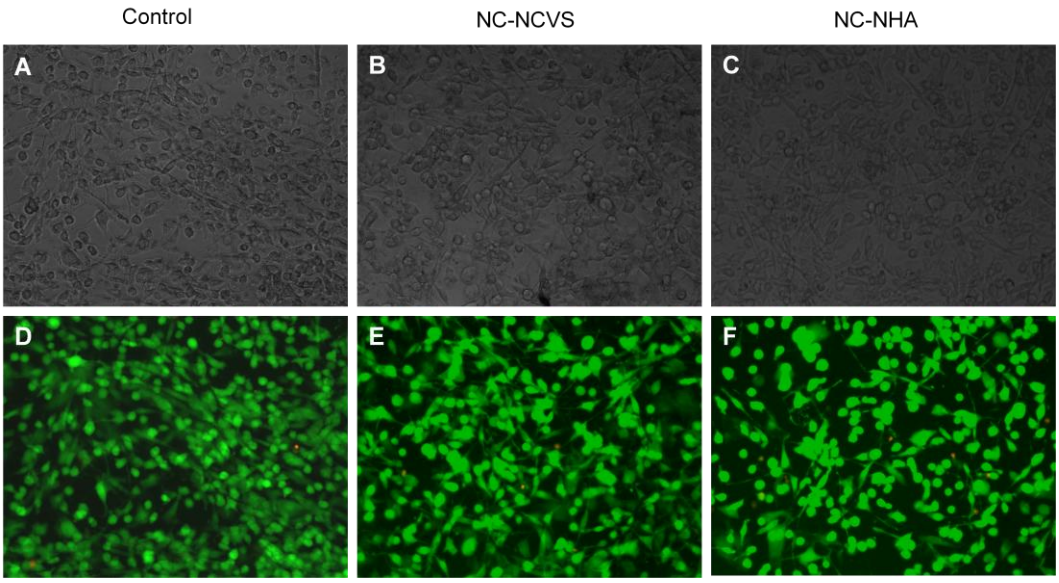

Figure 5.6 Images of live/dead assay on mouse fibroblasts as brightfield (A-C) and fluorescence (D-F). Observations of live (green) and dead (red) fluorescing cells between the live control (A & D) and the NC-NCVS gelling system (B & E) and the NC-NHA gelling system (C & F) demonstrate no difference in cell viability.

Images A through C are the bright field captures of the cells while D through F are the fluorescent images. Images A and D represent the control studies on the polystyrene well plate, B and E are the cells after a 3 day exposure to the NC-NCVS gel and C and F correspond to the cells after a 3 day exposure to the NC-NHA gel. By visualizing the bright field images, the fibroblasts exposed to either gel maintained their shape and confluency when compared to the control. In the fluorescent images, it appears that the majority of cells under both gel treatments are alive and healthy. Only very few cells are fluorescing red, which indicates minimal cytotoxic effects of the gels on the cells. When compared to the control,

the cells incubated with the gels do not seem to differ. To quantify cell viability of the live control and the two hydrogels, Image J Cell Counter was used to count live and dead cells for each treatment (n=3). Results demonstrate that the live control had 93% (± 5.6%) cell viability. For the gelling systems, the NC-NCVS hydrogel had 93% (± 3%) cell viability and the NC-NHA hydrogel had 91% (± 3.1%) cell viability. This indicates that the hydrogels possessed just as good cell viability as the live control. Thus, the cytotoxicity data demonstrate that both NC-NCVS and NC-NHA gels are safe to use as injectable agents for embolization of intracranial aneurysms.

Polymer concentration can have an effect on cell viability. With higher polymer concentrations, changes in cell morphology can occur and may result in cell lysis (Fischer, Li, Ahlemeyer, Krieglstein, & Kissel, 2003). Depending on the need for higher concentrations according to application, this can have a tragic effect on material interaction with cells or tissues, and its overall biocompatibility *in vivo.* To quantify the number of viable cells present after 3 days of exposure to the different concentration of gels, a proliferation assay was performed. The MTT assay measures the mitochondrial activity in cells (Vihola et al., 2005). Using the MTT solution which contains tetrazolium salt, live cells can be quantified as active mitochondria reduce the yellow MTT solution to a formazan product dark blue in color. For this experiment, two concentrations of polymer solutions were used to assess cell viability. The high (60 wt%) and low (15 wt%) concentrations were used to investigate the effect of different polymer concentrations on cell survival. Previous studies have shown that at 30 wt%, cell viability when exposed

to both gels did not differ from the control, thus indicating good biocompatibility (Chapter 4)(Bearat et al.,). Here, double and half the polymer concentrations that were previously tested were investigated to detect if any changes in cell viability occur. The studies were performed using inserts in which the gels were injected and then immerged into the media containing the cells. Inserts were used due to complications observed in prior tests without inserts. When the gels were injected directly on top of the cells, the weight of the gel on the cells may have resulted in difficult exchange of nutrients and CO_2 for the cells. Additionally, the gels posed some trouble in removing them by either adhering to the well surface or leaving behind debris which was difficult to remove by PBS washing. The remaining gel debris interfered with absorbance measurements since the gels are opaque. Figure 5.7 reports the cell viability when mouse fibroblasts were exposed to the NC-NHA and NC-NCVS gels at 15 wt% (A) and 60 wt% (B) for 3 days.

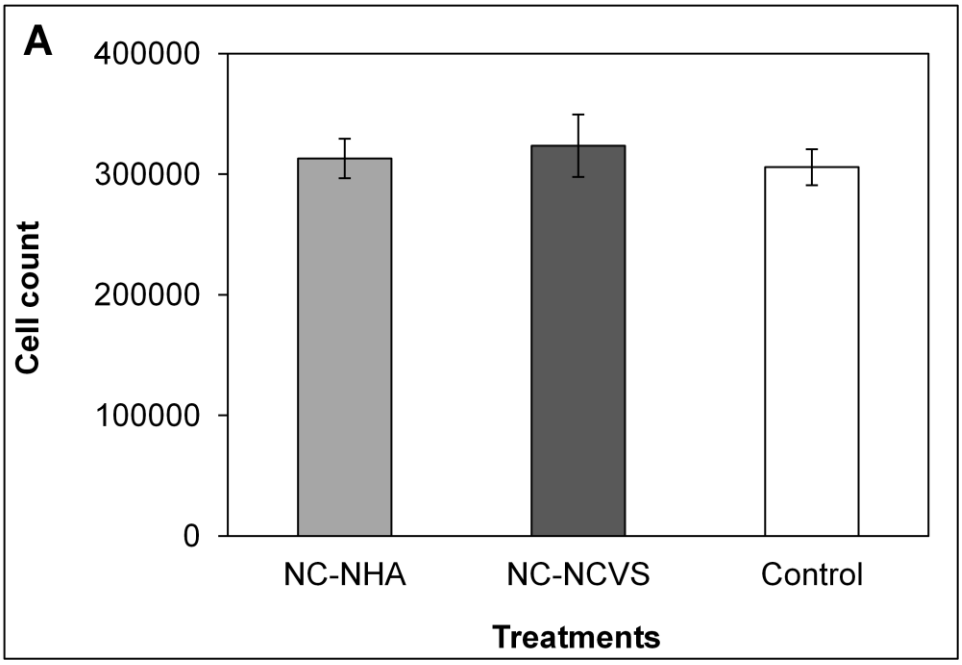

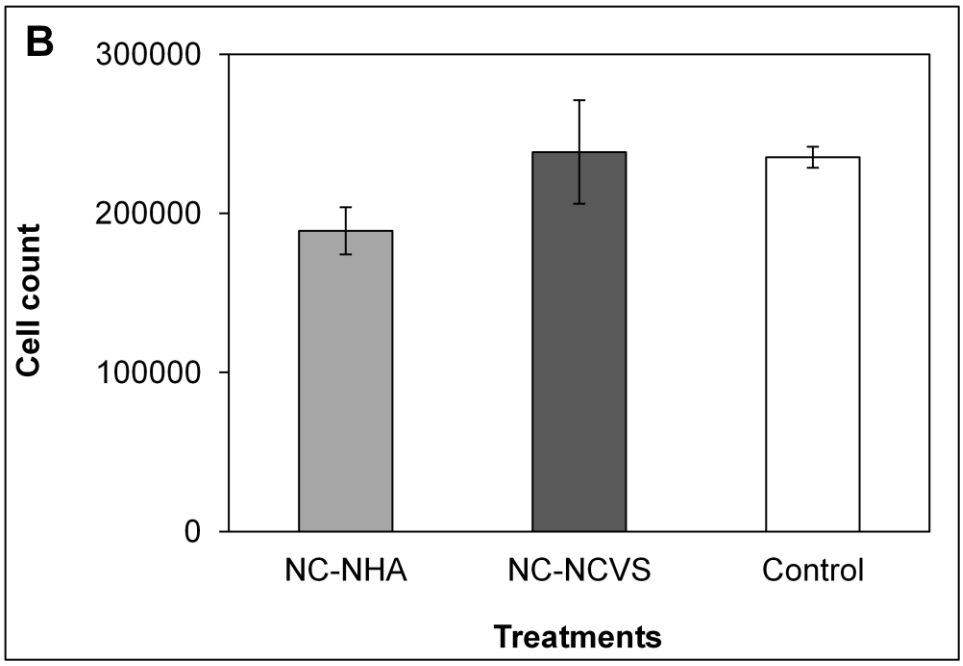

Figure 5.7 Proliferation of mouse fibroblasts exposed to both hydrogels for 3 days at polymer concentrations of A) 15 wt% and B) 60 wt%.

At 15 wt%, no difference was observed between the gels when compared with the control. This indicates that the cells proliferated normally and in good condition when exposed to both gels prepared at 15 wt%. As the concentration was increased to 60 wt%, no difference was detected between the NC-NCVS gel and the control, demonstrating that even at fairly high concentrations, this hydrogel promotes cell proliferation and does not possess any cytotoxic effects. For the NC-NHA gel, a difference was observed when compared with the control, showing less biocompatible properties of this hydrogel when compared to the NC-NCVS gel. Although it did not demonstrate proliferation rates as high as the control, the 60 wt% concentration of NC-NHA did not seem to completely inhibit growth of the cell population when compared to the control. Higher

concentrations of polymer could not be tested due to the difficulty in mixing the copolymers to form homogeneous gels and injection of the gel into inserts. The studies demonstrate that even at high concentrations of polymer, the hydrogels either continued to report good biocompatibility, as in the case with NC-NCVS, or did not reach the IC_{50} value, as seen with NC-NHA. If needed, concentrations higher than 30 wt% of polymer may be used for gel formation and potential injection *in vivo*. Results from both cytotoxicity assays, MTT and live/dead, indicate good cytocompatibility of the hydrogels, an important characteristic for a material to be used *in vivo*.

5.3.2 *In Vivo* Swine Study

To examine the efficacy of endovascular technologies, preclinical animal tests are highly needed. Ideally, animal models for human saccular aneurysms should imitate human histomorphologic and hemodynamic properties, while also reproducing a similar cellular and molecular environment (Dai et al., 2005). Past studies have used surgically created saccular aneurysms in swine models to mimic human aneurysms (Dawson et al., 1995; Murayama, Tateshima, Gonzalez, & Vinuela, 2003). Preliminary *in vivo* testing of the dual-gelling system was conducted on one swine as proof-of-concept for ability to inject the dual-gelling material and to observe its occlusion capabilities. The swine underwent aneurysm creation in the left and right common carotid arteries.

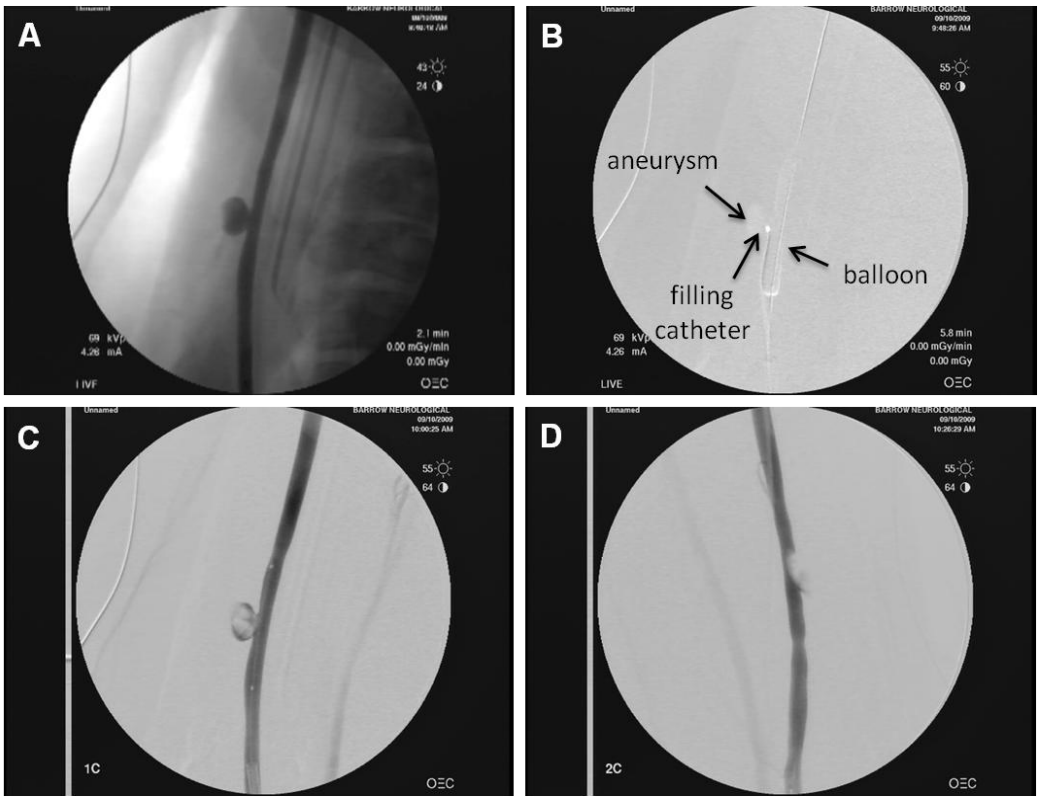

Figure 5.8 *In vivo* injectability and embolization assessment of NC-NHA hydrogel in swine model. A) Surgically created aneurysm pre-embolization, B) filling catheter positioned in aneurysm sac with balloon inflated across aneurysm neck, C) post-embolization results of the left common carotid artery and D) right common carotid artery, taken immediately after procedure, showing slight recanalization.

Angiographic verification of the aneurysm state prior to embolization was conducted, as seen in Figure 5.8A. Using a guide catheter inserted through the femoral artery, the balloon catheter was placed along the length of the aneurysm neck and beyond, and the filling catheter was inserted in the aneurysm. Figure 5.8B illustrates the position of the inflated balloon, preventing outflow from the

aneurysm neck, as well as the position of the filling catheter within the aneurysm. After 3 minutes of mixing the copolymers to achieve chemical gelation, the balloon was inflated while the filling catheter was monitored to ensure its position within the aneurysm. The gel solution was then administered, via the filling catheter, into the aneurysm sac. To ensure that no overfilling occurred and that the volume injected was close to complete filling, injection of the gel was supervised via digitally subtracted angiography due to the slightly lighter shade of the gel. The appropriate gel injection volume was also examined by injecting a volume close to the calculated aneurysm volume and by monitoring the injected volume displayed on the graduated syringe. The calculated aneurysm volumes were 0.23mL and the dead volume of the catheter was indicated to be 0.5mL. A total volume of approximately 0.73mL of gel was calculated to be the total injectable volume. After injection of the gel, the balloon remained inflated for 10 minutes to ensure physical gelation had taken place at physiological temperature. The balloon was then deflated and blood flow was resumed through the parent vessel. Conray^{TM}, a liquid agent containing iodine for radio-opacity, was injected into blood circulation to monitor the status of the aneurysm via angiography. In Figure 5.8C, the aneurysm on the left common carotid artery was imaged. Recanalization occurred in the aneurysm, as witnessed by the blood circulated within the aneurysm sac. Possible recanalization may be due to the inadequate volume of gel injected. A gel volume of 0.75mL was administered into the filling catheter. As can be seen in the image, the gel fills most of the aneurysm, but does not provide a complete filling of the volume. An incomplete fill facilitates penetration of

blood into the aneurysm sac and causes recanalization. In Figure 5.8D, the aneurysm created on the right common carotid artery is observed, post embolization. A very slight degree of recanalization is observed in this aneurysm, with a small volume of blood appearing at the dome of the aneurysm. For this aneurysm, the total volume of gel to be injected was increased to 0.9mL to provide for a more complete fill of the aneurysm volume. Better occlusion resulted in this aneurysm due to the slightly greater volume injected into the aneurysm, providing for close to a complete fill of the aneurysm sac.

To our knowledge, no dual-gelling system has been designed or tested *in vivo* as an embolic agent for aneurysm occlusion. The NC-NHA gel was tested in a swine model as proof-of-concept for the injectability and feasibility of the simultaneous physically and chemically gelling system. Ideal properties for a polymer gel to be used for endovascular embolization comprise of initial low viscosity to permit mixing of the copolymers and to facilitate initial delivery of the material through a catheter. Once the material is delivered *in vivo*, the system physically cross-links within the catheter and upon delivery in the aneurysm sac. Further curing of the gel then occurs within the aneurysm as chemical cross-links continue to form. Temperature responsive polymers, which transition from a liquid to a solid upon change in temperature (room to body), have been investigated as potential materials for various vascular applications. However, these purely physical gels can undergo creep deformation (F. Tanaka & Edwards, 1992b). Chemically cross-linked polymers require precise estimation of the delivery window for injection *in vivo.* Due to the chemical cross-links forming with time, rapid changes in

viscosity can take place. The material can potentially become too thick to deliver via catheters and therefore, the delivery window of the polymer solution becomes a crucial parameter. By combining both gelation mechanisms, improved properties of the polymer solution are developed. As far as injectability is concerned, the dual-gelling system was delivered via catheters with ease, as reported by the surgeon. The gel was delivered in the aneurysm sac and remained in the aneurysm for the period of time that it was observed (~1hr). When the aneurysm volume was close to being completely filled with the material, the hydrogel occluded the aneurysm with slight recanalization observed. For potential use as an embolic agent, this dual-gelling system will need some optimization to completely occlude aneurysms.

5.3.3 *In Vitro* Models

After having observed the recanalization taking place in the *in vivo* preliminary swine study, further examination of the delivery and occlusion properties of the dual gels was necessary. Since the gels were not radio-opaque, it was thus difficult to observe how they were delivered, how they were injected in the aneurysm sac, and the extent of the volume filling. It was also crucial to visually observe what occurred once the balloon was deflated and flow was resumed, especially in terms of the material remaining in the aneurysm sac, its occlusion properties and any potential leaks. By testing the gel in glass aneurysm models, the feasibility of injection and gelation of the material in a system mimicking physiological conditions can be obtained and aids in determining the

procedure and feasibility for *in vivo* work. Soga et al. have also used similar glass aneurysm models to evaluate their embolic agents (Soga, Preul, Furuse, Becker, & McDougall, 2004). In our study, saccular glass aneurysms were employed to imitate the physiology of saccular aneurysms *in vivo.* After placement of the balloon and filling catheters, the mixed polymer solutions were injected via filling catheter into the dome of the aneurysm. Injections of the materials at 37°C did not undergo complications; on the contrary, the surgeon was able to deliver the polymer mixtures easily, with minimal pressure. In Figure 5.9, the different stages for the delivery and feasibility of the NC-NHA gelling system are observed.

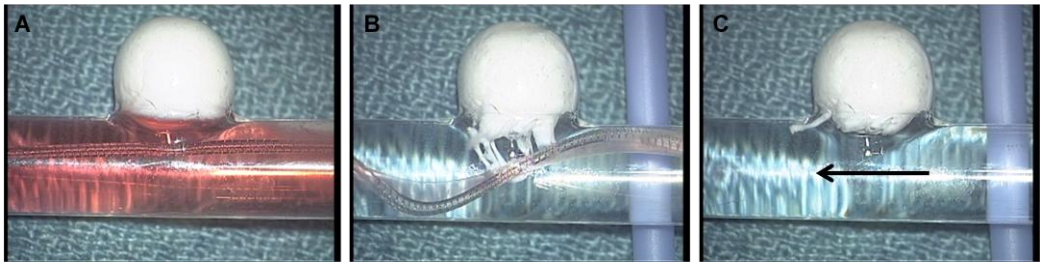

Figure 5.9 Various stages of the *in vitro* catheter delivery of the NC-NHA hydrogel in aneurysm glass model. A) balloon inflated and hydrogel injected in aneurysm sac, B) balloon taken down and C) flow resumed to observe embolization results of the NC-NHA gelling system.

In (A), the NC-NHA gel was fully delivered in the aneurysm to occlude as much of the aneurysm volume as possible. The balloon was left inflated (as indicated with the red coloring) for 10min to allow for physical gelation to take place at 37°C. As the balloon was taken down after 10min (B), one can detect that the gel

appears to slightly stick to the balloon catheter. The adhesion of the material to the balloon catheter may be as a result of the surface properties of the balloon catheter. Since these catheters were not designed for this specific application, the surface interaction between gels and the balloon were not optimized. When flow was allowed to resume in the parent vessel (C), the gel remained in place, occluding the neck of the aneurysm and preventing flow into the aneurysm dome. A small strand of the gel, however, can be seen to stray into the parent vessel. This may be due to the adhesion of the gel to the catheter and thus, this strand resulted from the detachment of the surface of the gel in contact with the catheter, which could not be incorporated into the cohesive gel mass within the aneurysm. In Figure 5.10, the similar stages of delivery and feasibility are illustrated for the NC-NCVS gelling system.

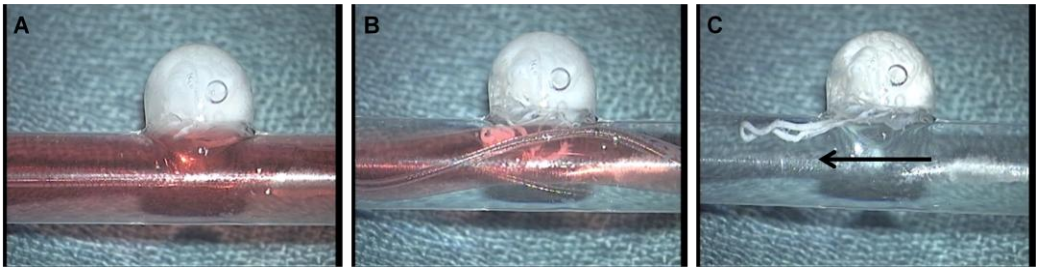

Figure 5.10 Various stages of the *in vitro* catheter delivery of the NC-NCVS hydrogel in aneurysm glass model. A) balloon inflated and hydrogel injected in aneurysm sac, B) balloon taken down and C) flow resumed to observe embolization results of the NC-NCVS gelling system.

As the material was injected via filling catheter into the aneurysm, a less cohesive gel was formed. As seen in (A), the gel strings did not seem to merge together to form a dense gel mass in the aneurysm. As the balloon was deflated (B), some of the gel strings also appear to adhere to the balloon catheter, again due to the lack of characterization of balloon surface properties and interaction with hydrogels. Once the balloon was removed and the flow resumed in the parent vessel (C), the gel remained in the aneurysm; however, it did not form a cohesive gel mass to completely occlude the aneurysm. An air bubble as well as some voids can be witnessed in the aneurysm. When the gel was administered, the strands failed to mesh into a larger gel but instead maintained their individual strand forms to fill the aneurysm volume. Additionally, small strings are also hanging from the aneurysm neck, which may have resulted from the gel portion that was detached from the adhesion to the catheter.

The difference observed between the delivery, feasibility and occlusion properties of the two gels can be attributed to the fundamentally different gelation properties of the NC-NCVS system, when compared to the NC-NHA gelling system. Both gels undergo dual gelation mechanisms: physical gelation via temperature-sensitivity of poly(NIPAAm) and chemical gelation by covalent cross-link formation between thiols and vinyls via a Michael-type addition reaction. In the NC-NHA system, the thermoresponsive properties of the gel are more dominant than its chemical cross-link formation. Because the rate of reaction between the thiol on the cysteamine and the vinyl on the acrylate is slow, the formation of covalent cross-links and chemical gelation occur at a slower rate.

Thus, once the mixed solution is injected at 37°C, physical gelation takes place almost immediately to form a gel. In the case of the NC-NCVS gelling system, the rate of reaction between the thiol on the cysteamine and the vinyl on the vinylsulfone is much faster, leading to a faster formation of covalent cross-links and chemical gelation. The chemical gelation component of the NC-NCVS system plays a more important role in the overall gelation mechanism. Therefore, when the mixed solution is injected, it has already pre-formed a majority of covalent cross-links and then undergoes further curing at 37°C. This explains the reason for the lack of integration of the gel strands into a gel mass once injected in the aneurysm. Nonetheless, the NC-NCVS gelling system may provide for stronger and more stable properties in the aneurysm because of the further degree of covalent cross-linking resulting from chemical reaction. However, to prevent the string-like behavior of this gel upon injection, the copolymers should be mixed for lesser time to diminish the chemical cross-links formed and result in an injection which allows for formation of a gel mass. Whereas the NC-NHA gelling system forms a well integrated gel upon injection, the less chemically cross-linked aspect of the gel may cause instability and weakness in the properties of the gel. Although both gelling systems showed slight adhesion of the surface of the gel in contact with the catheter and each gel possesses its set of benefits and drawbacks, overall, both gelling systems were easily administered via catheters into the aneurysm and remained in the aneurysm once flow resumed, providing in one case almost full occlusion (NC-NHA) and in the other, partial occlusion of the aneurysm (NC-NCVS). From the *in vitro* glass models, it was determined that

further optimization is needed to provide for a better injectable and embolic material. This can be done by performing more *in vitro* testing by changing variables, such as mixing time, polymer concentration in the hydrogel and possibly cross-link density.

5.3.4 Creep and Degradation Analysis

Hydrogels behave as viscoelastic materials. Viscoelasticity takes into account elasticity, flow and the molecular motion in the polymeric materials (Anseth, Bowman, & Brannon-Peppas, 1996). This viscoelastic response is dependent on the nature of the mechanical motion that the material is subjected to and on the time scale of this mechanical motion, whether applied stress or strain. Once a mechanical stress is applied, a time-dependent strain results due to the movement of the various parts of the polymer chains. By performing a creep test, the viscoelastic behavior of a material can be analyzed. A creep curve demonstrates how strain changes with time, under constant stress (Alfrey & Doty, 1945). In Figure 5.11, the creep compliance is plotted against time for the NC-NHA gel (Fig 5.11A) and NC-NCVS gel (Fig 5.11B) at different mixing times of 30s, 1min and 2min.

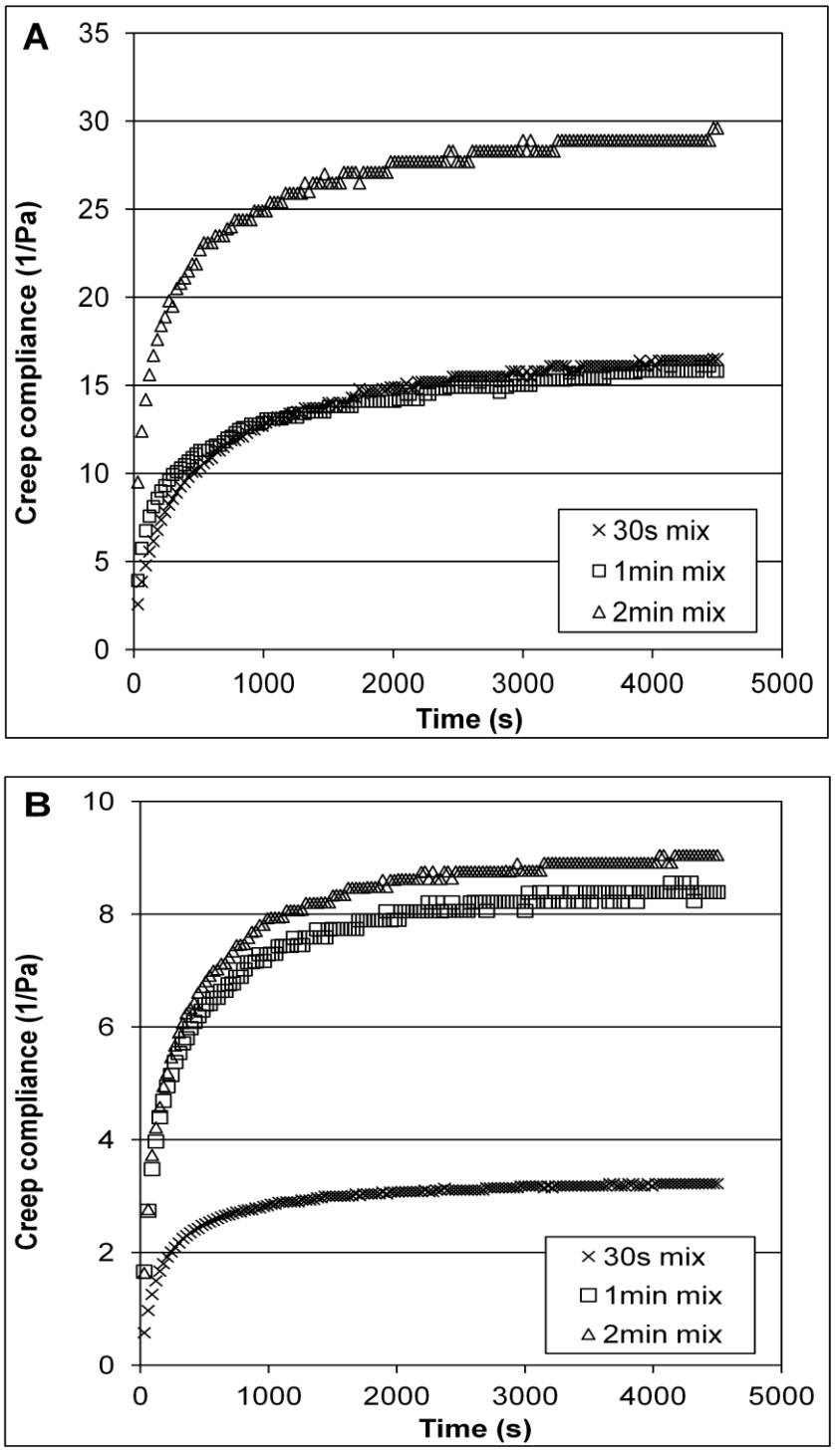

Figure 5.11 Rheological creep tests for A) NC-NHA and B) NC-NCVS at different mixing times of 30s, 1min and 2min, demonstrating viscoelastic behavior of both hydrogels.

Creep compliance represents the ratio of time-dependent shear strain to the applied stress. As observed by the shape of the curves in both figures, regardless of mixing times, the hydrogels demonstrate typical viscoelastic behavior, with creep deformation occurring over time. A rapid elastic response occurs initially, followed by a slow viscous response (Skrzeszewska et al., 2009). The gel systems experienced a fast deformation rate within the first 1000 seconds. After that point, deformation slowed down and reached a plateau. Although all mixing times demonstrate viscoelastic behavior, both hydrogels experience greater creep compliance with longer mixing times. It has previously been reported that polymers which have less chain mobility underwent a lesser degree of creep compliance than polymers with greater chain mobility (Tweedie & Van Vliet, 2006). At shorter mixing times, the copolymers are able to form chemical cross-links as well as physically entangle with temperature. However, as mixing time was increased, the chemical cross-links remained within the network but the physical entanglements were disrupted. The movement of the solution in the syringe over a longer period of time resulted in more rearrangement of the physical cross-links, which in turn, diminished the overall degree of cross-linking in the gel network. With less cross-links present, the gel is less rigid and thus possesses greater chain mobility, which leads to an increase in the creep compliance experienced by the gel. Although the behavior of increased creep compliance with increased mixing time was observed in both gelling systems, the magnitude of the creep compliance which each gel underwent is different. As observed in Figure 5.11A, the NC-NHA gelling system experienced creep

compliance almost reaching 30 (1/Pa), whereas the NC-NCVS gelling system, seen in Figure 5.11B, had creep compliance values reaching 9 (1/Pa). It is thus noticeable that the NC-NHA gel experienced a greater degree of creep compliance than the NC-NCVS gelling system. The main factor contributing to the difference in creep compliance within the gels is due to the degree of chemical cross-links formed. It was previously observed that the chemical reaction between thiols and vinyls in the NC-NHA system is slower than in the NC-NCVS system (Chapter 4)(Bearat et al.,). The NC-NCVS system allows for faster and more efficient chemical cross-link formation than the NC-NHA system. Because more chemical cross-links are present in the NC-NCVS system, there is less chain mobility as the chemical cross-links provide rigidity in the network structure. This leads to less creep compliance experienced. Since the NC-NHA system has fewer chemical cross-links due to its slower Michael-type addition reaction, the system relies more on physical entanglements for gelation. With few chemical cross-links and more opportunities for disruption of physical entanglements, more chain mobility is presented in this system, resulting in higher creep compliance experienced. For use *in vivo* as injectable gelling systems, the NC-NCVS gelling system appears to be more favorable due to its reduced creep compliance as a result of greater chemical cross-linking. The presence of more cross-links in the NC-NCVS gel diminishes the potential for creep deformation occurring *in vivo* over use of the NC-NHA gel.

For an injectable and implantable material, its degradation is an important feature of its properties, specifically for a material intended to be used

permanently, as is the case for an embolic agent for aneurysm occlusion. Degradation of a hydrogel can be influenced by hydrolysis, enzymatic action or dissolution (K. Y. Lee & Mooney, 2001). For the hydrogels addressed here, the mode of potential degradation would undergo hydrolysis, mainly the breaking of ester bonds by water. To analyze degradation of the materials, the gels were incubated in water at 37°C and their swelling ratios were measured over the course of 1.5 year. As observed in Figure 5.12, the swelling ratios of both hydrogels remained stable throughout the course of the study.

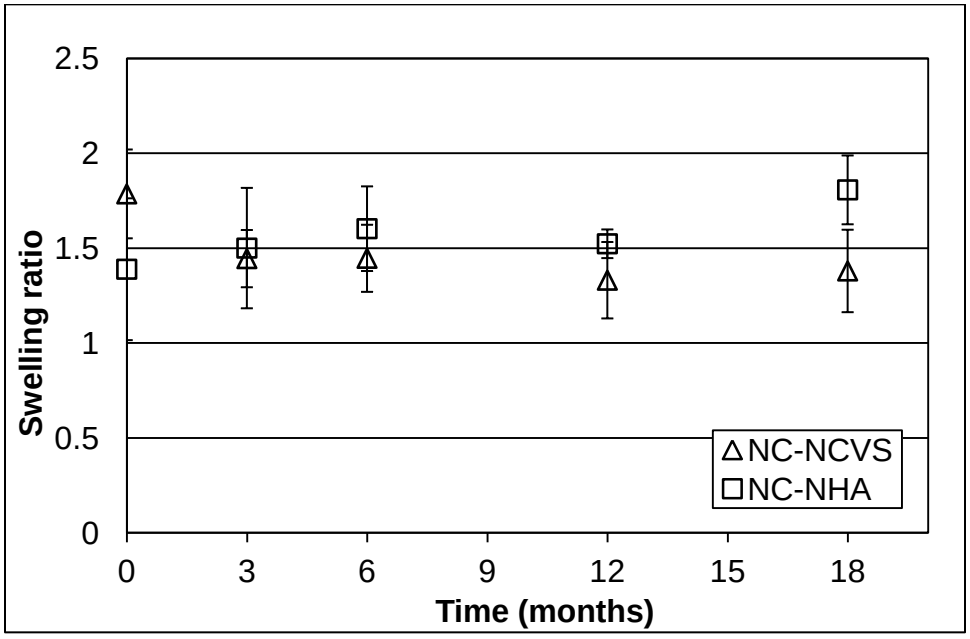

Figure 5.12 Degradation study of NC-NHA and NC-NCVS over the course of 1.5 yr, with both hydrogels remaining stable over the course of time.

For the NC-NHA gelling system, the swelling ratio ranged between 1.38 and 1.6, whereas for the NC-NCVS gelling system, it remained between 1.33 and 1.78.

The physical state of both hydrogels incubated in PBS in vials can be seen in Figure 5.13 (NC-NHA on the left, NC-NCVS on the right). Both gels remained stable and maintained their original shapes. Statistical analysis via ANOVA indicated that there is no significant difference between the swelling ratios at the various time points for each gelling system. Thus, both hydrogels did not show signs of degradation and maintained their stability. This characteristic is in great need for permanent implantation of the hydrogel within the aneurysm *in vivo*. With both gels remaining stable and not undergoing degradation, essentially via hydrolysis, renders them plausible for long term embolization.

Figure 5.13 Image of stable samples of NC-NHA (left) and NC-NCVS (right) hydrogels incubated in PBS at 37°C after 1.5 yr.

5.4 Conclusions

In this study, dual-gelling materials were investigated as potential liquid-to-solid embolic agents for endovascular occlusion of intracranial aneurysms. These hydrogels undergo gelation via two mechanisms: physical and chemical. Physical gelation occurs due to the temperature responsive nature of poly(NIPAAm), which transitions from a liquid to a gel around 31°C. Chemical gelation takes place via a chemical reaction between thiol and vinyl functional groups on the copolymers, ultimately forming a covalent cross-link. The hydrogels (NC-NHA and NC-NCVS) demonstrated great biocompatibility. The MTT and live/dead assays performed showed that cells proliferated normally when exposed to the gels for 3 days. This provides for a good indicator of biocompatible interaction between the gels and cells/tissues *in vivo*. As proof-of-concept, the NC-NHA gel was tested in a swine model for analysis of its injectable and occluding properties. The gel was able to be delivered endovascularly via microcatheters and injected into the aneurysm sac. The aneurysms filled with the gel exhibited some recanalization after flow resumption. When the aneurysm was not fully filled with the gelling material, greater recanalization was observed. However, as the injected volume was increased to result in a more complete fill of the aneurysm sac, very little recanalization was observed. The preliminary *in vivo* study demonstrated that the hydrogel was successfully delivered endovascularly and by optimizing injection volume and other gelling properties, almost complete occlusion could be achieved. Nonetheless, these results were taken immediately after embolization thus to

better analyze the occlusion properties of the gel, longer flow duration and X-ray observation would be needed. Using aneurysm glass models, the efficacy of the hydrogels was assessed visually, with regards to their injectability and extent of occlusion capabilities. From the observations, the NC-NHA gelling system allowed for a more cohesive gel mass to form and to fully fill the aneurysm volume. The NC-NCVS gelling system was administered in more string-like form, resulting in a less compact gel mass and partial occlusion of the aneurysm. Although both gelling systems showed slight adhesion to the balloon catheter and a gel strand protruding from the aneurysm, they were easily injected via catheters into the aneurysms and the gels remained in the aneurysm after deflation of the balloon and reintroduction of flow. The rheological creep tests demonstrated that a possible explanation for the observed recanalization and partial occlusion may be due to the viscoelastic behavior of these hydrogels. Although using simultaneous physical and chemical gelation reduced some of the creep experienced by purely physical gels and increased the strength, further work is needed to optimize the properties of these hydrogels to attain full occlusion of aneurysms via endovascular routes. However, being a waterborne system which is biocompatible and undergoes both modes of gelation at physiological temperature and pH allows it to be unique in its characteristics. The benefit of using a poly(NIPAAm)-based material is the possibility to engineer hydrogels with different properties. Using different solvents, comonomers and polymerization techniques, an array of polymer systems can be developed to better fit the requirements for particular applications.

CHAPTER 6

CONCLUSIONS AND FUTURE WORK

6.1 Dual-Gelling Polymer Systems as Embolic Agents for Cerebral Aneurysms

The work compiled in this thesis examined the use of dual-gelling polymer systems as liquid-to-solid materials for endovascular embolization of cerebral aneurysms. These dual gels are based on a thermoresponsive polymer, poly(N-isopropylacrylamide) (poly(NIPAAm)), which was functionalized with thiols and vinyls to undergo chemical reaction. The polymer systems undergo dual gelation due to the transition from a solution to a gel as temperature is increased from room to body, as well as the covalent cross-link formation via the chemical reaction between thiols and vinyls on the copolymers. The focus of this work is to develop these polymers, assess their properties and phase transition behavior, and to test their biocompatibility and delivery for potential use in occluding cerebral aneurysms.

6.2 Synthesis of Gelling Polymer Systems

The polymers presented herein were synthesized via free radical polymerization and conjugated with functional groups to produce poly(NIPAAm-*co*-HEMA-acrylate), poly(NIPAAm-*co*-cysteamine) and poly(NIPAAm-cysteamine-*co*-vinylsulfone), abbreviated as poly(NHA), poly(NC) and poly(NCVS), respectively. Poly(NC) was functionalized with cysteamine to provide thiol groups on its side chains. Poly(NHA) and poly(NCVS) were

functionalized to present terminal vinyl groups on the side chains. When either of the vinyl-conjugated polymers (NHA or NCVS) are mixed with the thiol-conjugated counterpart (NC), a Michael-type addition reaction occurs. At a pH of 7.4, the thiol groups are deprotonated, allowing for a nucleophilic substitution reaction onto the vinyl groups. As a result, covalent cross-links are formed between the mixed entities. This chemical reaction takes place at physiological pH and temperature, making it a feasible method to form chemical gels at physiological conditions.

The major portion (95 to 98 wt%) of the synthesized polymers consists of poly(NIPAAm). This polymer exhibits a lower critical solution temperature (LCST) around 31°C in an aqueous environment. Below the LCST, the polymer is hydrophilic and soluble, remaining in solution form. As temperature is increased above the LCST, the polymer becomes hydrophobic causing the polymer to collapse, forming a gel. By conjugating various monomers onto the homopolymer, this phase transition could be altered. Hydrophobic monomers which are conjugated onto poly(NIPAAM), such as HEMA-acrylate, decrease the LCST of the overall polymer, while hydrophilic monomers, such as cysteamine or vinylsulfone, increase the LCST.

The advantage of these polymer systems is that they can be engineered in a bottom-up approach. By synthesizing the polymers, the characteristics can be changed to fit the desired needs. The choice of many different solvents, monomers, polymerization techniques and feed ratios gives a plethora of polymers with various properties. Here, tetrahydrofuran was used as the solvent to

result in lower molecular weight polymers, with the intent that they can be cleared by the kidney in case of byproducts or leakage. The chosen monomers were utilized to functionalize thiols and vinyls in order to chemically react via Michael-addition reaction, while poly(NIPAAm) was chosen as a thermoresponsive polymer for physical gelation, for which both can undergo transition at physiological conditions.

6.3 Characterization of Properties of Polymer Gels

Various characterization methods were used to examine the properties obtained of the synthesized polymers. The ^{1}H NMR and FTIR spectra depicted the chemical and structural composition of the polymers by indicating the location of all protons and functional groups present in the structure, therefore confirming the successful synthesis of the polymers. It was crucial to analyze the thermal properties of the synthesized polymers, performed using DSC and cloud point. Poly(NHA) exhibited a decrease in the LCST, around 29.1°C, due to its hydrophobic components. Additionally, its broad DSC curve and early onset of opacity in cloud point indicated a less homogeneous composition of the polymer, with some chains undergoing transition at low temperatures. Poly(NC) and poly(NCVS) showed slightly higher LCSTs of 30.4°C and 34.7°C, respectively, due to their hydrophilicity. The narrow shape of their DSC curves and sharp drop in transmission in cloud point data demonstrate that these copolymers have a more homogeneous composition, with the majority of chains collapsing near the LCST temperature. All polymers exhibit LCSTs below physiological temperature

(37°C), thus making them feasible for liquid-to-solid gelling systems *in vivo*, as they would form gels once injected in the body.

Via rheological studies, many properties of the polymers were investigated. Time sweeps on the physical-chemical gels done at different mixing times revealed that the longer the copolymers are mixed, the faster gelation point is reached. A longer duration of mixing presents more opportunities for the thiol and vinyl groups to interact and form cross-links, as well as form a more homogeneous mixture, resulting in the faster formation of a gel. Frequency sweeps showed that purely physical gels are frequency-dependent and undergo creep flow, while purely chemical gels have low strength. By combining physical and chemical gelation, the benefits from both gelation mechanisms could be taken advantage of. The physical-chemical gels demonstrated a reduction in frequency-dependence observed by purely physical gels while increasing the overall mechanical strength. Temperature sweeps confirmed the LCST of the polymers while showing that the polymers increase in strength when reaching LCST as the physical gelation adds on to chemical cross-linking.

For a hydrogel to be used *in vivo*, its swelling and degradation need to be monitored. Swelling studies conducted on the two physical-chemical gels, NC-NHA and NC-NCVS, illustrated temperature dependence of swelling ratios. As temperature was increased to 37°C, the gels experienced a slight degree of shrinking. At low temperatures, only chemical cross-links hold the gels together; however, as temperature is increased, physical gelation contributes to the overall gelation. The hydrogels presented here are designed to be used as permanent

implants for occlusion of aneurysm, therefore, degradation is unwanted. Degradation studies of both hydrogels revealed that their swelling ratios remain stable over the course of 1.5 years, thus no degradation was observed for either gel, a promising feature for long term use.

Since the chemical gelation component of the overall gelling process occurs via a chemical reaction between functional groups, the rate at which the moieties interact and form covalent cross-links is important. Kinetic studies were performed between NC and NHA as well as NC and NCVS at ratios of 1:1 and 1:10 (thiol: vinyl) at pH 7.4. Results indicated that as the molar ratio was increased, faster reaction occurred between the reactive species. More importantly, the kinetic studies revealed the much faster rate of reaction between NC and NCVS, compared to NC and NHA. The faster reaction rate of the NC-NCVS gelling system explained the more significant effect of chemical gelation to the gelling system, whereas for the NC-NHA gelling system, its slow reaction allowed for physical gelation to be the dominant gelation mechanism.

6.4 Structural Analysis of Phase Transition of Poly(NIPAAm) and Copolymers

To analyze the phase transition properties and behavior of poly(NIPAAm) and its copolymers, thermal and x-ray techniques were utilized. Cloud point was done on homopolymer, NC and NHA at different concentrations and revealed that as concentration is decreased, the phase transition temperature is increased. Similar behavior was observed with DSC studies. X-ray tools were used to investigate the structural changes of the polymers during phase transition at the

macromolecular level. In the SAXS temperature studies of the three polymers, a peak developed as temperature was increased corresponding to a d-spacing value of 11-12Å. This value represents the distance between polymer chains as water molecules are expelled and the chains associate at the LCST. SAXS kinetic studies demonstrated that the phase transition occurs rapidly, within 1 minute and 40 seconds, while equilibrium of the extent of reaction takes place within 15 minutes. SAXS chemical gelation experiments did not give rise to new peaks; however, the same peak seen in the temperatures studies is formed in the physical-chemical gel. XRD data exposed two peaks in the structure of the polymers (NIPAAm, NC and NHA) as well as in the chemical and physical-chemical gels. The first peak at 11-12Å corresponds to the peak witnessed in the SAXS studies, confirming the distance between polymer chains as they associate. A second peak was discovered at 4-5Å representing the distance between side chains on the polymer backbones. In the chemical gel, the ratio between peak intensities is different, with the first peak being dominant. This indicates that the covalent cross-links formed are the main contributors to the association of the chains. In the physical-chemical gel, the ratio of peak intensities is less different due to the contribution of both covalent cross-links and physical gelation in the association of the chains.

6.5 Cytotoxicity, *In Vitro* and *In Vivo* Testing of Polymer Gels

For any biomaterial, its biocompatibility and efficacy are crucial to its performance *in vivo*. Cytotoxicity studies were conducted using MTT

proliferation assays and live/dead assays on both hydrogels. The MTT assays indicated no difference between controls and cell count at 15 and 30 wt% for both NC-NHA and NC-NCVS gelling systems. As concentration was increased to 60 wt%, the NC-NCVS gelling system did not show any difference with controls; however, the NC-NHA gelling system indicated different cell counts from controls. Although 30-40 wt% concentrations are used *in vivo*, even higher concentrations can potentially show normal proliferation. The live/dead assays showed that normal shapes and proliferation rates of cells exposed to both gels, when compared to controls. More than 90% viability was witnessed in NC-NHA, NC-NCVS and the controls, demonstrating normal proliferation of cells when incubated with the gels for 3 days. The cytotoxicity results affirm the excellent interaction of the gels with fibroblast cells.

In vitro glass models were used to test for the injectability and occlusion properties of the gels, as well as provide for visualization of the procedure and results. Both gels were easily delivered via catheters and injected in the glass aneurysms. Once flow was resumed, the gels remained within the aneurysm sac; however, there was slight adhesion of the gel to the balloon catheter as well as small strings of gel protruding into the parent vessel. The *in vivo* swine study was conducted as a proof-of-concept for the use of the dual gelling systems for aneurysm embolization. The NC-NHA gel was delivered through a catheter and injected in the surgically created aneurysm with ease. After flow was resumed in the parent vessel, slight recanalization was observed in the aneurysms. Nonetheless, the dual gelling system was able to undergo liquid-to-solid transition

at physiological temperature while remaining deliverable through catheters. Although further optimization is needed to provide better mechanical properties, these dual gelling polymer systems have shown feasible characteristics in terms of biocompatibility, as well as delivery and gelation *in vivo*.

6.6 Limitations

Although the current work highlights the achievements made with the dual-gelling systems, some limitations were encountered and need addressing. With hydrogels, the degree of swelling or shrinking can be a significant challenge, especially when the intended application is as a permanent implant in a confined volume. As was observed, the presented hydrogels experienced some shrinking when incubated at 37°C. This could potentially result in the gel shrinking within the aneurysm sac, leading to the gel becoming an embolus if leaked out of the sac. Additionally, the hydrogels demonstrated viscoelastic behavior which could result in creep deformation *in vivo*. If the gels undergo creep deformation *in vivo*, it could eventually cause leaching of the gel into the parent vessel, leading to further complications. The observed limitations to the hydrogel properties can be adjusted for via synthesis, as explained in the future work section below.

For use as embolic agents, the dual gels will also need to be optimized for the essential properties needed *in vivo*. This includes the need to account for incorporation of a radio-opaque modality within its network to allow for X-ray visualization, further discussed in the future work section. As was seen in the glass models, strings of gel emerged from the aneurysm sac due to incomplete

filling and longer mixing time. The preliminary swine model demonstrated that the filling volume is very important in obtaining complete occlusion. When the aneurysm was underfilled, major recanalization occurred post-embolization, whereas when the volume of gel injected was increased to provide for a more complete filling of the aneurysm, very little recanalization was witnessed. Thus, further optimization of mixing, delivery and injectability will need to be performed to obtain better results, in terms of complete occlusions, *in vitro* as well as *in vivo*.

6.7 Future Work

The work presented here was designed to develop and test properties of a dual gelling polymer system for occlusion of cerebral aneurysms. The studies highlighted the ability of gelation via chemical reaction and temperature-sensitivity at physiological conditions, as well as the excellent biocompatibility and ease of delivery via catheters. The aforementioned characteristics of these dual hydrogels demonstrated the potential for use as embolic agents for aneurysm occlusion. Nonetheless, further optimization is required to result in better suited hydrogels for such endovascular embolization applications.

The benefit of synthesizing the polymers stems from the ability and control to engineer the hydrogels for particular needs. In order to improve the properties of the current hydrogels, the mechanical strength, creep and shrinking will have to be altered. To do so, synthesis could be done in nonpolar solvents (1, 4-dioxane or benzene) to decrease the prevalence of chain transfer and therefore

result in higher molecular weight polymers. An increase in molecular weight correlates to an increase in mechanical strength. To reduce the creep experienced by the current hydrogels, the amount of covalent cross-linking in the system could be increased with higher molar feed ratios of functional groups or by using other functional groups which have higher affinity towards Michael-type addition reaction for more efficient chemical cross-linking. Additionally, the shrinking behavior of the gels could be prevented by conjugating a controlled quantity of hydrophilic groups, such as acrylic acid, into the polymer. Hydrophilicity aids in forming hydrogen bonds between water molecules and hydrophilic portions of the polymer, therefore, retaining water and preventing shrinking.

For use of these dual gels *in vivo,* it is important to be able to monitor the hydrogel while it is being injected and while positioned in the aneurysm sac. Current treatments ensure that the materials contain some form of radio-opacity, mainly a contrast agent. The hydrogels presented here do not incorporate any contrast agents and were therefore difficult to monitor via fluoroscopy. Future work should aim at making the hydrogels radio-opaque, possibly by either using commercially available contrast agents mixed into the gel, such as Conray^{TM} or Omnipaque^{TM}, or by conjugating radio-opaque moieties into the polymer system during synthesis. Ideally, conjugation of radio-opaque components, such as an iodine-based species, would be preferred to prevent leakage of the contrast agent and to maintain biocompatibility. Additional testing of the gels for their mixing, deliverability and injectability will need to be done in glass models to achieve better occlusion with no gel strings detected in the parent vessel and to master the

technique to achieve full volume filling with the optimized gelling properties. Once further optimized, these dual gels could then be tested in acute swine models for occlusion properties and eventually in chronic swine models for observation of long-term occlusion, biocompatibility and possible neointimal tissue formation over the neck of the aneurysm.

The reported dual gelling polymer systems have overall shown feasible properties for potential use *in vivo* as embolic agents for cerebral aneurysms. With further optimization and testing of these hydrogels, enhanced knowledge of the behavior as well as the advantages and shortcomings of these dual gels could be uncovered. Since there are no current FDA-approved treatments which provide a non-invasive technique combined with full occlusion, further research into hydrogels could potentially offer an improved treatment method for patients suffering from cerebral aneurysms.

REFERENCES

Alfrey, T., & Doty, P. (1945). The methods of specifying the properties of viscoelastic materials. *Journal of Applied Physics, 16*(11), 700-713.

Allen, F. H., Kennard, O., Watson, D. G., Brammer, L., Orpen, A. G., & Taylor, R. (1987). Tables of bond lengths determined by X-ray and neutron diffraction. part 1. bond lengths in organic compounds. *J.Chem.Soc., Perkin Trans.2,* (12), S1-S19.

Anseth, K. S., Bowman, C. N., & Brannon-Peppas, L. (1996). Mechanical properties of hydrogels and their experimental determination. *Biomaterials, 17*(17), 1647-1658.

Awad, H. A., Quinn Wickham, M., Leddy, H. A., Gimble, J. M., & Guilak, F. (2004). Chondrogenic differentiation of adipose-derived adult stem cells in agarose, alginate, and gelatin scaffolds. *Biomaterials, 25*(16), 3211-3222.

Babiker, M. H., Gonzalez, L. F., Ryan, J., Albuquerque, F., Collins, D., Elvikis, A., & Frakes, D. H. (2012). Influence of stent configuration on cerebral aneurysm fluid dynamics. *Journal of Biomechanics, 45*, 440-447.

Bae, Y. C., Lambert, S. M., Soane, D. S., & Prausnitz, J. M. (1991). Cloud-point curves of polymer solutions from thermooptical measurements. *Macromolecules, 24*, 4403-4407.

Bae, Y. H., Okano, T., & Kim, S. W. (1991). "On–Off" thermocontrol of solute transport. I. temperature dependence of swelling of N-isopropylacrylamide networks modified with hydrophobic components in water. *Pharmaceutical Research, 8*(4), 531-537.

Balasubramaniam, S., Pothayee, N., Lin, Y., House, M., Woodward, R. C., St. Pierre, T. G., . . . Riffle, J. (2011). Poly (N-isopropylacrylamide)-coated superparamagnetic iron oxide nanoparticles: Relaxometric and fluorescence behavior correlate to temperature-dependent aggregation. *Chemistry of Materials, 23*(14), 3348-3356.

Batrakova, E. V., & Kabanov, A. V. (2008). Pluronic block copolymers: Evolution of drug delivery concept from inert nanocarriers to biological response modifiers. *Journal of Controlled Release, 130*(2), 98-106.

Batrakova, E. V., Kelly, D. L., Li, S., Li, Y., Yang, Z., Xiao, L., . . . Kabanov, A. V. (2006). Alteration of genomic responses to doxorubicin and prevention of MDR in breast cancer cells by a polymer excipient: Pluronic P85. *Molecular Pharmaceutics, 3*(2), 113.

Bearat, H. H., Lee, B. H., Valdez, J., & Vernon, B. L. (2011). Synthesis, characterization and properties of a physically and chemically gelling polymer system using poly (NIPAAm-co-HEMA-acrylate) and poly (NIPAAm-co-cysteamine). *Journal of Biomaterials Science, Polymer Edition, 22*(10), 1299-1318.

Becker, T. A., Preul, M. C., Bichard, W. D., Kipke, D. R., & McDougall, C. G. (2007). Preliminary investigation of calcium alginate gel as a biocompatible material for endovascular aneurysm embolization in vivo. *Neurosurgery, 60*(6), 1119.

Brain aneurysm statistics and facts | the brain aneurysm foundation. Retrieved March 13, 2012, from http://www.bafound.org/Statistics_and_Facts

Brannon-Peppas, L., & Peppas, N. A. (1991). Equilibrium swelling behavior of pH-sensitive hydrogels. *Chemical Engineering Science, 46*(3), 715-722.

Brazel, C. S., & Peppas, N. A. (1995). Synthesis and characterization of thermo- and chemomechanically responsive poly (N-isopropylacrylamide-co-methacrylic acid) hydrogels. *Macromolecules, 28*(24), 8016-8020.

Brilstra, E. H., Rinkel, G. J. E., van der Graaf, Y., van Rooij, W. J. J., & Algra, A. (1999). Treatment of intracranial aneurysms by embolization with coils: A systematic review. *Stroke, 30*(2), 470-476.

Bruice, T. C., & Fife, T. H. (1962). Hydroxyl group catalysis. III. 1 the nature of neighboring hydroxyl group assistance in the alkaline hydrolysis of the ester bond. *Journal of the American Chemical Society, 84*(10), 1973-1979.

Byrne, J. V., Sohn, M. J., & Molyneux, A. J. (1999). Five-year experience in using coil embolization for ruptured intracranial aneurysms: Outcomes and incidence of late rebleeding. *Journal of Neurosurgery, 90*(4), 656-663.

Can, E., Küsefoğlu, S., & Wool, R. (2001). Rigid, thermosetting liquid molding resins from renewable resources. I. synthesis and polymerization of soy oil monoglyceride maleates. *Journal of Applied Polymer Science, 81*(1), 69-77.

Cekirge, H. S., Saatci, I., Ozturk, M. H., Cil, B., Arat, A., Mawad, M., . . . Turk, S. (2006). Late angiographic and clinical follow-up results of 100 consecutive aneurysms treated with onyx reconstruction: Largest single-center experience. *Neuroradiology, 48*(2), 113-126.

Cellesi, F., Tirelli, N., & Hubbell, J. A. (2004). Towards a fully-synthetic substitute of alginate: Development of a new process using thermal gelation and chemical cross-linking. *Biomaterials, 25*(21), 5115-5124.

Censi, R., Fieten, P. J., di Martino, P., Hennink, W. E., & Vermonden, T. (2010). In situ forming hydrogels by tandem thermal gelling and michael addition reaction between thermosensitive triblock copolymers and thiolated hyaluronan. *Macromolecules, 43*(13), 5771-5778.

Cerebral aneurysms information page: National institute of neurological disorders and stroke, national institutes of health. Retrieved March 13, 2012, from http://www.ninds.nih.gov/disorders/cerebral_aneurysm/cerebral_aneurysms.htm

Chalal, M., Ehrburger-Dolle, F., Morfin, I., Bley, F., Aguilar de Armas, M. R., López Donaire, M. L., . . . Ziane, O. (2010). SAXS investigation of the effect of temperature on the multiscale structure of a macroporous poly (N-isopropylacrylamide) gel. *Macromolecules, 43*(4), 2009-2017.

Chaloupka, J. C., Huddle, D. C., Alderman, J., Fink, S., Hammond, R., & Vinters, H. V. (1999). A reexamination of the angiotoxicity of superselective injection of DMSO in the swine rete embolization model. *American Journal of Neuroradiology, 20*(3), 401-410.

Chambon, F., & Winter, H. H. (1987). Linear viscoelasticity at the gel point of a crosslinking PDMS with imbalanced stoichiometry. *Journal of Rheology, 31*, 683-697.

Chang, C. W., Choi, D., Kim, W. J., Yockman, J. W., Christensen, L. V., Kim, Y. H., & Kim, S. W. (2007). Non-ionic amphiphilic biodegradable PEG–PLGA–PEG copolymer enhances gene delivery efficiency in rat skeletal muscle. *Journal of Controlled Release, 118*(2), 245-253.

Cheng, V., Lee, B. H., Pauken, C., & Vernon, B. L. (2007). Poly (N-isopropylacrylamide-co-poly (ethylene glycol))-acrylate simultaneously physically and chemically gelling polymer systems. *Journal of Applied Polymer Science, 106*(2), 1201-1207.

Chenite, A., Chaput, C., Wang, D., Combes, C., Buschmann, M. D., Hoemann, C. D., . . . Selmani, A. (2000). Novel injectable neutral solutions of chitosan form biodegradable gels in situ. *Biomaterials, 21*(21), 2155-2161.

Chu, B., & Hsiao, B. S. (2001). Small-angle X-ray scattering of polymers. *Chemical Reviews-Columbus, 101*(6), 1727-1762.

Chung, H. J., Lee, Y., & Park, T. G. (2008). Thermo-sensitive and biodegradable hydrogels based on stereocomplexed pluronic multi-block copolymers for controlled protein delivery. *Journal of Controlled Release, 127*(1), 22-30.

Clarke, M. (2008). Systematic review of reviews of risk factors for intracranial aneurysms. *Neuroradiology, 50*(8), 653-664.

Cui, Z., Lee, B. H., Pauken, C., & Vernon, B. L. (2010). Manipulating degradation time in a N-isopropylacrylamide-based co-polymer with hydrolysis-dependent LCST. *Journal of Biomaterials Science, Polymer Edition, 21, 6*(7), 913-926.

Cui, Z., Lee, B. H., & Vernon, B. L. (2007). New hydrolysis-dependent thermosensitive polymer for an injectable degradable system. *Biomacromolecules, 8*(4), 1280-1286.

Dai, D., Ding, Y. H., Danielson, M. A., Kadirvel, R., Lewis, D. A., Cloft, H. J., & Kallmes, D. F. (2005). Histopathologic and immunohistochemical comparison of human, rabbit, and swine aneurysms embolized with platinum coils. *American Journal of Neuroradiology, 26*(10), 2560-2568.

Dandy, W. E. (1938). Intracranial aneurysm of the internal carotid artery: Cured by operation. *Annals of Surgery, 107*(5), 654-659.

Dawson, R. C., Krisht, A. F., Barrow, D. L., Joseph, G. J., Shengelaia, G. G., & Bonner, G. (1995). Treatment of experimental aneurysms using collagen-coated microcoils. *Neurosurgery, 36*(1), 133-140.

de Salamanca, A. E., Diebold, Y., Calonge, M., Garcia-Vazquez, C., Callejo, S., Vila, A., & Alonso, M. J. (2006). Chitosan nanoparticles as a potential drug delivery system for the ocular surface: Toxicity, uptake mechanism and in vivo tolerance. *Investigative Ophthalmology & Visual Science, 47*(4), 1416-1425.

Debrun, G. M., Aletich, V., Ausman, J. I., Charbel, F., & Dujovny, M. (1997). Embolization of the nidus of brain arteriovenous malformations withn-butyl cyanoacrylate. *Neurosurgery, 40*(1), 112-121.

Denkbas, E. B., & Ottenbrite, R. M. (2006). Perspectives on: Chitosan drug delivery systems based on their geometries. *Journal of Bioactive and Compatible Polymers, 21*(4), 351-368.

Deshmukh, S. A., Sankaranarayanan, S. K. R. S., & Mancini, D. C. (2012). Atomic scale characterization of the conformational dynamics of a thermo-sensitive and a non-thermo-sensitive oligomer using vibrational spectra obtained from molecular dynamics. *Polymer, 53*(6), 1306-1320.

Deshmukh, S. A., Sankaranarayanan, S. K. R. S., Suthar, K., & Mancini, D. C. (2012). Role of solvation dynamics and local ordering of water in inducing conformational transitions in poly (N-isopropylacrylamide) oligomers through the LCST. *The Journal of Physical Chemistry B, 116*(9), 2651-2663.

Diebold, Y., Jarrín, M., Sáez, V., Carvalho, E. L. S., Orea, M., Calonge, M., Alonso, M. J. (2007). Ocular drug delivery by liposome–chitosan nanoparticle complexes (LCS-NP). *Biomaterials, 28*(8), 1553-1564.

Dingenouts, N., Norhausen, C., & Ballauff, M. (1998). Observation of the volume transition in thermosensitive core-shell latex particles by small-angle X-ray scattering. *Macromolecules, 31*(25), 8912-8917.

Dudeck, O., Jordan, O., Hoffmann, K., Okuducu, A., Tesmer, K., Kreuzer-Nagy, T., Felix, R. (2006). Organic solvents as vehicles for precipitating liquid embolics: A comparative angiotoxicity study with superselective injections of swine rete mirabile. *American Journal of Neuroradiology, 27*(9), 1900-1906.

Duvvuri, S., Janoria, K. G., & Mitra, A. K. (2005). Development of a novel formulation containing poly (d, l-lactide-co-glycolide) microspheres dispersed in PLGA–PEG–PLGA gel for sustained delivery of ganciclovir. *Journal of Controlled Release, 108*(2-3), 282-293.

Elliott, J. E., Macdonald, M., Nie, J., & Bowman, C. N. (2004). Structure and swelling of poly (acrylic acid) hydrogels: Effect of pH, ionic strength, and dilution on the crosslinked polymer structure. *Polymer, 45*(5), 1503-1510.

Ellman, G. L. (1958). A colorimetric method for determining low concentrations of mercaptans. *Archives of Biochemistry and Biophysics, 74*(2), 443-450.

Farhat, H. I., Elhammady, M. S., & Aziz-Sultan, M. A. (2010). N-butyl-2-cyanoacrylate use in intraoperative ruptured aneurysms as a salvage rescue: Case report. *Neurosurgery, 67*(1), E216-E217.

Feil, H., Bae, Y. H., Feijen, J., & Kim, S. W. (1993). Effect of comonomer hydrophilicity and ionization on the lower critical solution temperature of N-isopropylacrylamide copolymers. *Macromolecules, 26*, 2496-2500.

Feil, H., Bae, Y., Feijen, J., & Kim, S. (1992). Mutual influence of pH and temperature on the swelling of ionizable and thermosensitive hydrogels. *Macromolecules, 25*(20), 5528-5530.

Fellah, B. H., Weiss, P., Gauthier, O., Rouillon, T., Pilet, P., Daculsi, G., & Layrolle, P. (2006). Bone repair using a new injectable self-crosslinkable bone substitute. *Journal of Orthopaedic Research, 24*(4), 628-635.

Fiorella, D., Woo, H. H., Albuquerque, F. C., & Nelson, P. K. (2008). Definitive reconstruction of circumferential, fusiform intracranial aneurysms with the pipeline embolization device. *Neurosurgery, 62*(5), 1115.

Fischer, D., Li, Y., Ahlemeyer, B., Krieglstein, J., & Kissel, T. (2003). In vitro cytotoxicity testing of polycations: Influence of polymer structure on cell viability and hemolysis. *Biomaterials, 24*(7), 1121-1131.

Ford, M. D., Alperin, N., Lee, S. H., Holdsworth, D. W., & Steinman, D. A. (2005). Characterization of volumetric flow rate waveforms in the normal internal carotid and vertebral arteries. *Physiological Measurement, 26*(4), 477-488.

Forget Jr, T. R., Benitez, R., Veznedaroglu, E., Sharan, A., Mitchell, W., Silva, M., & Rosenwasser, R. H. (2001). A review of size and location of ruptured intracranial aneurysms. *Neurosurgery, 49*(6), 1322-1326.

Frank, H. S., & Evans, M. W. (1945). Free volume and entropy in condensed systems. III. entropy in binary liquid mixtures; partial molar entropy in dilute solutions; structure and thermodynamics in aqueous electrolytes. *The Journal of Chemical Physics, 13*(11), 507-532.

Friedman, M., Cavins, J., & Wall, J. (1965). Relative nucleophilic reactivities of amino groups and mercaptide ions in addition reactions with α,β-unsaturated Compounds1, 2. *Journal of the American Chemical Society, 87*(16), 3672-3682.

Fuchs, T., Richtering, W., Burchard, W., Kajiwara, K., & Kitamura, S. (1998). Gel point in physical gels: Rheology and light scattering from thermoreversibly gelling schizophyllan. *Polymer Gels and Networks, 5*(6), 541-559.

Fujimoto, K. L., Ma, Z., Nelson, D. M., Hashizume, R., Guan, J., Tobita, K., & Wagner, W. R. (2009). Synthesis, characterization and therapeutic efficacy of a biodegradable, thermoresponsive hydrogel designed for application in chronic infarcted myocardium. *Biomaterials, 30*(26), 4357-4368.

Ganachaud, F., Monteiro, M. J., Gilbert, R. G., Dourges, M. A., Thang, S. H., & Rizzardo, E. (2000). Molecular weight characterization of poly (N-isopropylacrylamide) prepared by living free-radical polymerization. *Macromolecules, 33*(18), 6738-6745.

Garbern, J. C., Hoffman, A. S., & Stayton, P. S. (2010). Injectable pH-and temperature-responsive poly (N-isopropylacrylamide-co-propylacrylic acid) copolymers for delivery of angiogenic growth factors. *Biomacromolecules, 11*(7), 1833-1839.

GhoshMitra, S., Diercks, D. R., Mills, N. C., Hynds, D. A. L., & Ghosh, S. (2011). Excellent biocompatibility of semiconductor quantum dots encased in multifunctional poly (N-isopropylacrylamide) nanoreservoirs and nuclear specific labeling of growing neurons. *Applied Physics Letters, 98*, 103702.

Gopferich, A. (1996). Mechanisms of polymer degradation and erosion. *Biomaterials, 17*(2), 103-114.

Guglielmi, G., Vinuela, F., Dion, J., & Duckwiler, G. (1991). Electrothrombosis of saccular aneurysms via endovascular approach. *Journal of Neurosurgery, 75*(1), 8-14.

Guo, J., Yang, W., Wang, C., He, J., & Chen, J. (2006). Poly (N-isopropylacrylamide)-coated luminescent/magnetic silica microspheres: Preparation, characterization, and biomedical applications. *Chemistry of Materials, 18*(23), 5554-5562.

Gupta, A. K., & Curtis, A. S. G. (2004). Surface modified superparamagnetic nanoparticles for drug delivery: Interaction studies with human fibroblasts in culture. *Journal of Materials Science: Materials in Medicine, 15*(4), 493-496.

Hacker, M. C., Klouda, L., Ma, B. B., Kretlow, J. D., & Mikos, A. G. (2008). Synthesis and characterization of injectable, thermally and chemically gelable, amphiphilic poly (N-isopropylacrylamide)-based macromers. *Biomacromolecules, 9*(6), 1558-1570.

Hayakawa, M., Murayama, Y., Duckwiler, G. R., Gobin, Y. P., Guglielmi, G., & Viñuela, F. (2000). Natural history of the neck remnant of a cerebral aneurysm treated with the guglielmi detachable coil system. *Journal of Neurosurgery, 93*(4), 561-568.

Henderson, E., Lee, B. H., Cui, Z., McLemore, R., Brandon, T. A., & Vernon, B. L. (2008). In vivo evaluation of injectable thermosensitive polymer with time-dependent LCST. *Journal of Biomedical Materials Research Part A, 90A*(4), 1186-1197.

Heskins, M., & Guillet, J. E. (1968). Solution properties of poly (N-isopropylacrylamide). *Journal of Macromolecular Science—Chemistry, 2*(8), 1441-1455.

Hiemstra, C., van der Aa, L. J., Zhong, Z., Dijkstra, P. J., & Feijen, J. (2007). Rapidly in situ-forming degradable hydrogels from dextran thiols through michael addition. *Biomacromolecules, 8*(5), 1548-1556.

Hoffman, A. S. (2002). Hydrogels for biomedical applications. *Advanced Drug Delivery Reviews, 54*(1), 3-12.

Jeong, B., & Gutowska, A. (2002). Lessons from nature: Stimuli-responsive polymers and their biomedical applications. *Trends in Biotechnology, 20*(7), 305-311.

Jeong, B., Kim, S. W., & Bae, Y. H. (2002). Thermosensitive sol-gel reversible hydrogels. *Advanced Drug Delivery Reviews, 54*(1), 37-51.

Jin, K. M., & Kim, Y. H. (2008). Injectable, thermo-reversible and complex coacervate combination gels for protein drug delivery. *Journal of Controlled Release, 127*(3), 249-256.

Kabanov, A. V., Batrakova, E. V., & Alakhov, V. Y. (2002). Pluronic® block copolymers as novel polymer therapeutics for drug and gene delivery. *Journal of Controlled Release, 82*(2-3), 189-212.

Kabiri, K., Omidian, H., Hashemi, S., & Zohuriaan-Mehr, M. (2003). Synthesis of fast-swelling superabsorbent hydrogels: Effect of crosslinker type and concentration on porosity and absorption rate. *European Polymer Journal, 39*(7), 1341-1348.

Kakudo, M., & Kasai, N. (1972). *X-ray diffraction by polymers* Kodansha Tokyo.

Kataoka, K., Harada, A., & Nagasaki, Y. (2001). Block copolymer micelles for drug delivery: Design, characterization and biological significance. *Advanced Drug Delivery Reviews, 47*(1), 113-131.

Kato, N., Sakai, Y., & Shibata, S. (2003). Wide-range control of deswelling time for thermosensitive poly (N-isopropylacrylamide) gel treated by freeze-drying. *Macromolecules, 36*(4), 961-963.

Kavanagh, G. M., & Ross-Murphy, S. B. (1998). Rheological characterisation of polymer gels. *Progress in Polymer Science, 23*(3), 533-562.

Keedy, A. (2006). An overview of intracranial aneurysms. *McGill Journal of Medicine: MJM, 9*(2), 141-146.

Khanna, R. K., Malik, G. M., & Qureshi, N. (1996). Predicting outcome following surgical treatment of unruptured intracranial aneurysms: A proposed grading system. *Journal of Neurosurgery, 84*(1), 49-54.

Kim, S. Y., Cho, S. M., Lee, Y. M., & Kim, S. J. (2000). Thermo-and pH-responsive behaviors of graft copolymer and blend based on chitosan and N-isopropylacrylamide. *Journal of Applied Polymer Science, 78*(7), 1381-1391.

Kim, S. Y., & Lee, S. C. (2009). Thermo-responsive injectable hydrogel system based on poly (N-isopropylacrylamide-co-vinylphosphonic acid). I. biomineralization and protein delivery. *Journal of Applied Polymer Science, 113*, 3460-3469.

Klouda, L., & Mikos, A. G. (2008). Thermoresponsive hydrogels in biomedical applications. *European Journal of Pharmaceutics and Biopharmaceutics, 68*(1), 34-45.

Koffi, A. A., Agnely, F., Besnard, M., Kablan Brou, J., Grossiord, J. L., & Ponchel, G. (2008). In vitro and in vivo characteristics of a thermogelling and bioadhesive delivery system intended for rectal administration of quinine in children. *European Journal of Pharmaceutics and Biopharmaceutics, 69*(1), 167-175.

Kong, B., Choi, J. S., Jeon, S., & Choi, I. S. (2009). The control of cell adhesion and detachment on thin films of thermoresponsive poly [(N-isopropylacrylamide)-r-((3-(methacryloylamino) propyl)-dimethyl (3-sulfopropyl) ammonium hydroxide)]. *Biomaterials, 30*(29), 5514-5522.

Krauland, A. H., Guggi, D., & Bernkop-Schnürch, A. (2006). Thiolated chitosan microparticles: A vehicle for nasal peptide drug delivery. *International Journal of Pharmaceutics, 307*(2), 270-277.

Kretlow, J. D., Hacker, M. C., Klouda, L., Ma, B. B., & Mikos, A. G. (2010). Synthesis and characterization of dual stimuli responsive macromers based on poly (N-isopropylacrylamide) and poly (vinylphosphonic acid). *Biomacromolecules, 11*(3), 797-805.

Kuckling, D., Adler, H. J. P., Arndt, K. F., Ling, L., & Habicher, W. D. (2000). Temperature and pH dependent solubility of novel poly (N-isopropylacrylamide)-copolymers. *Macromolecular Chemistry and Physics, 201*(2), 273-280.

Kulcsár, Z., Ernemann, U., Wetzel, S. G., Bock, A., Goericke, S., Panagiotopoulos, V., . . . Wanke, I. (2010). High-profile flow diverter (silk) implantation in the basilar artery. *Stroke, 41*(8), 1690-1696

Kumar, M. N. V. R., Muzzarelli, R. A. A., Muzzarelli, C., Sashiwa, H., & Domb, A. J. (2004). Chitosan chemistry and pharmaceutical perspectives. *Chem.Rev, 104*(12), 6017-6084.

Lanzino, G., Kanaan, Y., Perrini, P., Dayoub, H., & Fraser, K. (2005). Emerging concepts in the treatment of intracranial aneurysms: Stents, coated coils, and liquid embolic agents. *Neurosurgery, 57*(3), 449-459.

Lee, B. H., & Vernon, B. (2005). In situ-gelling, erodible N-isopropylacrylamide copolymers. *Macromolecular Bioscience, 5*(7), 629-635.

Lee, B. H., West, B., McLemore, R., Pauken, C., & Vernon, B. L. (2006). In-situ injectable physically and chemically gelling NIPAAm-based copolymer system for embolization. *Biomacromolecules, 7*(6), 2059-2064.

Lee, K. Y., & Mooney, D. J. (2001). Hydrogels for tissue engineering. *Chemical Reviews, 101*(7), 1869-1880.

Lee, P. Y., Cobain, E., Huard, J., & Huang, L. (2007). Thermosensitive hydrogel PEG–PLGA–PEG enhances engraftment of muscle-derived stem cells and promotes healing in diabetic wound. *Molecular Therapy, 15*(6), 1189-1194.

Lee, S. C., Cho, Y. W., & Park, K. (2005). Control of thermogelation properties of hydrophobically-modified methylcellulose. *Journal of Bioactive and Compatible Polymers, 20*(1), 5-13.

Lee, W. F., & Yeh, Y. C. (2005). Studies on preparation and properties of NIPAAm/hydrophobic monomer copolymeric hydrogels. *European Polymer Journal, 41*(10), 2488-2495.

Leon, C. M., Lee, B. H., Preul, M., McLemore, R., & Vernon, B. L. (2009). Synthesis and characterization of radio-opaque thermosensitive poly [N-isopropylacrylamide-2, 2′-(ethylenedioxy) bis (ethylamine)-2, 3, 5-triiodobenzamide]. *Polymer International, 58*(8), 847-850.

Li, H., & Luo, R. (2009). Modeling and characterization of glucose-sensitive hydrogel: Effect of young's modulus. *Biosensors and Bioelectronics, 24*(12), 3630-3636.

Lin, C., Zhao, P., Li, F., Guo, F., Li, Z., & Wen, X. (2010). Thermosensitive in situ-forming dextran-pluronic hydrogels through michael addition. *Materials Science and Engineering: C, 30*(8), 1236-1244.

Lin, T., Fox, A. J., & Drake, C. G. (1989). Regrowth of aneurysm sacs from residual neck following aneurysm clipping. *Journal of Neurosurgery, 70*(4), 556-560.

Liu, H. Y., & Zhu, X. X. (1999). Lower critical solution temperatures of N-substituted acrylamide copolymers in aqueous solutions. *Polymer, 40*(25), 6985-6990.

Liu, K. L., Zhu, J., & Li, J. (2010). Elucidating rheological property enhancements in supramolecular hydrogels of short poly [(R, S)-3-hydroxybutyrate]-based amphiphilic triblock copolymer and α-cyclodextrin for injectable hydrogel applications. *Soft Matter, 6*(10), 2300-2311.

Liu, X. M., Pramoda, K., Yang, Y. Y., Chow, S. Y., & He, C. (2004). Cholesteryl-grafted functional amphiphilic poly (< i> N</i>-isopropylacrylamide-< i> co</i>-< i> N</i>-hydroxylmethylacrylamide): Synthesis, temperature-sensitivity, self-assembly and encapsulation of a hydrophobic agent. *Biomaterials, 25*(13), 2619-2628.

Lubicz, B., Collignon, L., Raphaeli, G., Pruvo, J. P., Bruneau, M., De Witte, O., & Leclerc, X. (2010). Flow-diverter stent for the endovascular treatment of intracranial aneurysms. *Stroke, 41*(10), 2247-2253.

Lubicz, B., Piotin, M., Mounayer, C., Spelle, L., & Moret, J. (2005). Selective endovascular treatment of intracranial aneurysms with a liquid embolic: A single-center experience in 39 patients with 41 aneurysms. *American Journal of Neuroradiology, 26*(4), 885-893.

Lutolf, M., & Hubbell, J. (2003). Synthesis and physicochemical characterization of end-linked poly (ethylene glycol)-co-peptide hydrogels formed by michael-type addition. *Biomacromolecules, 4*(3), 713-722.

Lylyk, P., Miranda, C., Ceratto, R., Ferrario, A., Scrivano, E., Luna, H. R., . . . Fiorella, D. (2009). Curative endovascular reconstruction of cerebral aneurysms with the pipeline embolization device: The buenos aires experience. *Neurosurgery, 64*(4), 632.

Maeda, Y., Higuchi, T., & Ikeda, I. (2000). Change in hydration state during the coil-globule transition of aqueous solutions of poly (N-isopropylacrylamide) as evidenced by FTIR spectroscopy. *Langmuir, 16*(19), 7503-7509.

Mather, B. D., Viswanathan, K., Miller, K. M., & Long, T. E. (2006). Michael addition reactions in macromolecular design for emerging technologies. *Progress in Polymer Science, 31*(5), 487-531.

Matsuo, E. S., & Tanaka, T. (1988). Kinetics of discontinuous volume–phase transition of gels. *The Journal of Chemical Physics, 89*, 1695-1703.

McLemore, R., Lee, B. H., & Vernon, B. (2009). Surfactant effects on the kinetics of Michael-type addition reaction in reverse emulsion polymeric systems. *Journal of Biomedical Materials Research Part B: Applied Biomaterials, 89*(1), 191-198.

Meenach, S. A., Anderson, A. A., Suthar, M., Anderson, K. W., & Hilt, J. Z. (2009). Biocompatibility analysis of magnetic hydrogel nanocomposites based on poly (N-isopropylacrylamide) and iron oxide. *Journal of Biomedical Materials Research Part A, 91*(3), 903-909.

Meng, F., Hennink, W. E., & Zhong, Z. (2009). Reduction-sensitive polymers and bioconjugates for biomedical applications. *Biomaterials, 30*(12), 2180-2198.

Metters, A., & Hubbell, J. (2005). Network formation and degradation behavior of hydrogels formed by michael-type addition reactions. *Biomacromolecules, 6*(1), 290-301.

Moelbert, S., & De Los Rios, P. (2003). Hydrophobic interaction model for upper and lower critical solution temperatures. *Macromolecules, 36*(15), 5845-5853.

Moffatt, S., & Cristiano, R. J. (2006). PEGylated J591 mAb loaded in PLGA-PEG-PLGA tri-block copolymer for targeted delivery: In vitro evaluation in human prostate cancer cells. *International Journal of Pharmaceutics, 317*(1), 10-13.

Molyneux, A. J., Cekirge, S., Saatci, I., & Gál, G. (2004). Cerebral aneurysm multicenter european onyx (CAMEO) trial: Results of a prospective observational study in 20 european centers. *American Journal of Neuroradiology, 25*(1), 39-51.

Mosmann, T. (1983). Rapid colorimetric assay for cellular growth and survival: Application to proliferation and cytotoxicity assays. *Journal of Immunological Methods, 65*(1-2), 55-63.

Mottu, F., Gailloud, P., Massuelle, D., Rüfenacht, D., & Doelker, E. (2000). In vitro assessment of new embolic liquids prepared from preformed polymers and water-miscible solvents for aneurysm treatment. *Biomaterials, 21*(8), 803-811.

Mottu, F., Laurent, A., Rüfenacht, D. A., & Doelker, E. (2000). Organic solvents for pharmaceutical parenterals and embolic liquids: A review of toxicity data. *PDA Journal of Pharmaceutical Science and Technology, 54*(6), 456-469.

Murayama, Y., Nien, Y. L., Duckwiler, G., Gobin, Y. P., Jahan, R., Frazee, J., . . . Viñuela, F. (2003). Guglielmi detachable coil embolization of cerebral aneurysms: 11 years' experience. *Journal of Neurosurgery, 98*(5), 959-966.

Murayama, Y., Tateshima, S., Gonzalez, N. R., & Vinuela, F. (2003). Matrix and bioabsorbable polymeric coils accelerate healing of intracranial aneurysms. *Stroke, 34*(8), 2031-2037.

Murayama, Y., Viñuela, F., Ulhoa, A., Akiba, Y., Ducwiler, G. R., Gobin, Y. P., . . . Greff, R. J. (1998). Nonadhesive liquid embolic agent for cerebral arteriovenous malformations: Preliminary histopathological studies in swine rete mirabile. *Neurosurgery, 43*(5), 1164-1172.

Nisbet, D. R., Crompton, K. E., Hamilton, S. D., Shirakawa, S., Prankerd, R. J., Finkelstein, D. I., . . . Forsythe, J. S. (2006). Morphology and gelation of thermosensitive xyloglucan hydrogels. *Biophysical Chemistry, 121*(1), 14-20.

Norisuye, T., Masui, N., Kida, Y., Ikuta, D., Kokufuta, E., Ito, S., . . . Shibayama, M. (2002). Small angle neutron scattering studies on structural inhomogeneities in polymer gels: Irradiation cross-linked gels vs chemically cross-linked gels. *Polymer, 43*(19), 5289-5297.

Ono, Y., & Shikata, T. (2006). Hydration and dynamic behavior of poly (N-isopropylacrylamide) s in aqueous solution: A sharp phase transition at the lower critical solution temperature. *Journal of the American Chemical Society, 128*(31), 10030-10031.

Ono, Y., & Shikata, T. (2007). Contrary hydration behavior of N-isopropylacrylamide to its polymer, P (NIPAm), with a lower critical solution temperature. *The Journal of Physical Chemistry B, 111*(7), 1511-1513.

Otake, K., Inomata, H., Konno, M., & Saito, S. (1990). Thermal analysis of the volume phase transition with N-isopropylacrylamide gels. *Macromolecules, 23*(1), 283-289.

Ougizawa, T., Inoue, T., & Kammer, H. W. (1985). Upper and lower critical solution temperature behavior in polymer blends. *Macromolecules, 18*, 2092-2094.

Pan, Y., Bao, H., Sahoo, N. G., Wu, T., & Li, L. (2011). Water-Soluble poly (N-isopropylacrylamide)–Graphene sheets synthesized via click chemistry for drug delivery. *Advanced Functional Materials, 21*(14), 2754-2763.

Park, K. M., Lee, S. Y., Joung, Y. K., Na, J. S., Lee, M. C., & Park, K. D. (2009). Thermosensitive chitosan–Pluronic hydrogel as an injectable cell delivery carrier for cartilage regeneration. *Acta Biomaterialia, 5*(6), 1956-1965.

Parkinson, R. J., Eddleman, C. S., Batjer, H. H., & Bendok, B. R. (2006). Giant intracranial aneurysms: Endovascular challenges. *Neurosurgery, 59*(5), S3-282-S3-286.

Peppas, N. A., Keys, K. B., Torres-Lugo, M., & Lowman, A. M. (1999). Poly (ethylene glycol)-containing hydrogels in drug delivery. *Journal of Controlled Release, 62*(1), 81-87.

Perez, P., Plieva, F., Gallardo, A., San Roman, J., Aguilar, M. R., Morfin, I., . . . Galaev, I. Y. (2007). Bioresorbable and nonresorbable macroporous thermosensitive hydrogels prepared by cryopolymerization. role of the cross-linking agent. *Biomacromolecules, 9*(1), 66-74.

Peters, D. G., Kassam, A. B., Feingold, E., Heidrich-O'Hare, E., Yonas, H., Ferrell, R. E., & Brufsky, A. (2001). Molecular anatomy of an intracranial aneurysm: Coordinated expression of genes involved in wound healing and tissue remodeling. *Stroke, 32*(4), 1036-1042.

Plummer, P. L. M., & Chen, T. S. (1983). A molecular dynamics study of water clathrates. *Journal of Physical Chemistry, 87,* 4190-4197.

Pratt, A. B., Weber, F. E., Schmoekel, H. G., Müller, R., & Hubbell, J. A. (2004). Synthetic extracellular matrices for in situ tissue engineering. *Biotechnology and Bioengineering, 86*(1), 27-36.

Qi, H., Chen, W., Huang, C., Li, L., Chen, C., Li, W., & Wu, C. (2007). Development of a poloxamer analogs/carbopol-based in situ gelling and mucoadhesive ophthalmic delivery system for puerarin. *International Journal of Pharmaceutics, 337*(1-2), 178-187.

Qiu, Y., & Park, K. (2001). Environment-sensitive hydrogels for drug delivery. *Advanced Drug Delivery Reviews, 53*(3), 321-339.

Ramakrishna, S., Mayer, J., Wintermantel, E., & Leong, K. W. (2001). Biomedical applications of polymer-composite materials: A review. *Composites Science and Technology, 61*(9), 1189-1224.

Ramanan, R. M. K., Chellamuthu, P., Tang, L., & Nguyen, K. T. (2006). Development of a Temperature-Sensitive composite hydrogel for drug delivery applications. *Biotechnology Progress, 22*(1), 118-125.

Raymond, J., Metcalfe, A., Desfaits, A. C., Ribourtout, E., Salazkin, I., Gilmartin, K., . . . Boock, R. J. (2003). Alginate for endovascular treatment of aneurysms and local growth factor delivery. *American Journal of Neuroradiology, 24*(6), 1214-1221.

Regli, L., Uske, A., & de Tribolet, N. (1999). Endovascular coil placement compared with surgical clipping for the treatment of unruptured middle cerebral artery aneurysms: A consecutive series. *Journal of Neurosurgery, 90*(6), 1025-1030.

Ribeiro, C., Arizaga, G. G. C., Wypych, F., & Sierakowski, M. R. (2009). Nanocomposites coated with xyloglucan for drug delivery: In vitro studies. *International Journal of Pharmaceutics, 367*(1-2), 204-210.

Ricci, E. J., Lunardi, L. O., Nanclares, D. M. A., & Marchetti, J. M. (2005). Sustained release of lidocaine from poloxamer 407 gels. *International Journal of Pharmaceutics, 288*(2), 235-244.

Rijcken, C. J., Snel, C. J., Schiffelers, R. M., Van Nostrum, C. F., & Hennink, W. E. (2007). Hydrolysable core-crosslinked thermosensitive polymeric micelles: Synthesis, characterisation and in vivo studies. *Biomaterials, 28*(36), 5581-5593.

Rinkel, G. J. E., Djibuti, M., Algra, A., & Van Gijn, J. (1998). Prevalence and risk of rupture of intracranial aneurysms: A systematic review. *Stroke, 29*(1), 251-256.

Robb, S. A., Lee, B. H., McLemore, R., & Vernon, B. L. (2007). Simultaneously physically and chemically gelling polymer system utilizing a poly (NIPAAm-co-cysteamine)-based copolymer. *Biomacromolecules, 8*(7), 2294-2300.

Ruel-Gariepy, E., Chenite, A., Chaput, C., Guirguis, S., & Leroux, J. C. (2000). Characterization of thermosensitive chitosan gels for the sustained delivery of drugs. *International Journal of Pharmaceutics, 203*(1-2), 89-98.

Ruel-Gariepy, E., & Leroux, J. C. (2004). In situ-forming hydrogels--review of temperature-sensitive systems. *European Journal of Pharmaceutics and Biopharmaceutics, 58*(2), 409-426.

Ruel-Gariépy, E., Shive, M., Bichara, A., Berrada, M., Le Garrec, D., Chenite, A., & Leroux, J. C. (2004). A thermosensitive chitosan-based hydrogel for the local delivery of paclitaxel. *European Journal of Pharmaceutics and Biopharmaceutics, 57*(1), 53-63.

Rzaev, Z. M. O., Dinçer, S., & Piskin, E. (2007). Functional copolymers of N-isopropylacrylamide for bioengineering applications. *Progress in Polymer Science, 32*(5), 534-595.

Sá-Lima, H., Tuzlakoglu, K., Mano, J. F., & Reis, R. L. (2011). Thermoresponsive poly (N-isopropylacrylamide)-g-methylcellulose hydrogel as a three-dimensional extracellular matrix for cartilage-engineered applications. *Journal of Biomedical Materials Research Part A, 98A*(4), 596-603.

Sampei, K., Hashimoto, N., Kazekawa, K., Tsukahara, T., Iwata, H., & Takaichi, S. (1996). Histological changes in brain tissue and vasculature after intracarotid infusion of organic solvents in rats. *Neuroradiology, 38*(3), 291-294.

Santos, J. R., Alves, N. M., & Mano, J. F. (2010). New thermo-responsive hydrogels based on poly (N-isopropylacrylamide)/Hyaluronic acid semi-interpenetrated polymer networks: Swelling properties and drug release studies. *Journal of Bioactive and Compatible Polymers, 25*(2), 169-184.

Sarkar, N. (1979). Thermal gelation properties of methyl and hydroxypropyl methylcellulose. *Journal of Applied Polymer Science, 24*(4), 1073-1087.

Schievink, W. I. (1997). Intracranial aneurysms. *New England Journal of Medicine, 336*(1), 28-40.

Schievink, W. (1998). Genetics and aneurysm formation. *Neurosurgery Clinics of North America, 9*(3), 485-495.

Schild, H. G., & Tirrell, D. A. (1990). Microcalorimetric detection of lower critical solution temperatures in aqueous polymer solutions. *Journal of Physical Chemistry, 94*(10), 4352-4356.

Scott, E. A., Nichols, M. D., Cordova, L. H., George, B. J., Jun, Y. S., & Elbert, D. L. (2008). Protein adsorption and cell adhesion on nanoscale bioactive coatings formed from poly (ethylene glycol) and albumin microgels. *Biomaterials, 29*(34), 4481-4493.

Seliktar, D., Zisch, A., Lutolf, M., Wrana, J., & Hubbell, J. (2004). MMP-2 sensitive, VEGF-bearing bioactive hydrogels for promotion of vascular healing. *Journal of Biomedical Materials Research Part A, 68*(4), 704-716.

Shamji, M. F., Hwang, P., Bullock, R. W., Adams, S. B., Nettles, D. L., & Setton, L. A. (2008). Release and activity of anti-TNFα therapeutics from injectable chitosan preparations for local drug delivery. *Journal of Biomedical Materials Research Part B: Applied Biomaterials, 90B*(1), 319-326.

Shi, J., Alves, N. M., & Mano, J. F. (2008). Chitosan coated alginate beads containing poly (N-isopropylacrylamide) for dual-stimuli-responsive drug release. *Journal of Biomedical Materials Research Part B: Applied Biomaterials, 84*(2), 595-603.

Shibayama, M., Mizutani, S., & Nomura, S. (1996). Thermal properties of copolymer gels containing N-isopropylacrylamide. *Macromolecules, 29*(6), 2019-2024.

Shibayama, M., Morimoto, M., & Nomura, S. (1994). Phase separation induced mechanical transition of poly (N-isopropylacrylamide)/water isochore gels. *Macromolecules, 27*(18), 5060-5066.

Siepmann, J., & Peppas, N. A. (2001). Modeling of drug release from delivery systems based on hydroxypropyl methylcellulose (HPMC). *Advanced Drug Delivery Reviews, 48*(2-3), 139-157.

Silverstein, R., & Webster, F. (2006). *Spectrometric identification of organic Compounds6* Wiley-India.

Skrzeszewska, P. J., de Wolf, F. A., Werten, M. W. T., Moers, A. P. H. A., Stuart, M. A. C., & van der Gucht, J. (2009). Physical gels of telechelic triblock copolymers with precisely defined junction multiplicity. *Soft Matter, 5*(10), 2057-2062.

Soga, Y., Preul, M. C., Furuse, M., Becker, T., & McDougall, C. G. (2004). Calcium alginate provides a high degree of embolization in aneurysm models: A specific comparison to coil packing. *Neurosurgery, 55*(6), 1401-1409.

Solis, F. J., Weiss-Malik, R., & Vernon, B. (2005). Local monomer activation model for phase behavior and calorimetric properties of LCST gel-forming polymers. *Macromolecules, 38*(10), 4456-4464.

Solomon, R. A., Fink, M. E., & Pile-Spellman, J. (1994). Surgical management of unruptured intracranial aneurysms. *Journal of Neurosurgery, 80*(3), 440-446.

Southall, N. T., Dill, K. A., & Haymet, A. D. J. (2002). A view of the hydrophobic effect. *Journal of Physical Chemistry B-Condensed Phase, 106*(3), 521-533.

Sriadibhatla, S., Yang, Z., Gebhart, C., Alakhov, V. Y., & Kabanov, A. (2006). Transcriptional activation of gene expression by pluronic block copolymers in stably and transiently transfected cells. *Molecular Therapy, 13*(4), 804-813.

Stile, R. A., Burghardt, W. R., & Healy, K. E. (1999). Synthesis and characterization of injectable poly (N-isopropylacrylamide)-based hydrogels that support tissue formation in vitro. *Macromolecules, 32*(22), 7370-7379.

Szikora, I., Berentei, Z., Kulcsar, Z., Marosfoi, M., Vajda, Z., Lee, W., . . . Nelson, P. (2010). Treatment of intracranial aneurysms by functional reconstruction of the parent artery: The budapest experience with the pipeline embolization device. *American Journal of Neuroradiology, 31*(6), 1139-1147.

Tanaka, F., & Edwards, S. (1992a). Viscoelastic properties of physically crosslinked networks. 1. transient network theory. *Macromolecules, 25*(5), 1516-1523.

Tanaka, F., & Edwards, S. (1992b). Viscoelastic properties of physically crosslinked networks: Part 1. non-linear stationary viscoelasticity. *Journal of Non-Newtonian Fluid Mechanics, 43*(2-3), 247-271.

Tanaka, T., Sato, E., Hirokawa, Y., Hirotsu, S., & Peetermans, J. (1985). Critical kinetics of volume phase transition of gels. *Physical Review Letters, 55*(22), 2455-2458.

Tarasevich, B. J., Gutowska, A., Li, X. S., & Jeong, B. M. (2009). The effect of polymer composition on the gelation behavior of PLGA-g-PEG biodegradable thermoreversible gels. *Journal of Biomedical Materials Research Part A, 89A*(1), 248-254.

Toru, T., & Bolm, C. (2008). *Organosulfur chemistry in asymmetric synthesis* Vch Verlagsgesellschaft Mbh.

Tweedie, C.A., & Van Vliet, K.J. (2006). Contact creep compliance of viscoelastic materials via nanoindentation. *Journal of Materials Research, 21*(6), 1576-1589.

Vernengo, J., Fussell, G. W., Smith, N. G., & Lowman, A. M. (2008). Evaluation of novel injectable hydrogels for nucleus pulposus replacement. *Journal of Biomedical Materials Research Part B: Applied Biomaterials, 84A* (1), 64-69.

Vernon, B., Kim, S. W., & Bae, Y. H. (2000). Thermoreversible copolymer gels for extracellular matrix. *Journal of Biomedical Materials Research, 51*(1), 69-79.

Vernon, B., & Martinez, A. (2005). Gel strength and solution viscosity of temperature-sensitive, in-situ-gelling polymers for endovascular embolization. *Journal of Biomaterials Science, Polymer Edition, 16*(9), 1153-1166.

Vernon, B., Tirelli, N., Bächi, T., Haldimann, D., & Hubbell, J. A. (2003). Water-borne, in situ crosslinked biomaterials from phase-segregated precursors. *Journal of Biomedical Materials Research Part A, 64*(3), 447-456.

Vihola, H., Laukkanen, A., Valtola, L., Tenhu, H., & Hirvonen, J. (2005). Cytotoxicity of thermosensitive polymers poly (N-isopropylacrylamide),

poly (N-vinylcaprolactam) and amphiphilically modified poly (N-vinylcaprolactam). *Biomaterials, 26*(16), 3055-3064.

Viñuela, F., Duckwiler, G., & Mawad, M. (1997). Guglielmi detachable coil embolization of acute intracranial aneurysm: Perioperative anatomical and clinical outcome in 403 patients. *Journal of Neurosurgery, 86*(3), 475-482.

Wadajkar, A. S., Koppolu, B., Rahimi, M., & Nguyen, K. T. (2009). Cytotoxic evaluation of N-isopropylacrylamide monomers and temperature-sensitive poly (N-isopropylacrylamide) nanoparticles. *Journal of Nanoparticle Research, 11*(6), 1375-1382.

Wang, C. C., Su, C. H., & Chen, C. C. (2008). Water absorbing and antibacterial properties of N-isopropyl acrylamide grafted and collagen/chitosan immobilized polypropylene nonwoven fabric and its application on wound healing enhancement. *Journal of Biomedical Materials Research Part A, 84A* (4), 1006-1017.

Wang, X., Qiu, X., & Wu, C. (1998). Comparison of the coil-to-globule and the globule-to-coil transitions of a single poly (N-isopropylacrylamide) homopolymer chain in water. *Macromolecules, 31*(9), 2972-2976.

Weber, W., Siekmann, R., Kis, B., & Kuehne, D. (2005). Treatment and follow-up of 22 unruptured wide-necked intracranial aneurysms of the internal carotid artery with onyx HD 500. *American Journal of Neuroradiology, 26*(8), 1909-1915.

Wei, H., Cheng, C., Cheng, C., Chang, C., Chen, W. Q., Cheng, S. X., . . . Zhuo, R. X. (2008). Synthesis and applications of shell cross-linked thermoresponsive hybrid micelles based on poly (N-isopropylacrylamide-co-3-(trimethoxysilyl) propyl methacrylate)-b-poly (methyl methacrylate). *Langmuir, 24*(9), 4564-4570.

Weiss, P., Layrolle, P., Clergeau, L. P., Enckel, B., Pilet, P., Amouriq, Y., . . . Giumelli, B. (2007). The safety and efficacy of an injectable bone substitute in dental sockets demonstrated in a human clinical trial. *Biomaterials, 28*(22), 3295-3305.

Weng, L., Pan, H., & Chen, W. (2008). Self-crosslinkable hydrogels composed of partially oxidized hyaluronan and gelatin: In vitro and in vivo responses. *Journal of Biomedical Materials Research Part A, 85A*(2), 352-365.

Wiebers, D. O. (2003). Unruptured intracranial aneurysms: Natural history, clinical outcome, and risks of surgical and endovascular treatment. *The Lancet, 362*(9378), 103-110.

Wiebers, D. O., Whisnant, J. P., & O'Fallon, W. M. (1981). The natural history of unruptured intracranial aneurysms. *New England Journal of Medicine, 304*(12), 696-698.

Wirth, F., Laws Jr, E., Piepgras, D., & Scott, R. (1983). Surgical treatment of incidental intracranial aneurysms. *Neurosurgery, 12*(5), 507-511.

Wu, J., Wei, W., Wang, L. Y., Su, Z. G., & Ma, G. H. (2007). A thermosensitive hydrogel based on quaternized chitosan and poly (ethylene glycol) for nasal drug delivery system. *Biomaterials, 28*(13), 2220-2232.

Xu, F., Zhu, Y., Liu, F., Nie, J., Ma, J., & Yang, W. (2010). Comb-shaped conjugates comprising hydroxypropyl cellulose backbones and low-molecular-weight poly (N-isopropylacryamide) side chains for smart hydrogels: Synthesis, characterization, and biomedical applications. *Bioconjugate Chemistry, 21*(3), 456-464.

Yasuda, S., Townsend, D. W., Michele, D. E., Favre, E. G., Day, S. M., & Metzger, J. M. (2005). Dystrophic heart failure blocked by membrane sealant poloxamer. *Nature, 436*(7053), 1025-1029.

Yin, X., Hoffman, A. S., & Stayton, P. S. (2006). Poly (N-isopropylacrylamide-co-propylacrylic acid) copolymers that respond sharply to temperature and pH. *Biomacromolecules, 7*(5), 1381-1385.

Yu, Q., Zhang, Y., Chen, H., Zhou, F., Wu, Z., Huang, H., & Brash, J. L. (2010). Protein adsorption and cell Adhesion/Detachment behavior on dual-responsive silicon surfaces modified with poly (N-isopropylacrylamide)-block-polystyrene copolymer. *Langmuir, 26*(11), 8582-8588.

Yun, K., & Moon, H. T. (2008). Inducing chondrogenic differentiation in injectable hydrogels embedded with rabbit chondrocytes and growth factor for neocartilage formation. *Journal of Bioscience and Bioengineering, 105*(2), 122-126.

Zhou, Q., Rutland, M. W., Teeri, T. T., & Brumer, H. (2007). Xyloglucan in cellulose modification. *Cellulose, 14*(6), 625-641.

Zhu, Y., Kaskel, S., Ikoma, T., & Hanagata, N. (2009). Magnetic SBA-15/poly (N-isopropylacrylamide) composite: Preparation, characterization and temperature-responsive drug release property. *Microporous and Mesoporous Materials, 123*(1-3), 107-112.

APPENDIX A

IACUC PROTOCOL APPROVAL

Institutional Animal Care and Use Committee (IACUC)
Office of Research Integrity and Assurance
Arizona State University
Tempe, Arizona 85287-1103
Phone: (480) 965-2179 *FAX:* (480) 965-7772

Animal Protocol Review

ASU Protocol Number: **11-1152TK**
Protocol Title: **"Liquid-to-Solid Gelling Polymer System for Intracranial Aneurysm Embolization"**
Principal Investigator: **Brent Vernon**
Date of Action: **09/03/2010**

The animal protocol review was considered by the Committee and the following decisions were made:

- ☐ The original protocol was APPROVED as presented.
- ☐ The revised protocol was APPROVED as presented.
- ☐ The protocol was APPROVED with RESTRICTIONS or CHANGES as noted below. The project can only be pursued, subject to your acceptance of these restriction or changes. If you are not agreeable, contact the IACUC Chairperson immediately.
- ☐ The Committee requests CLARIFICATIONS or CHANGES in the protocol as described in the attached memorandum. The protocol will be considered when these issues are clarified and the revised protocol is submitted.
- ☐ The protocol was approved, subject to the approval of a WAIVER of provisions of NIH policy as noted below. Waivers require written approval from the granting agencies.
- ☐ The protocol was DISAPPROVED for reasons outlined in the attached memorandum.
- ☐ The Committee requests you to contact _____ to discuss this proposal.
- ☐ A copy of this correspondence has been sent to the Vice President for Research.
- ☒ This tracking protocol references research in collaboration with Celeste Riley (ASU) and Mark Preul (BNI). BNI Protocol Number 388.

RESTRICTIONS, CHANGES OR WAIVER REQUIREMENTS:
Approval Period: **2/26/2010 – 2/25/2013**

Signature: _____ Date: 9/2/10
IACUC Chair or Designee

Original: Principal Investigator
Cc: IACUC Office
IACUC Chair

APPENDIX B

BNI PROTOCOL NUMBER 388

St. Joseph's Hospital and Medical Center
A member of CHW

Institutional Animal Care and Use Committee

APPROVAL FORM

Protocol # 388 Animal Welfare Assurance # A3519-01

Grant #

Investigator(s): Dr. Mark Preul

Title of Project "Advanced polymer for endovascular embolization

Species and Numbers of Animals: Swine - 21
Canines - 21

This is to certify that the project identified above has been reviewed by the Institutional Animal Care and Use Committee which has considered specifically the compliance with applicable requirements of the Animal Welfare Act and pertinent state and local laws, regulations and adherence to the PHS Policy, and NIH Guide.

The proposed study has been approved by the IACUC and complies with the institutional assurance certification of the Barrow Neurological Institute of St. Joseph's Hospital and Medical Center.

Unless otherwise stated, this protocol has been approved by the Committee for a period of three years from the date noted below. The protocol is also subject to annual review on or before this date by this Committee.

Date of Committee Approval: February 26, 2010

COMMITTEE APPROVAL:

Thomas M. Hamm, Ph.D. Chairman - Institutional Animal Care and Welfare Committee

INSTITUTIONAL APPROVAL:

Ronald J. Lukas, Ph.D. Vice President of Research

c: Principal Investigator: You are reminded that modifications of any type in the above research project pertaining to animal experimentation requires re-review by this Committee.

350 West Thomas Road
Phoenix, AZ 85013
602.406.3000 telephone

stjosephs-phx.org

APPENDIX C

STATEMENT OF PERMISSION FROM CO-AUTHORS

Co-authors on previously published or submitted articles "Synthesis, Characterization and Properties of a Physically and Chemically Gelling Polymer System Using Poly(NIPAAm-*co*-HEMA-acrylate) and Poly(NIPAAm-*co*-cysteamine)" and "Comparison of properties between NIPAAm-based simultaneously physically and chemically gelling polymer systems for use *in vivo*" have granted their permission for use of the articles in this dissertation.